

A COMPREHENSIVE STUDY ON THE DETECTION OF BLADE VIBRATION IN ROTATING MACHINERIES

By
A. Rama Rao

ENGG 01200904013

Bhabha Atomic Research Center, Mumbai

*A thesis submitted to the
Board of Studies in Engineering Sciences*

In partial fulfillment of requirements

for the Degree of

DOCTOR OF PHILOSOPHY

of

HOMI BHABHA NATIONAL INSTITUTE

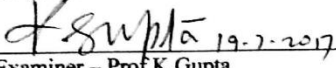
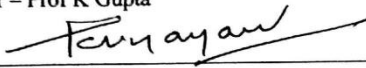
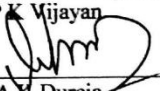


July 2017

Homi Bhabha National Institute

Recommendations of the Viva Voce Committee

As members of the Viva Voce Committee, we certify that we have read the dissertation prepared by Shri A. Rama Rao entitled "A comprehensive study on the detection of blade vibration in rotating machineries" and recommend that it may be accepted as fulfilling the thesis requirement for the award of Degree of Doctor of Philosophy.

 Chairman – Prof R B Grover	19 July 2017
 Guide / Convener – Prof B K Dutta	19 July 2017
Co-guide - ----	19 July 2017
 Examiner – Prof K Gupta	19 July 2017
 Member 1- Prof P K Vijayan	19 July 2017
 Member 2- Prof A K Dureja	19 July 2017

Final approval and acceptance of this thesis is contingent upon the candidate's submission of the final copies of the thesis to HBNI.

I hereby certify that I have read this thesis prepared under my direction and recommend that it may be accepted as fulfilling the thesis requirement.

Date: 19 July 2017

Place: Mumbai

Guide

STATEMENT BY AUTHOR

This dissertation has been submitted in partial fulfillment of requirements for an advanced degree at Homi Bhabha National Institute (HBNI) and is deposited in the Library to be made available to borrowers under rules of the HBNI.

Brief quotations from this dissertation are allowable without special permission, provided that accurate acknowledgement of source is made. Requests for permission for extended quotation from or reproduction of this manuscript in whole or in part may be granted by the Competent Authority of HBNI when in his or her judgment the proposed use of the material is in the interests of scholarship. In all other instances, however, permission must be obtained from the author.

A. Rama Rao

Place: Mumbai

Date 26th July 2017

DECLARATION

I, hereby declare that the investigation presented in the thesis has been carried out by me. The work is original and has not been submitted earlier as a whole or in part for a degree / diploma at this or any other Institution / University.

A. Rama Rao

Place: Mumbai

Date 26th July 2017

List of Publications arising from the thesis

International Journals: 03

1. Vibration Analysis for Detecting Failure of Compressor Blade. A.Rama Rao, B.K.Dutta. Engineering Failure Analysis (Elsevier) Volume 25, 2012 page 211-218
2. In situ Detection of Turbine Blade Vibration and prevention. Journal of Failure Analysis and Prevention. A.Rama Rao, B.K.Dutta DOI 10.1007/s11668-012-9597-6 Published online 01 August 2012
3. Blade vibration triggered by low load and high back pressure, A.Rama Rao, B.K.Dutta, Engineering Failure Analysis (Elsevier) Volume 46, 2014 page 40-48

International conference: 01

1. A.Rama Rao & B.K.Dutta “Non intrusive Technique for Monitoring Vibration of Operating Turbine Blades” (ID 581) 24th International Conference on Noise and Vibration Engineering 2010 ISMA 20-22 September 2010, Leuven, Belgium

National Conference: 01

1. A.Rama Rao, B.K.Dutta “Turbine Blades Vibration: Non Intrusive Monitoring Technique” Paper No C001 National Symposium on Rotor Dynamic (NSRD-2011) 19-21 Dec 2011. Indian Institute of Technology, Madras.

A. Rama Rao

Place: Mumbai

Date 26th July 2017

DEDICATION

This thesis is dedicated to the loving memory of my father

Shri. T. R. Ashwathanarayana Rao.

ACKNOWLEDGEMENTS

I express my sincere gratitude towards my guide Prof. Dr. B. K. Dutta, Dean, HBNI for his guidance, encouragement and support during my research work. He was the main motivator to convert my technical investigations in to a systematic research work. His guidance has helped me to publish three good research papers which have been widely referred by other researchers in the field of diagnostics for turbine blades.

I am deeply indebted to Prof. Dr. R. B. Grover, Ex Vice Chancellor, HBNI for relentlessly persuading me to complete the thesis work in a stipulated time. I am also grateful to Dr. R. K. Sinha, Ex Chairman, DAE who was very keen in getting me registered for Ph. D. work.

Contents

Synopsis	i
List of figures	ix
List of tables	xii

Chapters

1 Introduction and objective	1
1.1 Vulnerability of long blades to vibrate	2
1.2 Objective of the thesis	6
1.3 Organization of the thesis	6
2 Literature Survey	9
2.1 Challenges of Detecting Turbine Blade Vibration	10
2.2 Design features of long turbine blades	11
2.2.1 Velocity Diagram	12
2.2.2 Blade nodes and wheel modes	15
2.2.3 Effect of rotation on blade frequency	17
2.2.4 Stresses in blades	19
2.2.5 Fatigue in blades	20
2.2.6 Sources of blade vibration	21
2.3 Different methods of blade vibration measurement	23
2.3.1 Strain gage method	24
2.3.2 Blade tip timing method	25
2.3.3 Laser Doppler Anemometry method	26
2.3.4 Acoustic Doppler method	28

2.3.5	Torsion vibration method	30
2.3.6	Narrow beam radar signal method	31
2.3.7	Microwave method	32
2.3.8	Radionuclide method for non-magnetic blades	34
2.3.9	Optical method	36
2.3.10	Casing internal pressure measurement	37
2.3.11	Casing vibration method	38
2.3.12	Closure	39
3	Analysis method for detecting blade vibration	40
3.1	Problem definition	41
3.2	Relationship between BPF and Blade natural frequency	45
3.3	Analytical solution on amplitude reduction of BPF due to blade vibration	48
3.4	Closure	51
4	Application of blade vibration detection method on LP turbine on 900 MW Nuclear turbine	52
4.1	Problem definition	53
4.2	Casing vibration analysis	54
4.3	Closure	61
5	Blade vibration analysis during part load operation	63
5.1	Problem definition	64
5.2	Casing vibration analysis	64
5.3	Closure	69
6	Application of detecting technique on compressor blades in a power plant	71
6.1	Problem definition	72
6.2	Casing vibration analysis	73
6.3	Closure	77

7	Simulation of fluid structure interaction between blade and the surrounding steam by numerical method	79
7.1	Problem definition	80
7.2	Modeling long turbine blade	82
7.3	Fluid structure analysis	83
7.4	Closure	87
8	Conclusion, Contribution and Future work	88
8.1	Conclusions	88
8.2	Contribution	89
8.3	Future work	90
	References	91

Synopsis

1 Introduction

Steam turbine based power plants constitute more than 85% of the total installed capacity in the world. The long blades in the LP turbine are the most stressed components due to hostile steam environment. Survey has indicated that in over 40% of cases the exact reason for blade failure is not fully understood [2]. The mechanisms responsible for each of these failures are different and complex. In view of the serious consequences of blade failure, it is important to monitor blade vibration to assess overall health of the operating machine. Important steps are.

- Understanding the mechanism and root cause of failure
- Monitoring evolving precursors to take advance action that will prevent failure

Blades are not accessible for direct measurement. World over many research work are pursued to device methods to quantify blade vibration [1-10]. These methods are intrusive by design and need complicated analysis and extensive instrumentation for getting limited information. The aim of the study in this work is to comprehensively address the issue of detecting blade vibration by non-intrusive technique and to build a robust method for detecting blade vibration in plants.

2 Sources of Blade Excitation in the Turbine

Primary source of blade excitation have been put under four categories [2].

- Harmonic excitation: Per revolution excitation forces, more relevant to long blades.

- Non synchronous excitation: Complex interaction between rotor and stator
- Random excitation: Flow unsteadiness in the stationary flow passages
- Self excitation: During Low load and low vacuum in condenser.

2.1 Objective of the Present Research.

Detecting blade vibration through analysis of casing vibration is chosen in the present research. It is well known that the casing of a turbine is typically a pressure vessel which responds to all the dynamics that unfolds when the turbine rotor starts rolling. These are the cyclic components identified as blade passing frequency (BPF) which is directly related to the blades. The aim of the research is to analyze BPF and correlate it with blade vibration.

2.2 Outline of the Work

- To collect available information about the behavior of the long turbine blades.
- Propose a non-intrusive method for detecting blade vibration.
- To build a robust online method for detecting blade vibration in power plants.

3 Following studies are carried out as a part of present research programme.

3a A New Methodology for Monitoring Blade Vibration

Laboratory experiment involving rotating fan and jet of air was carried out to excite the blades of the fan. The fan in the setup simulates the rotating turbine, its blades as turbine blades and the air jet was meant to excite the blades of the fan to vibrate. A dynamic pressure transducer was used close to the tip of the blades to measure dynamic air pressure pulsation during rotation of the fan. Figure 1 shows frequency spectrum of the pressure signal measured by the sensor. Amplitude at BPF is pressure pulsation due to rotation of the fan. Experiment proved that amplitude at BPF reduces when the blade vibrates due to air jet impingement. All the attributes of BPF peak can be connected to the blades. A simple MatLab programme plot shows reduced amplitude at BPF due to blade vibration.

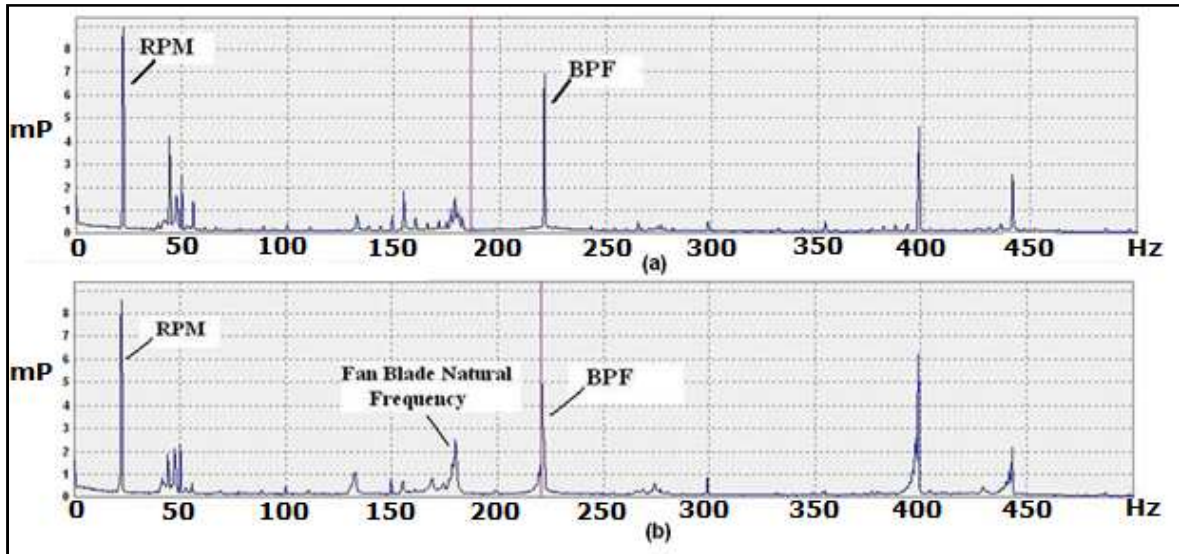


Figure 1 Spectrum of pressure signal (a) BPF & RPM (b) BPF, RPM & blade natural frequency

Finding.

The experiment connects BPF and the natural frequency of the blade.

3b LP Casing Vibration Analysis of 990 MW Nuclear Power Plant

Blades rotating inside the casing of LP turbine communicate information about the blade in the form of amplitude at BPF that can be measured by casing mounted accelerometer. Figure 2 (left) shows cascaded spectra with BPF of 8th stage at 2400 Hz (25 X 48). Figure 2 (right) shows cascaded spectra with peak at 78 Hz emerging from background noise when amplitude at BPF reduces. Blades were found to be vibrating at its natural frequency due to excitation by steam

Finding

Long LP blades are susceptible to vibration due to steam turbulence at extraction.

3c Detection of Blade Vibration During Part Load Plant Operation

Long LP turbine blades vibrate due to part load operation. Amplitude at BPF of the last stage blades of LP turbine showed variation matching with the variation of power and vacuum in the

condenser. A frequency peak at 107 Hz appears in the spectrum when the amplitude at BPF reduced. 107 Hz is natural frequency of the last stage blades (Campbell diagram).

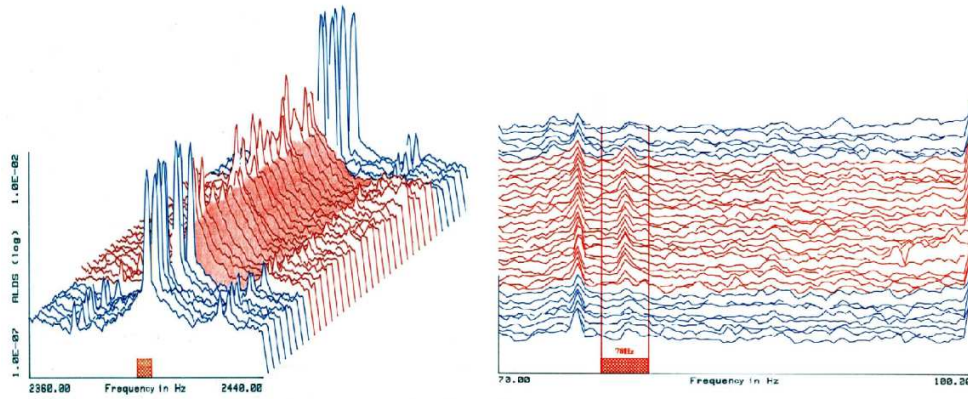


Figure 2 Water fall spectrum showing BPF and blade natural frequency in 900 MW plant

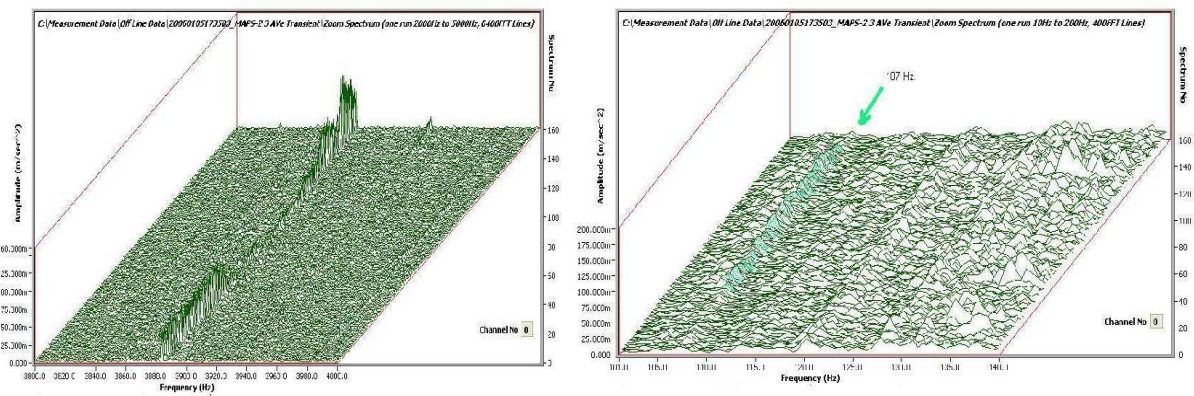


Figure 3 Water fall spectrum showing BPF and blade natural frequency in 220 MW plant

Finding

Long LP blades vibrate at its natural frequency under low load and low vacuum.

3d Validation of Proposed Method on Compressor of Gas Turbine

Vibration was induced in the compressor blades by reducing load by 10 MW for short time. The compressor blades respond during the transient. 508 Hz was confirmed as mode of the blades.

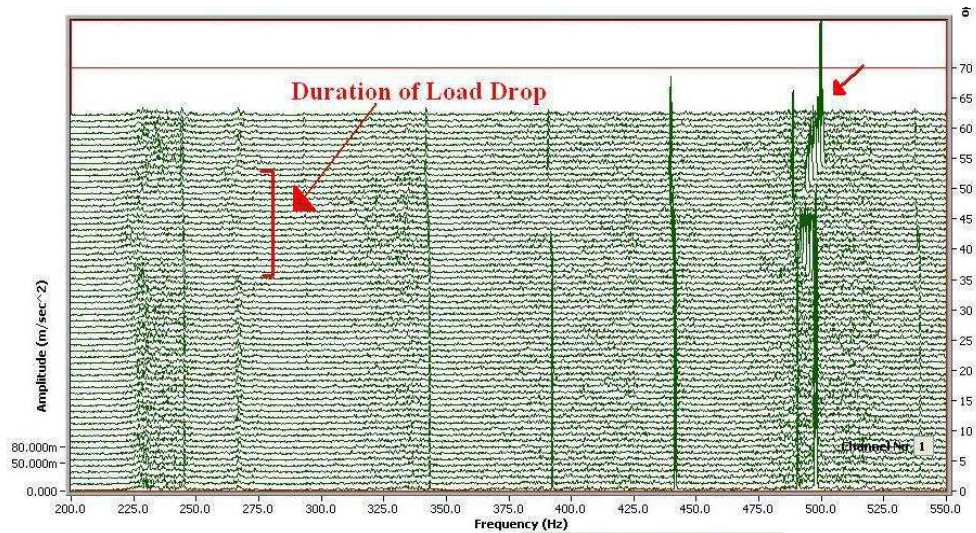


Figure 4 Water fall spectrum showing blade natural frequency interacting with 10X component

Finding

Short and rigid compress blades too respond to transient created in the compressors.

3e Simulation of fluid structure interaction between blade and surrounding steam [11]

Long LP blades vibrate under low load and low vacuum. The dragged 3-D blade model was meshed in Lagrangian formulation and fluid was meshed in Eulerian formulation. Along the leading edge of the blade, steam jet is modeled with steam velocity corresponding to the upper portion of the blade velocity for reaction type blade.

Figure 5 shows FE model of the blade submerged in the fluid domain.

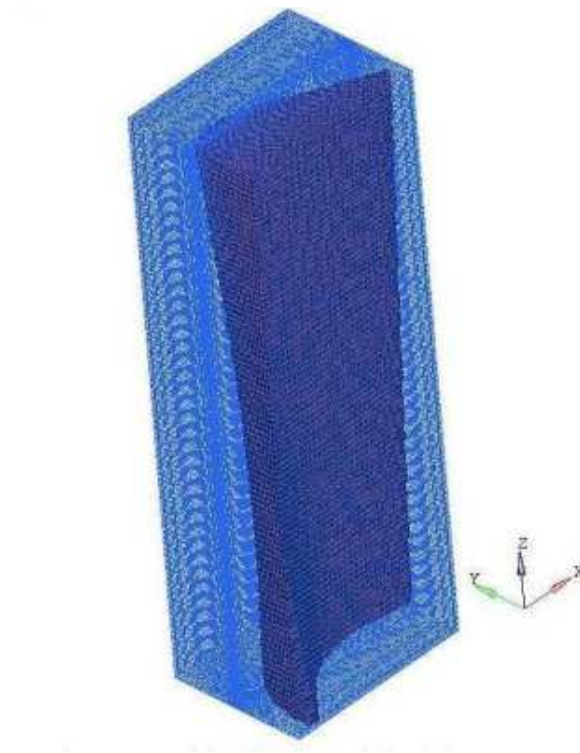


Figure 5 Model of the blade and the surrounding fluid

Figure 6 shows steam vectors along the cross section

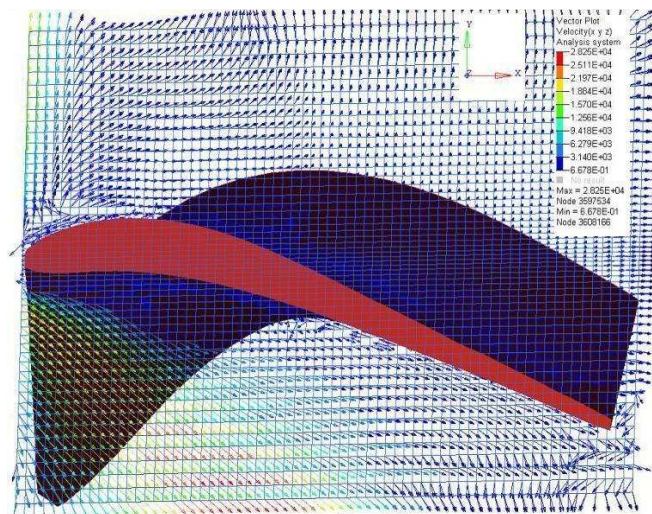


Figure 6 Flow of steam across the blade

Lagrangian elements of the blade are defined as master nodes and Eulerian elements of the fluid are defined as slave nodes. A spring element gets added between master and the slave node which remains active until slave node goes beyond the gap value. Blade vibration due to interaction with the jet of steam flowing across the blade at different angle of incidence is analyzed.

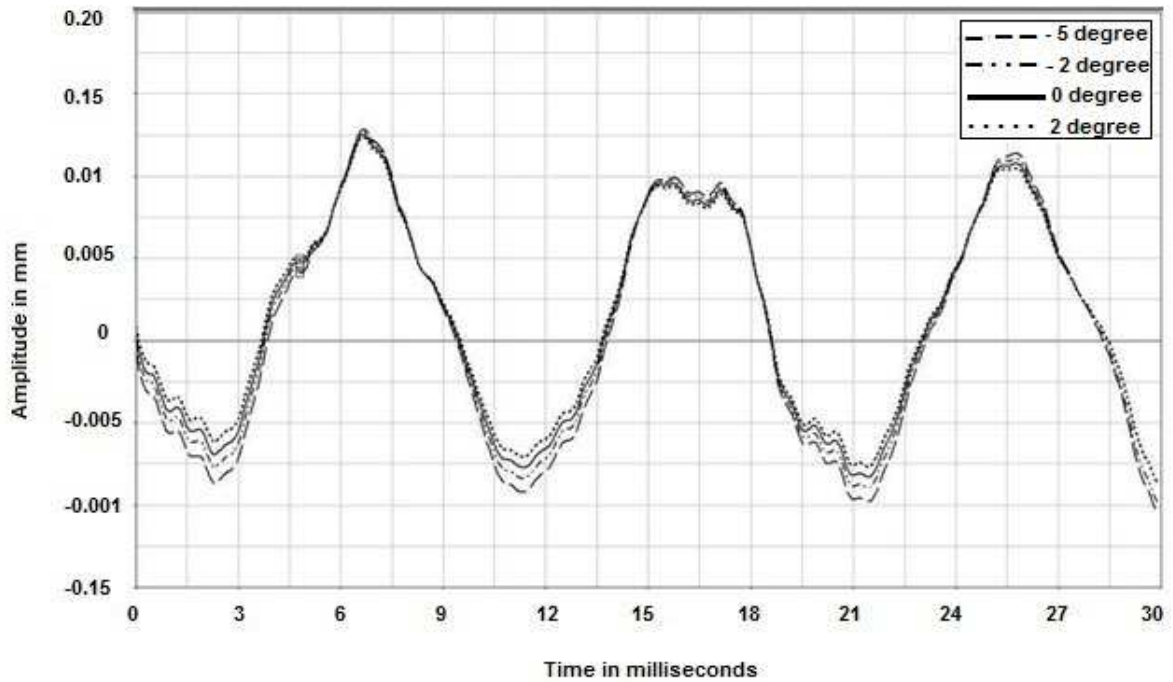


Figure 7 Increase in blade vibration due to large steam inlet angle

7 Contribution

1. The evolved method can be used for in situ validation of Campbell diagram.
2. The method detects blade vibration during self excitation demonstrated.
3. The method is robust and can be implemented in different types of power plants.

8 Conclusion

1. Casing vibration analysis is reliable method for detecting blade vibration.
2. Direct relationship is established between blade vibration and BPF.
3. Long blades are sensitive to changes to process parameters.
4. Steam extractions from the LP casing induces vibration in the long blades
5. Low load plants operation not good for long turbine blades

Reference

1. Alexander Leyzerovich. Large Power Steam Turbines. PennWell Books. ISBN 0-87814-717-9/ ISBN 0-87814-716-0. 1997
2. Bates, R.C.: Steam turbine blades: considerations in design and a survey of blade failures, EPRI Project Report No 912-1 CS-1967, August (1981)
3. Dewey, R., Rieger, N., McCloskey, T.: Survey of steam turbine blade failures. EPRI CS3891 Project 1856-1, March (1985)
4. Knappett D & J.Garcia. Blade tip timing and strain gage correlation on compressor blades. Proceeding of the Institution of Mechanical Engineers Part G, 222 (GA) pg 497-506 2008
5. Dvrst.F.A Melling & Whitelaw Principles and practices of Laser Doppler Anemometry. Academic press <http://www.dantecmt.com/Ida/princip/Indes.html>
6. Maynard K.P. Trethewey M.W. Application of torsional vibration measurement to blade and shaft crack detection in operating machinery. Maintenance and reliability Conference, Gatlinburg, Tennessee, May 2001.
7. Frank Woditschka. Steam turbine and method of measuring the vibration of a moving blade in a flow passage of a steam turbine Siemens Aktiengesellschaft US patent No 761956
8. Forbes G L & Robert B Randall. Non contact gas turbine blade vibration measurement from casing pressure and vibration signals- a review. Proceedings of the 8th IFToMM International Conf. in rotordynamics Sept 2010 KIST Seoul, Korea
9. Kearton W.J. Steam turbine theory and practice. Pitman, London 1999.
10. Matthew P. Castanier Modeling and analysis of mistuned bladed disk vibration status and emerging directions. Journal of Propulsion and power Vol 22 No 2 March-April 2006.
11. RADIOSS Theory and Manual, "Large displacement finite element analysis" January 2009

List of Figures

Figure 1.1	Schematic of turbine rotor, blades and bearings	3
Figure 2.1	Velocity diagram for reaction stage	13
Figure 2.2	Cross sections of long blades	13
Figure 2.3	Blade aerofoil section	14
Figure 2.4	Blade angle settings	14
Figure 2.5	Prismatic bar representation of turbine blade	15
Figure 2.6	Overlapped blade cross section and direction of blade modes	16
Figure 2.7	Coupled blade modes	16
Figure 2.8	Wheel mode in the 6 th nodal diameter	16
Figure 2.9	Nodal and wheel Modes.	17
Figure 2.10	Illustration of Campbell diagram	18
Figure 2.11	Vectorial representation of centrifugal force on the blades	18
Figure 2.12	Water fall spectrum showing critical speeds at 22 Hz and 43 Hz excited by speed component in turbine	19
Figure 2.13	Graph showing damage versus cycles	21
Figure 2.14	Illustration of Strain gage method for measuring blade vibration	24
Figure 2.15	Illustration of blade tip timing measurement	26
Figure 2.16	Illustration of Laser for blade tip vibration measurement	27
Figure 2.17	Typical Laser Doppler Vibrometer arrangement	28
Figure 2.18	Illustration of using Acoustic sensor inside the casing	29
Figure 2.19	Schematic of torsional vibration measurement of turbine shaft and the blades	31
Figure 2.20	Schematic of Radar probe used for blade vibration	32

Figure 2.21	Schematic of microwave method for blade vibration	33
Figure 2.22	Schematic of Radionuclide's method for blade vibration	35
Figure 2.23	Schematic of optical method for blade vibration	37
Figure 3.1	Response and phase angle during to forced excitation	43
Figure 3.2	Schematic of turbine casing and position of accelerometer on the casing	44
Figure 3.3	Wide band frequency response of the casing	44
Figure 3.4	Individual spectra of BPF at 2400 Hz.	45
Figure 3.5	Schematic of experimental setup	46
Figure 3.6	Spectrum of pressure signal (a) BPF & RPM (b) BPF, RPM & blade natural frequency	47
Figure 3.7	Illustration of pressure wave inside a turbine & effect of blade vibration	49
Figure 3.8	Amplitude reduction with increase in phase shift due to blade vibration.	50
Figure 3.9	Reduction in the amplitude at BPF due to increasing vibration of the blades.	50
Figure 4.1	BPF peak of the last four stages measured from the casing of LP turbine	55
Figure 4.2	Trend of Generated Power and Current of 990 MW turbine	56
Figure 4.3	Waterfall spectrum of showing BPF of 9 th stage at 1450 Hz.	56
Figure 4.4	Waterfall spectrum of showing BPF of 8 th stage at 2400 Hz.	57
Figure 4.5	Waterfall spectrum of casing vibration showing blade natural frequency at 78 Hz	60
Figure 4.6	Cross section of exhaust side of the LP casing	60
Figure 4.7	Results of CFD study carried out by M/s Hitachi	61
Figure 5.1	Trend of turbine load, condenser vacuum and speed	65
Figure 5.2	Waterfall frequency spectrum showing BPF of last stage LP blades	66
Figure 5.3	Waterfall spectrum showing blade natural frequency at 107 Hz	67
Figure 5.4	1 st Mode (Umbrella) and frequency (107.7098 Hz) of the last stage	68
Figure 6.1	Typical cross section of axial flow compressor	72

Figure 6.2	Waterfall spectrum of casing vibration response	73
Figure 6.3	Water fall spectrum of casing vibraion response during load drop	74
Figure 6.4	Amplitude trend of BPF of row R3	75
Figure 6.5	Frequency Response Function of row R3 blade	76
Figure 6.6	Cross section of the failed blade with beach marks	77
Figure 7.1	Model of the blade and the surrounding fluid	84
Figure 7.2	Steam inlet angle on the blade.	85
Figure 7.3	Flow of steam across the blade	86
Figure 7.4	Increase in blade vibration due to large steam inlet angle	86

List of Tables

Table 3.1	Amplitude of BPF and Blade Natural frequency in the setup.	48
Table 4.1	List of BPFs and number of blades in the last 6 stages of LP turbine	53
Table 5.1	First mode frequency of the last stage bladed dish	69
Table 6.1	List of natural frequencies of the blades in 4 rows of the spare rotor	76

Chapter 1

Introduction

Steam turbine based power plants constitute more than 85% of the total installed capacity in the world. Presently the largest steam turbine has reached installed capacity of over 1300-1500 MW and with the current development in design and materials this figure for single unit of turbine could rise still higher in the near future [1]. Modern turbines for power applications generally have a high level of reliability primarily because of rigid inspection regime backed up by ingenious methods of detecting impending failures. Together, they ensure that almost all failures are detected at the incipient stage and affected components removed from service before failure actually occurs. This has indeed led to low rate of actual failure during service. The component most commonly rejected in the screening process is the blades. In spite of applying stringent criteria of acceptance, blades do fail during operation. Survey indicates that in over 40% of cases the exact reason for blade failure is not fully understood [2].

The blades are the most critical component in the turbine. Enormous amount of work has been carried out in its design, selection of material, fabrication, profiling, surface treatment, tuning and in optimizing its position within the steam path to achieve the best

possible efficiency [3]. Today the best blade design and manufacturing technology is available with big companies in advanced countries of Europe, UK, USA, Russia and Japan only. In rest of the places generally the blades are made available under agreement with respective power generating companies. This shows how involved are the technologies of forging and manufacturing of turbine blades. Countries with limited infrastructure and manufacturing base, the challenges of designing and manufacturing turbine blades is still in infant stage. In view of large number of blade failures in power plants leading to huge economic loss, power companies are investing in expanding the limited expertise in diagnosing the cause of blade failure and industries as a whole have become sensitive to certain operating process parameters detrimental to the health of the blades identified over years of operating experience.

In the beginning of the nuclear power age, nuclear power plants (NPP) were seen only as base load source of electricity. The main reason was that the operating NPP at rated power was more efficient and simpler. Also, when nuclear power was introduced, its share in the countries energy mixes was very small and so the flexibility in operation were typically limited to safety needs (e.g. safe shutdowns in case off load rejection) and for frequency regulation. Since that time, the situation in several advanced countries has changed. The share of nuclear power in the national electricity mix have become so important that the utilities had to implement or improve the maneuvering ability of their NPPs, to be able to adapt the electricity supply to daily or seasonal variations of power demand. This typically demands plants to be operating in load following mode.

1.1 Vulnerability of Long Blades to Vibrate

In developing countries where grids are weak and where enforcing discipline among power producers is difficult, the plants have to operate over wide range of speeds. Weak grids

lead to frequent interruption to turbine operation. Turbine blades in low pressure (LP) turbine are most affected during interruption or during part load operation. Typically in 540 MW plant, the LP turbine have 6 stages of blades mounted on the discs. Of these, the blades in the last three stages generally are free standing which are more susceptible to vibration. Blades in each of the three stages have different natural frequencies. Figure 1.1 illustrates a schematic of a turbine rotor and the blades.

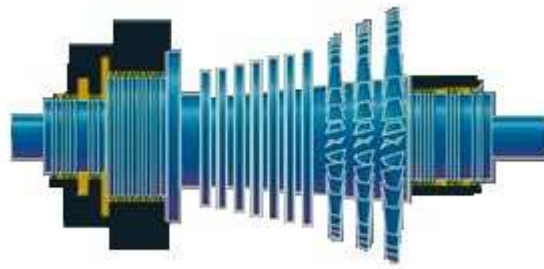


Figure 1.1 Schematic of turbine rotor, blades and bearings

During each startup and shut down of the plant, these blades undergo forced vibration excited by the speed component and its harmonics. Besides, whenever the plant operates at low load and low condenser vacuum (common in many power plants) blade tend to vibrate almost always. The combination of these high and low cycle fatigue loading on the blades lead to premature blade failure. In the developing countries the turbines are made to run beyond the original manufacturer's recommended running hours to meet the demand for uninterrupted supply. Under these circumstances, it is most important to have a built-in system to monitor blade vibration and assess it health on online mode. Blade and shaft vibration monitoring systems are common in all the power plants. In fact, standard turbo-supervisory systems have matured to an extent that the diagnosis has become a routine activity. Good level of expertise is available on the shop floor. However, diagnosis for rotating turbine blade is not common primarily because the technology is not readily available

and whatever it is available it is not easy to implement and is not economical. In the recent time, the power industry has realized the need to look for a reliable technology in view of the importance of monitoring health of operating blades. In the last decade, there are many concerted effort initiated between industry and research organization to evolve a reliable and affordable method of monitoring blade vibration. The aim is surely to minimize the cost and achieve simplicity to a level comparable with shaft and bearing vibration monitoring system.

Dynamic loads which generate blade vibration can arise from different sources. Rotor imbalances, steam pressure distributions due to non-concentric casings, irregularities in the stators located up and downstream of the rotor stage, rotating stall causing asynchronous vibration, unfavorable interaction between blades and flow and self-excited vibrations related to blade and rotor natural frequencies are some of the known sources [4]. The intensity and relevance of these sources are unique to different configuration of machines. The ensuing amplitude and frequency of these vibrations have a deep impact on fatigue life, performance and integrity of the machine. The accurate estimation of blade vibration characteristics according to rotational frequency is a crucial issue for the design of new design. It is important to realize that failure of even one blade out of hundreds of rotating blades in a turbine has a potential to cause grievous damage on many healthy blades and also to the machine. In view of the serious consequence of blade failure, it is most important and highly desirable to monitor the blade vibration that can help to infer the overall health of the operating blade.

In an online mode, it is not possible to directly monitor blade vibration. However, during Campbell analysis of blades on test rigs, strain gages are directly mounted on the blades and strain data is acquired through slip rings. For obvious reasons this method cannot be implemented on all the blades of working turbine in a power plant. Blade vibration

measurement by contact method is therefore not ideal and at the most can be used only during the validation stage of the blade design.

The other known methods are based on non-contacting type that use probes located around the narrow passage between the tip of the blades and the casing to measure the arrival times of individual blades. From the arrival time data, the blade vibration parameter is estimated through complicated formulations [5]. However blade tip timing methods suffer various drawbacks in particular on account of large number of probes needed to measure all blades simultaneously. Currently no single method exists for the complete measurement of the dynamic properties of blade vibrations in an operational turbine [5]. Additionally the complexity involved in implementing the known non-contacting method outweigh the need for explicit measurement of blade vibration.

The rotating turbine blades develop both spatially and temporally varying pressure forces acting on the casing. The internal pressure so developed presents an interesting loading condition on the casing. Vibration response of the casing which primarily is due to dynamic excitation by the working fluid, carry enormous amount of information about the turbine rotor, the blades and the steam path as a whole. The aim of the work presented in this thesis is to lay robust foundation for a simple and easily scheme for blade vibration measurement, which can be readily used to deduce the condition of blades inside any turbine in operation. It is proposed that this could ideally be achieved through the measurement of external casing vibrations thus eliminating the need for sensors to be placed inside the flow path. The method offers the desired advantage of the ease with which the sensors could be mounted on existing operating turbines in power plants. The measured casing vibration is recorded for further analysis involving correlation with process parameters, FFT for studying the content of the signal and for generating the 3D waterfall spectra for assessing the variation of different

frequencies in the signal with time and speed. Such an analysis can give the cause and effect relationship manifesting in the turbine casing.

1.2 Objective and Scope

Based on the extensive review of the literature on available methods of blade vibration the following objectives are set for the present investigation

1. To develop a reliable, versatile and non-intrusive blade vibration monitoring technique based on known mechanistic behavior of the long blades under hostile steam environment.
2. To extend the present methodology for detecting blade vibration in operating power plant and validate the Campbell diagram supplied by the designer.
3. Validate the robustness of the method by detecting blade vibration under part load operation, a condition known to excite the blades to vibrate during operation.
4. Verify the applicability of the methodology for detecting vibration of stiff blades in a compressors of a gas turbine
5. To propose a robust technique for in-situ detection of turbine blade vibration in all types of power plants.

These objectives constitute the core theme of the present thesis, in which we develop a model of a blade and simulate a condition conducive for blade vibration due to self excitation.

1.3 Organization of the Thesis

This thesis is organized in 8 chapters. Chapter 1 gives a brief introduction and objective of this study. A comprehensive review of the literature related design and working

of long blades is presented in Chapter 2. Different methods developed for blade vibration measurement and the science behind each method are also presented here. The working principle behind each method is discussed with illustrations for better understanding. As can be seen in the chapter, except for the strain gage method, the rest of the methods are intrusive by design which needs extensive arrangement to install, analyze and maintain the system.

Chapter 3 discusses an experimental model built to represent a rotating single stage turbine, means to excite the blades during rotation, sensor to pick up blade related frequencies and device to acquire and analyze the dynamic signal. This is followed by detailed analysis of the signal to investigate the relationship between rotating blade signals and the characteristic natural frequency of the blade. It is demonstrated that the amplitude at blade passing frequency (BPF) of a stage in the turbine, which is a readily measureable parameter from the casing of any turbine, is unique to a stage and can be connected to vibration of the blades. Based on the results, an important non intrusive method of detecting blade vibration in operating turbine is proposed.

In chapter 4, the extension of this proposed method to the actual application on a low pressure turbine of a 900 MW Nuclear power plant is described. The long blades of low pressure turbine are susceptible to vibration for several known and unknown sources of excitation in an operating turbine. In the particular case, blades were vibrating due to turbulence caused by steam extraction. The acquired signals of all the stages were analyzed and the amplitudes at BPFs were investigated. It was demonstrated that when blades vibrate due to steam induced turbulence, the amplitude at BPF modulate.

The testing of the application of the proposed method on low pressure turbine of 220 MW nuclear plant to detect simulated low load and low vacuum condition in the condenser is presented in chapter 5. It was demonstrated that the blades indeed vibrate under low load

operation and the proposed method is capable of detecting blade vibration. The results were compared with the published blade vibration characteristics.

It was further demonstrated in chapter 6 that the proposed method is also applicable for detecting vibration of short blades of compressor blades in a 250 MW gas power plant.

In chapter 7, a description of a model of actual blade and the surrounding fluid, (in this case steam) to simulate the condition of self excitation is presented. The blade is modeled in Lagrangian coordinates and the surrounding steam in Eulerian coordinates. Using a standard commercial Fluid Structure Interaction program, the master coordinates of the blade and the slave coordinates of the steam are coupled in the interface to simulate condition for self excitation. It was demonstrated that the amplitude of the blade increases due to self excitation. The important conclusions drawn from the present investigation together with contribution of the thesis work and future study are discussed in chapter 8.

Chapter 2

Literature Review

Extensive studies have been presented till date which addresses the urgent need for evolving an easy method for detecting blade vibration in an operating turbine. This chapter presents review of the literature related to methods evolved by several industries, researchers and institutions. It is always a challenge to monitor the health of rotating components housed in a pressurized casing like the turbine blades. Numerous cantilever like blades behave individually at the time of failure and as a group during healthy condition. This review is organized in four sections. Challenges faced in detecting turbine blade vibration in operating plants. The past investigation method still followed during design stages of the blades as a bench mark exercises. In the sequel, the intrusive methods available as commercial package and employed as trial approach in operating plants. This is followed by more recent proposal of non intrusive methods with limited validation. The chapter also covers review of essential characteristics of long turbine blades needed better understanding of applicability of proposed method and ends with conclusive closure with an emphasis on need for a robust detection method.

2.1 Challenges of Detecting Turbine Blade Vibration

By design, the rotating turbine blades are housed in casing(s) making direct measurement not feasible on a routine basis. Each stage in a turbine consists of several blades. The last stage blades in a low pressure turbine work in a hostile steam environment. Categorizing of all the forcing functions operating on the blades that lead to vibration and eventual failure is still an area of intense research. Despite the difficulties, because of the enormous advantages, many researchers and manufacturers have invested huge efforts in developing techniques for detecting blade vibration. Primary source of blade excitation have been broadly put under four categories [2][6].

- Harmonic excitation
- Non synchronous but discrete frequency excitation
- Random or broad band excitation
- Self excitation

Each of these sources either exist individually or in combination. They have the potential to induce vibration in the blade to an extent that it may lead to failure and subsequent damage to the plant. The long blades vibrate in different modes depending on its design and source of excitation. Individual blades could vibrate if it is severely mistuned or damaged due to local corrosion or due to presence of high concentration stress in the blade material. Generally such deviations are eliminated by thorough inspection. In spite of such care during inspection, several reported failure indicate as initiated by single blade failure. As fatigue in the blades are largely addressed by sources of high or low cycle excitations, all the blades of a stage together are set into vibration. Out of many vibrating blades in a stage, the stray blades could fail due to reasons mentioned above. Except for the strain gage method, all other methods target for detecting single blade vibration which does not indicate the condition of other

blades in the stage. The time between detecting and failure could be too short. Hence, it is important to detect global blade vibrations.

2.2 Design Feature of Long Turbine Blades

Steam turbine blades convert the heat energy in the steam to useful shaft work. In that respect it is important to understand how the turbine is designed, how the loads are determined that closely match actual loads during operation. This chapter aims to cover all aspects of long blades that help to make the objective of this study comprehensively clear.

One of the characteristic properties of large steam turbines is the long length of the last stage blades which are susceptible vibration. The low pressure turbine blades are designed to extract the final remnants of energy from the passing steam flow. The limit of the turbine output is thus decided by the length of the last stage blades (LSB). Remarkable improvement has been made in designing the long blades for improvement of efficiency and reliability over the last ten decades. Major part of the evolution has concentrated on behavior of individual blades. The key improvements have been in involving advanced analytical techniques for assessing the behavior of the entire bladed disk. Advancement in modal analysis and testing, fatigue analysis, creep analysis, fracture mechanics, fluid dynamic analysis and development of many new materials and manufacturing processes have accelerated design of powerful and reliable blades.

The blades in working turbine not only rotate due to change of steam flow direction but also due to the additional steam speed up within the blade channels that cause reactive forces. Hence the long turbine is named reaction type. In long blades, the degree of reaction varies with in the stage and along the height of the blade because of the centrifugal force. The degree of reaction is high in the upper section than in the root section. Raising the length of the blades is limited by the centrifugal stresses in the blades. The decreased rotational speed

makes it possible to use much longer blades. Steam pressure in the reaction turbine falls and undergoes expansion in each row of the blades. When the steam pressure is reduced outlet velocity increases at a much greater rate than the specific volume and an equilibrium point is reached when the equation of continuity is satisfied. To accommodate the gradual increase in the specific volume the heights of the blades in each stage is progressively increased.

Long LP blades are made of common types of stainless steel. The exact type of steel chosen for a particular LP application depends on the strength and corrosion resistance. Since the 1960s, titanium alloys, especially Ti-6Al-4V, have also been used for LP turbine stages. When the steam condenses on the blade surface, corrosion pits and dimples are formed. These are particularly harmful to the blade because they serve as stress concentrators.

2.2.1 Velocity Diagram

Velocity diagram [7] is fundamental for improving the overall efficiency of the turbine stage. Steam inlet and exit velocity triangles depict the differences between impulse and reaction blade and vectorially indicate the loads acting the turbine blade. It helps to explain the steam flow in to the blade during full load and part load operation. A reaction turbine is constructed of rows of fixed and rows of moving blades. The fixed blades act as nozzles. The moving blades move as a result of the impulse of steam received (caused by change in momentum) and also as a result of expansion and acceleration of the steam relative to them. In other words, they also act as nozzles. The moving blades of a reaction turbine are easily distinguishable from those of an impulse turbine by the non-symmetrical geometry and because they partly act as nozzles, have a shape similar to that of the fixed blades, although curved in the opposite direction. Figure 2.1 shows a typical velocity diagram for the reaction stage.

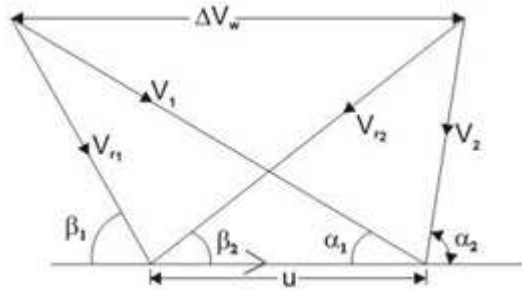


Figure 2.1 Velocity diagram for reaction stage

Blade efficiency is given as

$$\eta_b = \frac{\dot{m} U \Delta V_w}{\dot{m} \frac{V_1^2}{2}} \quad (2.1)$$

by putting $\rho = U/V_1$, the maximum attainable blade efficiency can be shown to be

$$(\eta_b)_{\max} = \cos^2 \alpha_1 \quad (2.2)$$

In designing the form of the blade, its length is divided into equal number of sections.

In view of the negative reaction at part load on the long blades towards the exhaust end of the turbine, certain degree of reaction is given at the lower section of the blade.

Typical blade profile at the root, middle and tip section of long section of the long LP blade is shown in Figure 2.2.

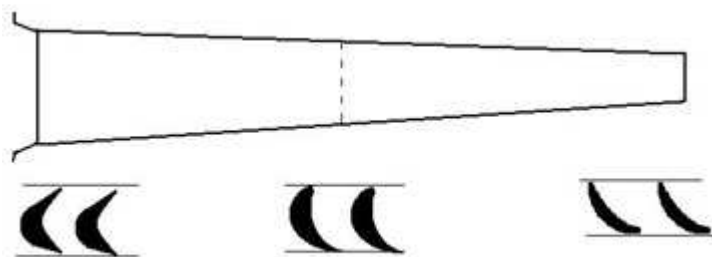


Figure 2.2 Cross sections of long blades

For best efficiencies, the degree of rotation is more at the root of the blade and then increase towards the tip. The taper and twist to the blade is given to the blade to resist inertia and blade bending forces during rotation. The blade is modified to compensate for the large variation in the inlet flow angle in the radial direction, by varying the angle of twist in the

cross section of the blade. Longer blades increase the steam flow capacity, the taper help in limiting the stresses in the blade due to centrifugal forces acting during rotation and twist help achieve constant specific steam flow lengthwise along the radius.

The form of the reaction blade is defined by its centre line called camber line. The camber line may be either circular arc or a parabolic arc as shown in Figure 2.3

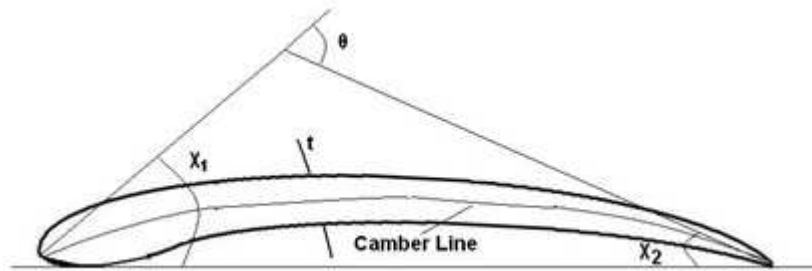


Figure 2.3 Blade aerofoil section

Typical setting of the blade is shown in Figure 2.4.

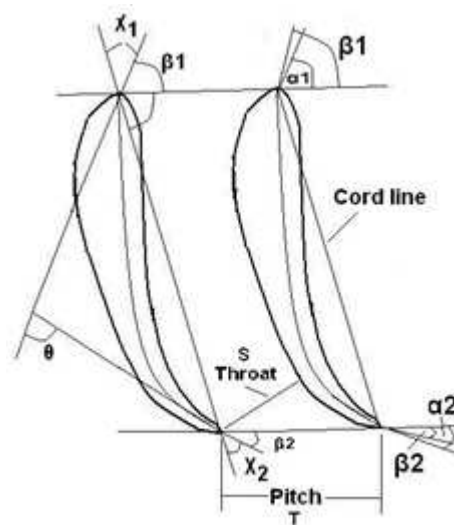


Figure 2.4 Blade angle settings

α_1 is the direction of flow into the blade. If α_1 is greater than β_1 , the incidence is said to be negative. The channel through the flow is gradually convergent and leads to a throat of width S (opening)

The throat to pitch ratio (S/T) is an aerodynamic design parameter that corresponds to the outlet flow angle of the blade. If S/T ratio is increased, the speed of axial flow component

increases and vice versa. In long blades, the pressure difference between the root section and tip section is large because of the tangential velocity component produced by the turbine nozzle blades. The S/T ratio for the blade is decided based on the pressure difference.

2.2.2 Blades Node and Wheel Modes

Dynamic behavior, meaning the frequency and the associated mode shapes are important in defining vibration of turbine blades or stage as a whole. This section aims to cover nodal diameter modes and wheel modes in long blades that help in understanding why a particular mode is excited and what design changes may be made to control blade vibrations. When a single blade is clamped at the root, at the lowest natural frequency, the mode of vibration will be similar to the prismatic bar as shown in Figure 2.5.

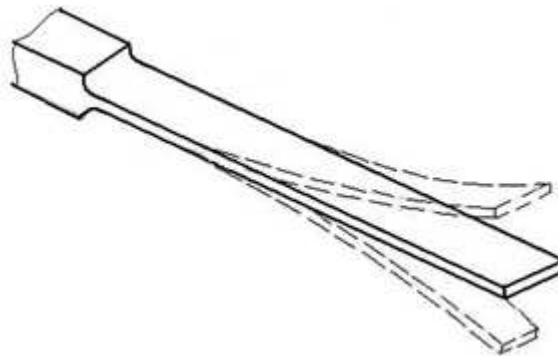


Figure 2.5 Prismatic bar representation of turbine blade

In the lowest mode the blade vibrates in the flap mode as shown in Figure 2.5. Figure 2.6 illustrates the direction of the three lower modes. The blades in a group oscillate in phase approximating in the same manner as though they were not joined. This is true for flap wise, edge wise and torsional modes. Figure 2.7 illustrates four modes of blades joined together. Figure 2.8 shows wheel mode with 6th nodal diameter

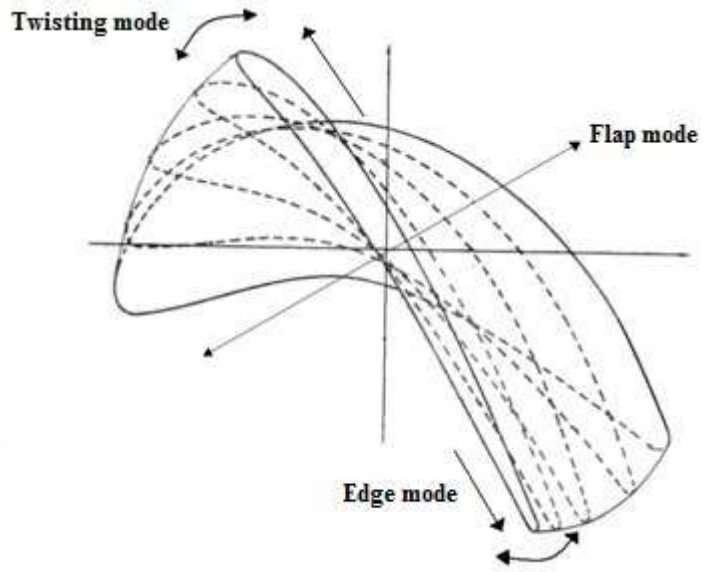


Figure 2.6 Overlapped blade cross section and direction of blade modes

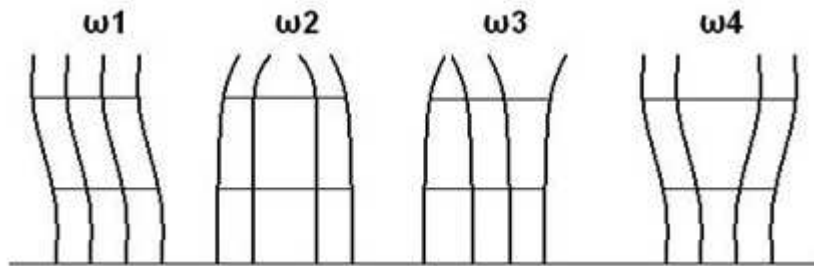


Figure 2.7 Coupled blade modes

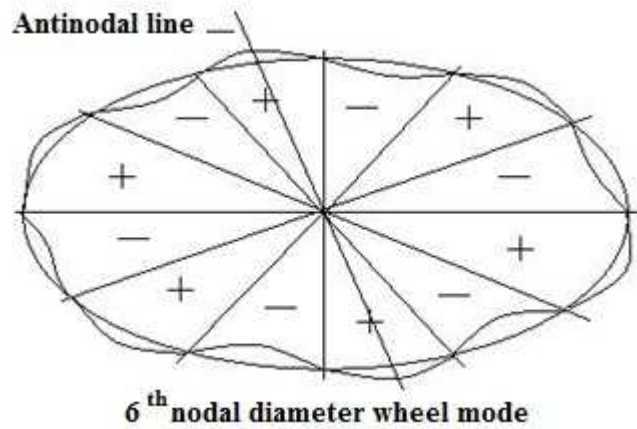


Figure 2.8 Wheel mode in the 6th nodal diameter

The wheel and the nodal modes are shown in Figure 2.9

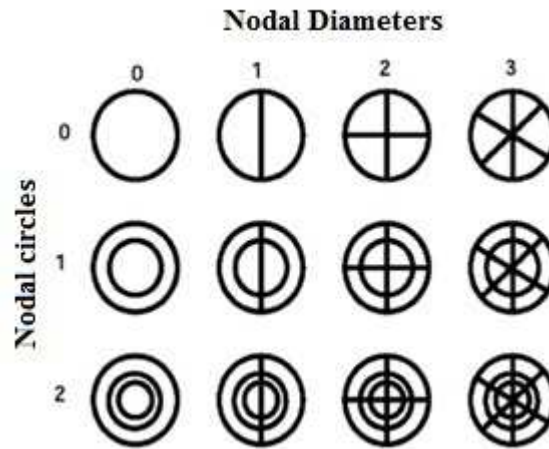


Figure 2.9 Nodal and wheel Modes.

2.2.3 Effect of Rotation on Blade Frequency

The centrifugal stress for most part is steady in nature and can be estimated accurately. It is almost never a principle cause of blade failure but may become important for numerous startup and shutdown cycles. Centrifugal forces stiffen the roots thus influencing the natural frequency of the blade. This effect can be seen on a Campbell diagram as shown in Figure 2.10

The curved trend of the first mode illustrates the stiffening effect due to centrifugal force during rotation at different speeds [8]. The rays coming from the origin of the ordinates presents the variation of disturbing forces with the rotational speed and its multiples. The intersection of these rays with the strip of the blades natural frequencies results in resonance of the blade at that speed. The steady centrifugal stresses in the last-row LP blades are typically $0.5\sigma_y$ for about 50% of the blade length, and greater than or equal to $0.25\sigma_y$ for 80% of that length, where σ_y is the yield stress of the material [3]. Figure 2.11 shows sketch of vectorial representation of centrifugal force on the blades.

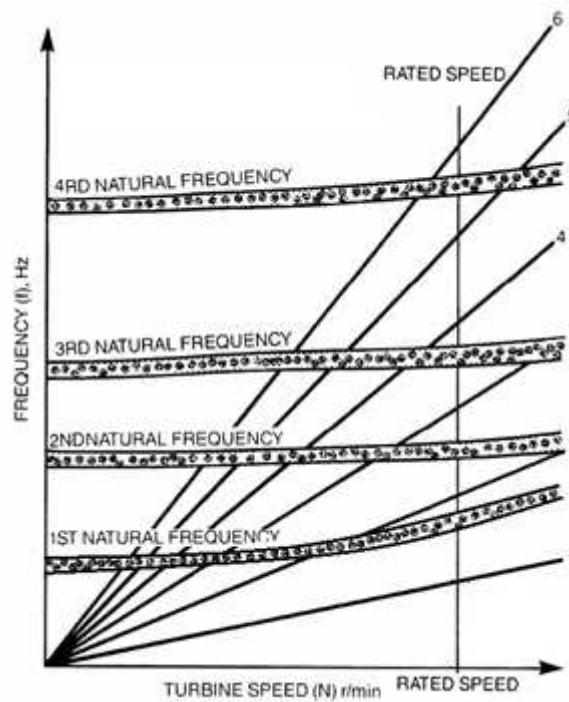


Figure 2.10 Illustration of Campbell diagram

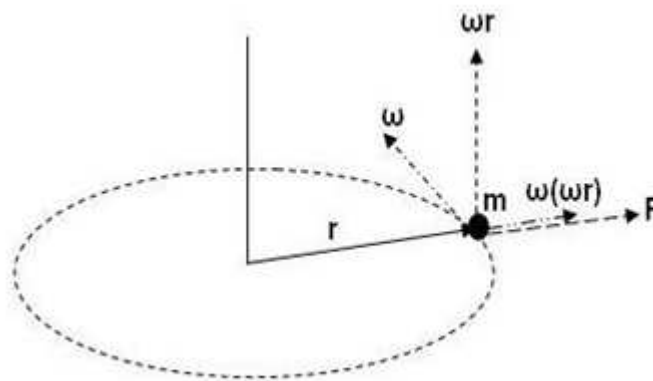


Figure 2.11 Vectorial representation of centrifugal force on the blades

Figure 2.12 shows waterfall spectra generated by taking FFT of the time domain signal of casing vibration during startup of 220 MWe Nuclear turbine. Vibration signals are measured with general purpose accelerometer and the time signal is analysed in the frequency domain using standard FFT analyzer. The several spectra are then plotted in waterfall mode to visualize change in frequency content with time. The progress of speed component can be seen from 10 to 50 Hz when the turbine was synchronized to the grid. On the way to rated

speed, the speed component excites different natural frequencies of the machine. As can be seen in the figure, the speed component excites the critical speeds of the LP turbine rotor at 20 and 42 Hz. The increase in the amplitude at these frequencies happens due to crossing of the first engine order with the natural frequency of the rotor. In a similar way when the engine order crosses the trace of natural frequencies of different modes of the blade, the blade resonates with higher amplitude.

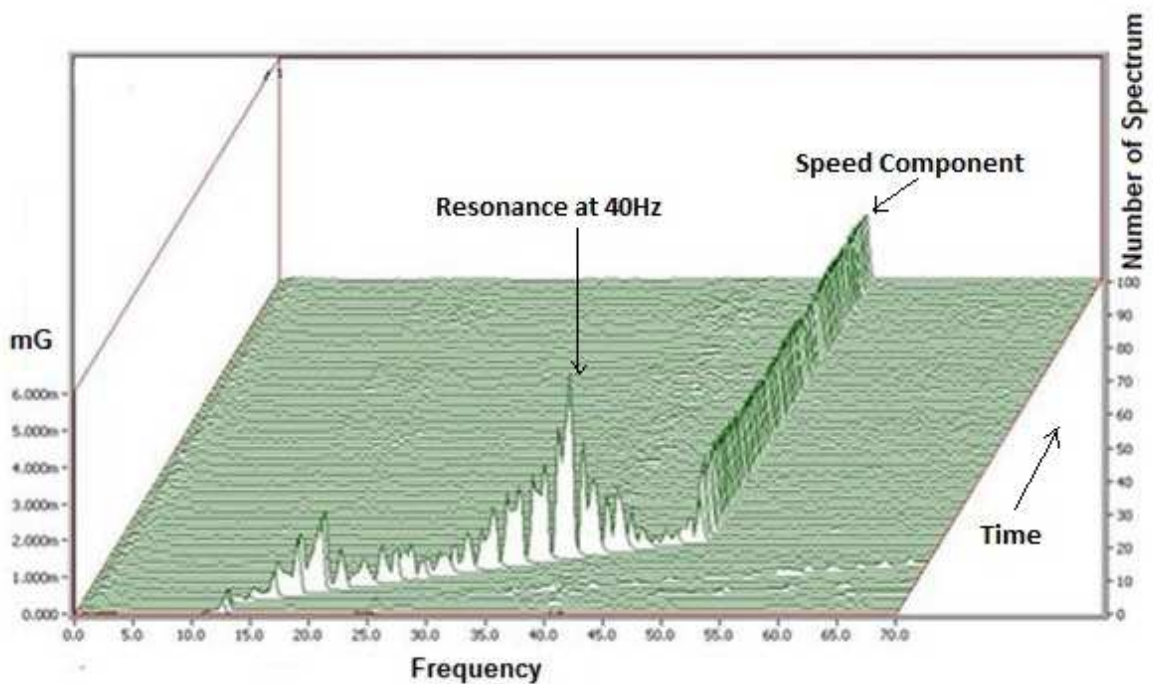


Figure 2.12 Water fall spectrum showing critical speeds at 22 Hz and 43 Hz excited by speed component in turbine

2.2.4 Stress in the Blades

The fundamental parameter in blade design is ratio between its length and width called aspect ratio. The vibratory stresses in a blade of blade group are roughly proportional to the square of aspect ratio multiplies by function related to its thickness and camber.

$$\sigma_{\text{vib}} = [\text{Length/Width}]^2 f \{ \text{camber, maximum thickness} \} \quad (2.3)$$

When the length of the blade is increased, its width also increases to control the vibratory stresses in the blade.

The tensile centrifugal stress in the blade section at the distance z from the root section is given by,

$$\sigma = N(z) / F(z), \quad (2.4)$$

where $F(z)$ is the current cross section area, and $N(z)$ is the centrifugal force in section z . For long blades, in order to decrease the maximum centrifugal stress, the blades are tapered with decreasing $F(z)$ towards their tip.

As the steam flows through the turbine blades, the steam pushes the blades causing them to bend. Like centrifugal bending, steam bending causes the blades to be bent lengthwise, creating regions of tensile and compressive stress in the blade. Although the movement of the steam does induce blade bending, the effect of steam bending in moving blades is not as pronounced as the effects of centrifugal forces. In fact, steam-bending stresses are typically only about 10% of the centrifugal stresses [4].

2.2.5 Fatigue in the Blades

Fatigue in a blade is caused by repeated cycling of the load on the blade. Both low and high cycle fatigue load applied on operating blade play important role in initiating, propagating the defects in the blade before final failure. Typically, most steam turbine rotor fractures are caused by low cycle fatigue (LCF) [8]. The high strains caused by LCF typically occurs during the cold start turbine operation. Due to high strain rates implicit in LCF, it is typically accompanied by plastic deformation. LCF occurs after relatively low number of cycles (typically <10000 cycles) of high stress amplitude. LCF happens only occasionally in the life of the actual machine. For example, the average design life of a steam turbine is about 30 years. Assuming the frequency of cold start is three times per year, the total number of cold starts will be 90 times in 30 years. Sandeep Kumar [9] proposed a damage model for low

cycle fatigue damage in a steam turbine developed using a continuum mechanics approach integrated with the finite element model.

Figure 2.13 shows that damage D varies quickly at the last stages of the whole cycling and slowly at the middle stage from 10% to 80% of the total cycles, which is a characteristic of LCF damage. High strain leads to faster failure of the material.

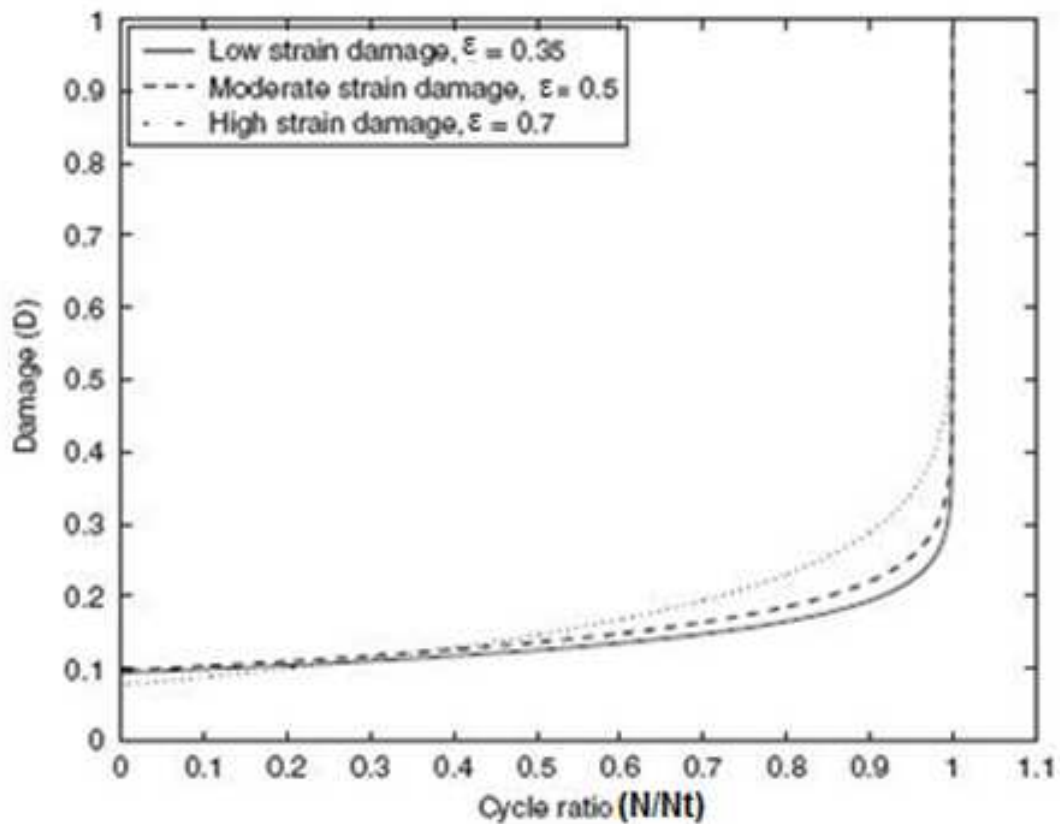


Figure 2.13 Graph showing damage versus cycles [9]

2.2.6 Sources of Blade Vibrations

This is truly a complicated topic involving fluid structure interaction which is not fully comprehended. There are still many complicated phenomenon yet to be unraveled. EPRI research project RP 912 in its report has brought several considerations in design mainly of

LP turbine blades for stochastic excitations as listed below [2].

- Non uniform steam pressure, velocities or angle of flow into the rotating blades/row cause harmonic excitation related to the rotational speeds. The non uniformity is caused by mismatch in the assembly of stationary blades, mismatch of diaphragm vanes at the horizontal split etc.
- Disturbances caused to the blades by the nozzle passing are one of the most studied sources of discrete frequency excitation. These forces arise mainly because the trailing edges of the nozzle vanes have finite thickness, and because the steam is discharged towards the moving blade after passing over several geometrical variations.
- Random excitation is caused by flow unsteadiness in the stationary flow passages. These are primarily due to acoustic resonance in the inlet passage and extraction line, unsteady flow separation from stationary blades, pressure fluctuations due to impingement of turbulent flow into rotating blades and flow unsteadiness in the rotating blades themselves.
- Stall flutter occurs in the last row of LP turbines at low load and high back pressures when the blades experience a negative angle of attack at least over the upper portion of their length. An important feature of flutter is that the resulting vibration is non integral and therefore the frequency-speed characteristics is not influenced by the engine order line as shown in Campbell diagram. Self excitation does not need external excitation frequency; instead, the frequency is internally generated. When the blade is perturbed from equilibrium, it will vibrate back to equilibrium at its natural frequency. If this vibration modulates the flow in such a way that the resulting dynamic forces act to sustain the vibration, then the blade is vibrating in self excited manner. The vibration is maintained right at the natural frequency. Such a vibration due to flutter is well recognized cause for fatigue in the blade. Some blades have the

tendency to flutter more than the others and the process is not linearly related to the load [4].

- Sudden changes in the steam extraction flow between the stages, negative angle of steam flow into the blade significantly change the operating condition of the blades resulting in stall flutter in the last stage blades.

2.3 Different Methods of Blade Vibration Measurements

Blade vibration monitoring is required and is very important to ensure that excessive vibration that could compromise the integrity of machine does not occur. Understandably, large differences exist between vibration techniques used during development stage of the blades and those implemented for online measurement. In-service blade vibration measurement is not just to know if the blades are excessively deflecting but is required to validate the dynamic characteristics of the blades in different stages at different speeds and to detect changes in the blade characteristics. There are reports on measurement of blade vibration due to resonance measured by bearing mounted accelerometers in an operating plant [10]. This method however depends on the transmissibility of blade vibrations through the bearings. Besides, this method can be used during coast up or coast down of turbine to excite the blades in resonance. Known tools like Campbell diagram and direct measurement by strain gage based technique are used. That does not mean that the known tools are easy to implement (during development stage). Implementation needs extra ordinary preparation just to verify and validate the measurement. This section discusses different methods of measuring blade vibration along with the merits and demerits in each of the cases accounting for the ease of implementation.

2.3.1 Strain Gage Method

Strain gage method is a time tested method and the only one technique that can be used directly on the blades to capture the modes and stresses due to vibration during operation. The type of strain gage to be used, locations on the blades, wiring and remote transmission of strain data are well mastered technique. Strain gage method is the only method which can capture all the modes of blade vibration under all working condition and is in fact a benchmark exercise to validate all other non-contacting methods.

Strain gauge methods involve attachment of several strain gauges on various critical blade areas with the associated instrumentation connected to the rotor itself. Figure 2.14 shows typical arrangement of using strain gauges on the rotating blades.

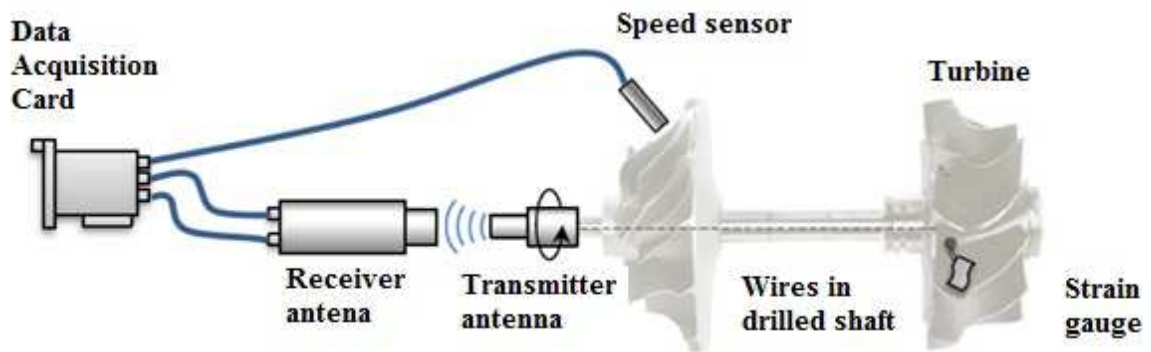


Figure 2.14 Illustration of Strain gage method for measuring blade vibration [11]

Strain gages are mounted on the blades and the signal cables are shown routed through the shaft and connected to a transmitting antenna. The measured strain signals are transmitted to a receiver for onward data acquisition and analysis along with a independent speed signal. The method is well established and is field-proven systems for obtaining information related to the alternating strains arising in certain critical areas of the blade. However, its implementation has several practical problems. The gages have limited life; connecting wires and associated instrumentation are prone to damages due to exposure to severe steam

environment [5]. The major problem, however, is related to the need to transmit the signals. Slip ring or telemetry systems are usually employed, but they are often contaminated by noise. Strain gauge based measurements are therefore part of a test method that can produce extremely valuable information on certain parts of the blades, but are statistically unreliable due to the irregularity of the blade tolerances.

2.3.2 Blade Tip Timing Measurement

Taking the advantage of developed non contacting techniques of measuring motions, many researchers have worked on capturing blade information by measuring the tip of the blade during operation. Advanced front end sensors and fast data acquisition systems backed with robust signal analysis technique has enabled researchers to try several approaches.

Currently large numbers of popular methods based on non-contact measurement of blade vibrations employ use of number of proximity probes located around the periphery of inner casing for measuring the blade tip time. In view of inherent difficulties in implementing direct measurement of blade vibration by strain gage and slip ring technique, non-contact blade vibration measurement has been sought.

Figure 2.15 shows peripherally positioned proximity sensors and cabling routed to measuring electronics. Despite increasing ability of this method, there still exist several constrains and limitations such as the requirement of a large number of sensors for each turbine stage, difficulties in dealing with multiple excitation frequencies, sensors being located in the flow path, and the inability to directly measure the frequency and mode of the blade[13][14].

Electromagnetic probes, capacitive and inductive based probes are some of the front end sensors. In order that maximum probe sensitivity is realized in the measurement, it is necessary to mount the detector in close proximity to the blade tip. When the gap becomes

large, required to avoid fouling with the blades, it results in reduced sensitivity and reduced signal to noise ratio in the data. This is a serious limitation in arriving at accurate arrival time of blade tips. Asynchronous vibrations, such as rotating stall, compressor surge and blade flutter, which usually occurs at a blade natural frequency, are not as easily analyzed from proximity probe measurements.

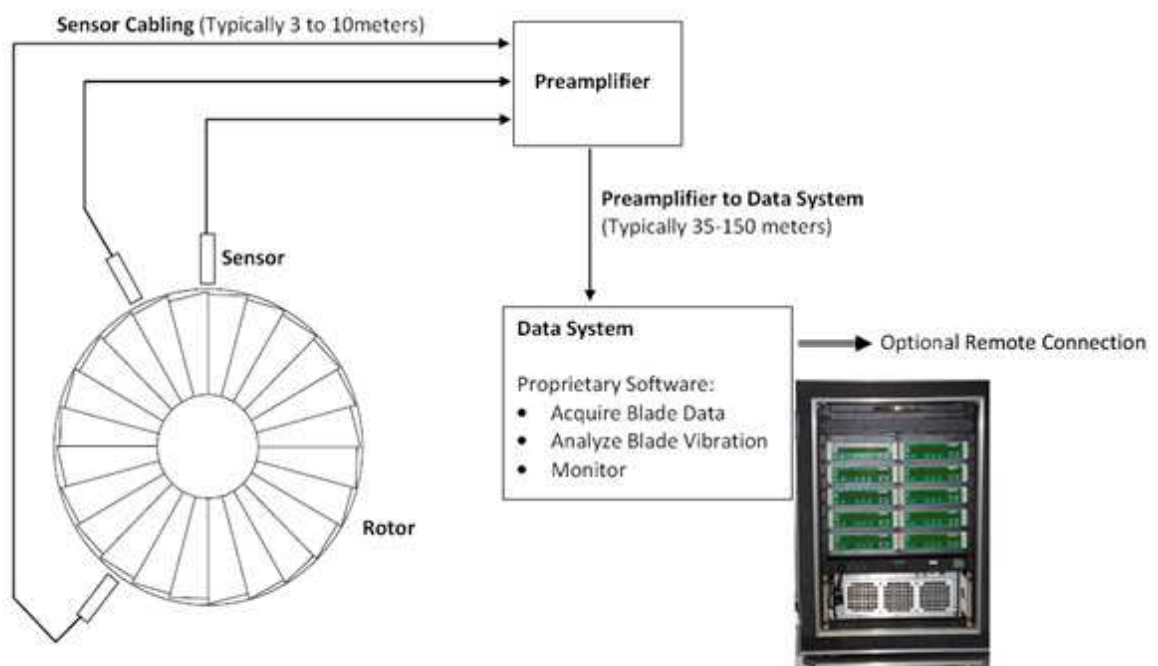


Figure 2.15 Illustration of blade tip timing measurement [12].

2.3.3 Laser Doppler Anemometry Method

The coherent wave structure of laser is indeed a big advantage is using them for measurement of velocity of vibrating body. The laser light can be used to measure both lateral and normal velocity of a body in motion. In fact this technique has been developed into a commercial product. With proper selection of location for installation of laser probes between the rotating and stationary rows, it is possible to measure blade vibration at any location along the length of the blade.

Figure 2.16 shows the Laser striking the leading and trailing edge of a blade. When the laser light is directed on the vibrating surface, the reflected light adds a Doppler shift to the frequency of the scattered light proportional to velocity of the surface [15].

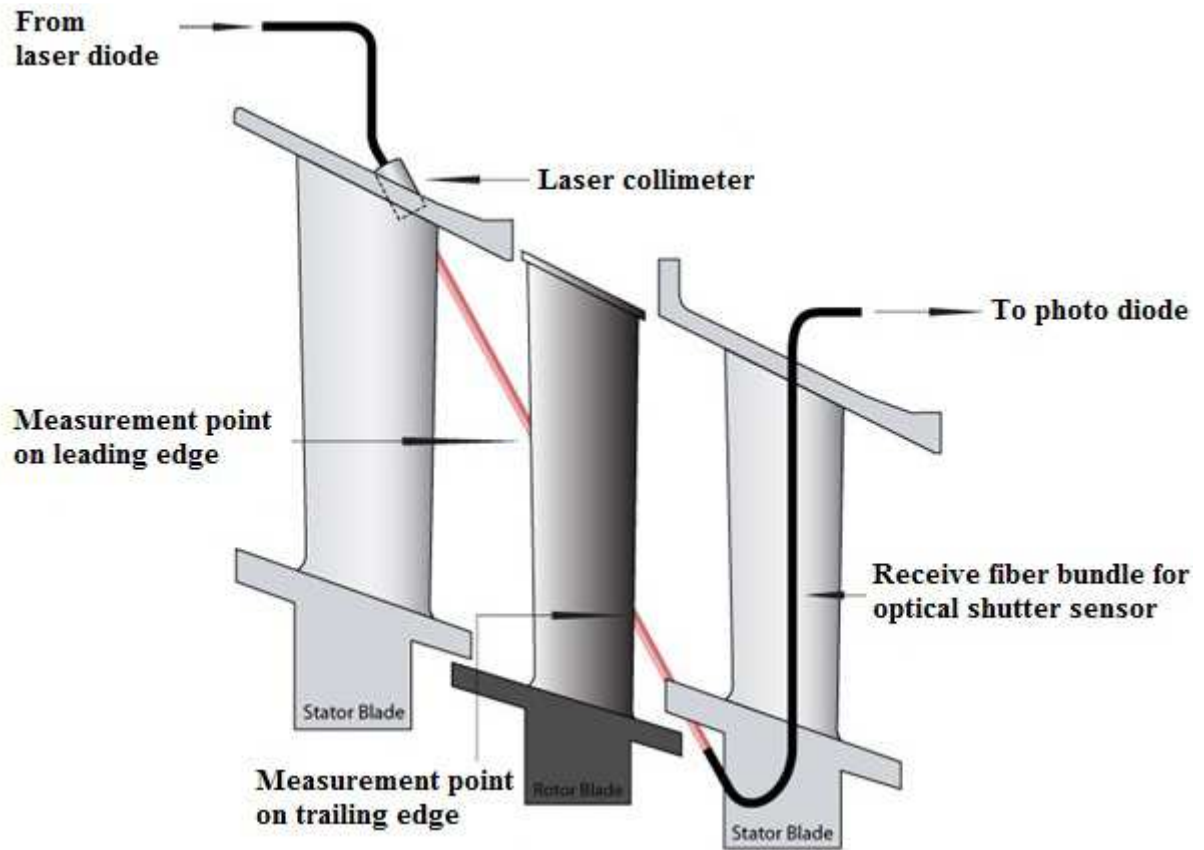


Figure 2.16 Illustration of Laser for blade tip vibration measurement [12]

The scattered light is detected by a photomultiplier tube, an instrument that generates a current proportional to absorbed photon energy, and then amplifies that current. The difference between the incident and scattered light frequencies is called the Doppler shift.

The Doppler shift f_D , depends on the speed V of the blade, direction of motion, the wavelength of the light λ , and the orientation of the observer. Figure 2.17 shows schematic of LDA. Then,

$$f_D = 2V/\lambda \tag{2.5}$$

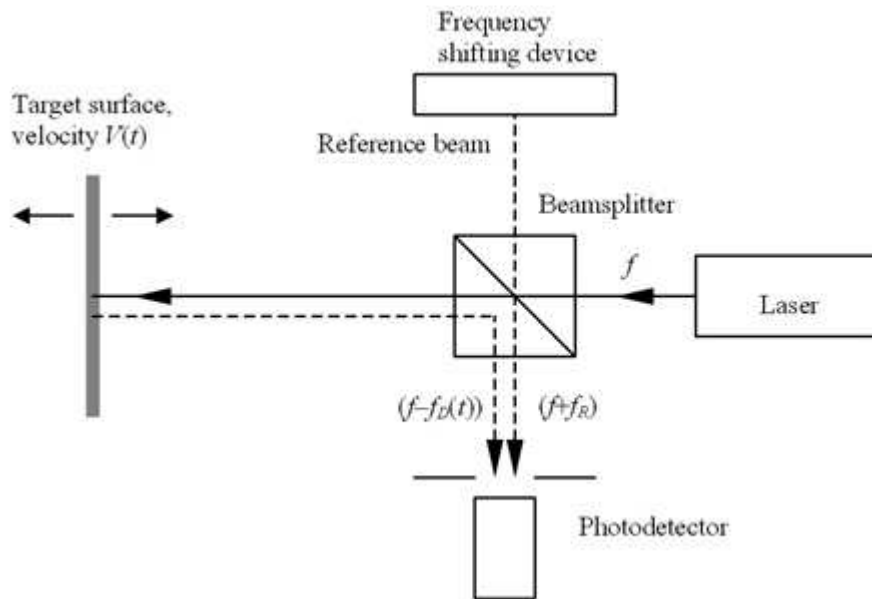


Figure 2.17 Typical Laser Doppler Vibrometer arrangement

2.3.4 Acoustic Doppler Method

Interior of any turbine is filled with rich acoustic information of which many are deterministic but low in strength. Well tuned acoustic sensor plus processing tools have high potential to decipher every signal received from rotating and other non rotating components in any turbine [16]. Small sized acoustic sensors that can with stand harsh steam environment inside the casing what makes this technique suitable for the purpose.

Non-interfering acoustic sensor fixed to the casing downstream of the blade row detects the sound radiated by the vibrating blades as shown in Figure 2.18. It involves analysis of the characteristic Doppler waveform sensed by a nearby stationary acoustic sensor. The Doppler waveform is the result of the single frequency acoustic energy radiated by the blades and the changing position and velocity of the blades relative to the sensor. The method comprises sensing the total acoustic energy at a fixed location and to generate a composite electrical signal. The radiated energy is detected by the stationary sensor and if the

energy radiating blade is simultaneously rotating such that it has a velocity component along a line joining the moving blade and the fixed sensor then the frequency of the energy radiated from the blade as detected by the sensor will be altered from the frequency actually radiated from the blade This concept is known as moving source Doppler.

The new frequency as detected by the sensor is given by the following formula,

$$f^1 = \frac{f(V + w)}{(V + w - v)} \tag{2.6}$$

where,

f^1 is the frequency of the vibrating blade

f is the frequency detected by the sensor

v is the instantaneous velocity of the blade toward the fixed sensor along a line joining the blade and the sensor

w is the average velocity of the surrounding operational fluid moving toward the fixed sensor along a line joining the blade and the sensor and

V is the velocity of sound in the operating fluid

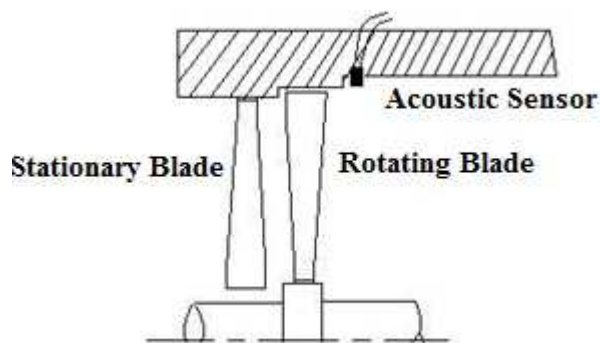


Figure 2.18 Illustration of using an acoustic sensor inside the casing

Signal manipulations are then performed upon the composite signal in both the time domain and the frequency domain to remove the undesirable noise generated in order to reveal the characteristic Doppler waveform. The analysis involves synchronous averaging out the non order related background noise followed by editing or blanking out the few order related components known to be contaminated with background error such as blade passing frequency and once per revolution and twice per revolution frequencies. The resulting signal is then displayed to reveal the characteristic Doppler waveform of the blade vibrations. An envelope detection technique is employed to accurately pick out the amplitude peak indicative of the location of the resonant blade.

2.3.5 Torsion Vibration Technique

A new direct approach of detecting the blade vibration through torsional vibration measurement of the rotor shaft was proposed by Maynard and Trethewey [17]. On research level they have demonstrated the feasibility of detecting changes in the blade natural frequency by measuring torsional vibration of the shaft. An incremental demodulator and angular domain converter is used for conditioning the measured signal. The signal level associated with the torsional vibration of the shaft is very low. To ensure clean capture of torsional vibration, signal of large dynamic range and high signal to noise is required. To meet these requirements, the torsional signal are order sampled followed by frequency sampling. For effective measurement of blade natural frequency, the prerequisite is that the blade natural frequency must have strong coupling with the torsional vibration of the shaft. Meaning, only those blade natural frequencies which are coupled with the torsional vibration of the shaft can be detected. Implementation of this method needs stationary rotor for installing the system and trouble shooting. For measurement on the shaft the infrared fiber optic probes are directed on the shaft to sense the zebra stripes as shown in Figure 2.19.

However, torsional vibration measurement techniques are many and are still in the development stage from both the aspects of pick-ups and data processing tools. The piezoelectric materials have been used as sensors for a long time in vastly different areas and the corresponding technologies have been well-developed. The survey paper by Sunar and Rao [18] has reported on various applications of piezoelectric materials. This involves firmly embedding piezoelectric sensor at the root of the blade and taking voltage signal from the transmitter which transmits the signal to the stationary receiver. The method is more suited for laboratory setup rather than its use in operating turbine.

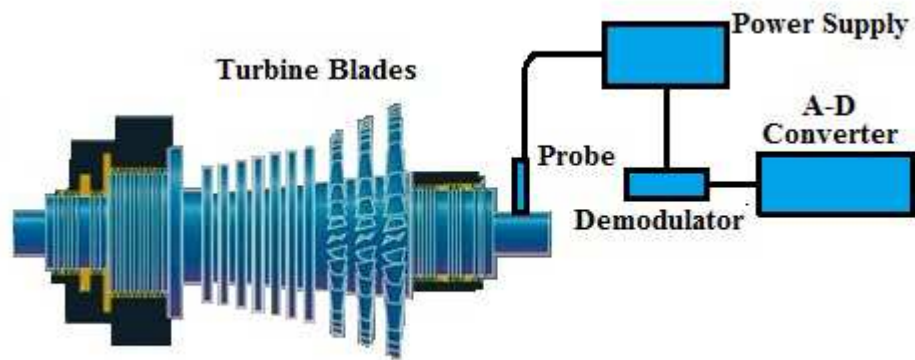


Figure 2.19 Schematic of torsional vibration measurement of turbine shaft and the blades

2.3.6 Narrow Beam Radar Signal Method

Radar is yet another remote technique that can be configured along with a reference signal of rotor rotation to determine which particular blade is vibrating [19]. The turbine blade detection system includes radar sensors operable to transmit a relatively narrow beam radar signal toward the rotating turbine blades of one or more blade rows as shown in Figure 2.20. The reflected radar signals from the blades are utilized to derive respective output signals indicative of relative blade movement toward and or away from the respective radar sensors.

In order to determine which particular blade is vibrating, the signal is coupled to reference signal giving each complete rotation or partial rotation of the turbine shaft. The processed reference signal provides respective running counts indicative of the number of turbine blades which have traversed a reference position to thereby specifically identify the particular blades.

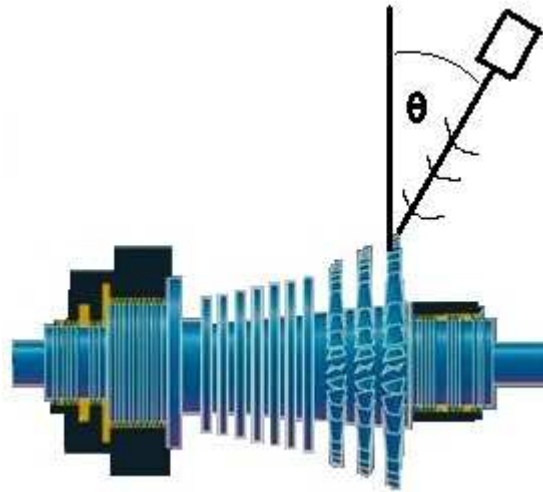


Figure 2.20 Schematic of Radar probe used for blade vibration

Gating method is used for selectively gating the radar output signal and the running counts. Signal processing enables arrival of the output signals at predetermined times. It provides an indication if the analyzed signal exceeds predetermined limits. For better estimation, the analyzed signal from each respective blade is averaged over a predetermined number of rotations of the turbine shaft

2.3.7 Microwave Method

Microwave method provides a relatively simple reliable and inexpensive blade vibration monitoring technique that operates at gigahertz frequency range that provides ultra high bandwidth [20]. In this method a microwave transceiver is located within a junction box on a guide tube kept external to the turbine.

Continuous wave is transmitted through a waveguide toward the rotating row of blades as shown in Figure 2.21. A reflected wave is produced when a blade tip is adjacent to the aperture of the waveguide. Each passage of an individual blade tip through the path of the continuous wave produces a signal indicative of the time at which each passage occurs. The reflected wave interacts with the transmitted wave to produce a standing wave inside the waveguide. The signal is monitored to detect any disturbance in the standing wave resulting from the passage of the blade tip past the aperture. Such disturbances are detected by measuring the current drawn by the transmitter, the voltage drop across a resistor carrying the transmitter current or any other means for measuring the change in Q of the microwave cavity or tube.

Alternatively the wave reflected by the blade tips as they pass the waveguide aperture is detected. This is done with a microwave detector connected to a hybrid power divider arranged to divert the reflected power to the detector. The ensuing voltage versus time waveform generally has more peaks. Each peak corresponds in time of passage of a blade tip through the path of the continuous wave. The time intervals between peaks are analyzed to yield the desired vibration information.

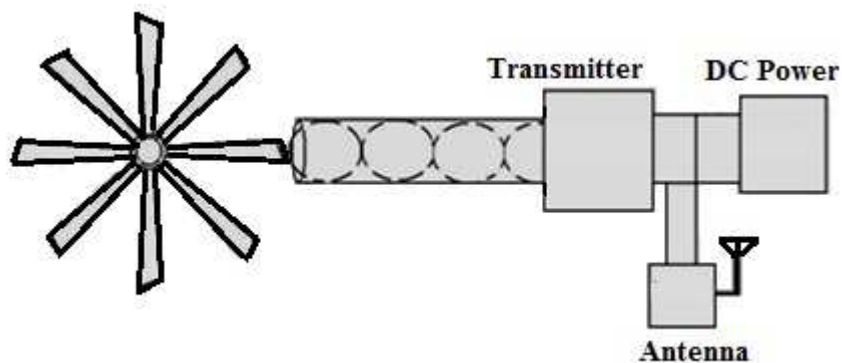


Figure 2.21 Schematic of microwave method for blade vibration

For example for a 3000 RPM machine the time required for a blade to complete one revolution is 0.02 s. For a unit with 100 blades per row the time between blade passing is $0.02 \text{ s} \times 100 \text{ blades per row} = 2.0 \times 10^{-4} \text{ sec}$ between blade passing. An eddy current sensor with a 1.6 MHz search frequency produces $(2.0 \times 10^{-4} \text{ s} \times 1.6 \text{ MHz}) = 320$ sensor cycles between blade passing. In contrast with a microwave frequency of 1 GHz there are $(2.0 \times 10^{-4} \text{ s} \times 10^9 \text{ sec}) = 2.0 \times 10^4$ cycles between blade passing. A zero crossing board clock of 24 MHz will produce $(2.0 \times 10^{-4} \text{ sec} \times 24 \times 10^6 \text{ sec}) = 4800$ clock pulses between blade passings. Blade vibration causes the measured clock counts to vary about 4800 which variation is measured to detect blade vibration

This method does not require the sensor to be positioned above the blade tip. The problem of placing the sensor in the small space above the blade tip is avoided. The system is immune to residual magnetism and does not require shielding.

2.3.8 Radionuclide Method for Nonmagnetic Blades

The eddy currents methods depend on the ability of the sensor to induce eddy currents in the blade. However, in turbine which has blades made of non magnetic materials it is extremely difficult to induce eddy currents. Eddy current method cannot be effective on the blades whose materials losses their magnetic properties at the operating temperatures and pressures. Besides, on blades which are made of non magnetic material, eddy current technique cannot be used. For such blades, radioactive nuclide method has been developed and holds promise in detecting blade modes when radioactive nuclides embedded at the tip of the blade is emitted during rotation [21]. A radioactive sensor is positioned on a fixed location with respect to the rotating portion of the turbine. One of the turbine blades together with the sensor is shown in detail in Figure 2.22. The tip of the blade carries radioactive nuclides which are produced as a result of Surface Layer Activation (SLA). SLA is achieved through

the use of an accelerator ion beam to generate the radioactive nuclides. It is known that SLA has no effect on the mechanical properties of the material to which it is applied. The characteristic gamma rays that are emitted from the induced radioactive nuclides are strong enough to be detected but do not present health hazard for personnel. The sensor is positioned within a shield and is mounted in a fixed location with respect to the rotating blades. The shield has a portion shaped to act as a collimator.

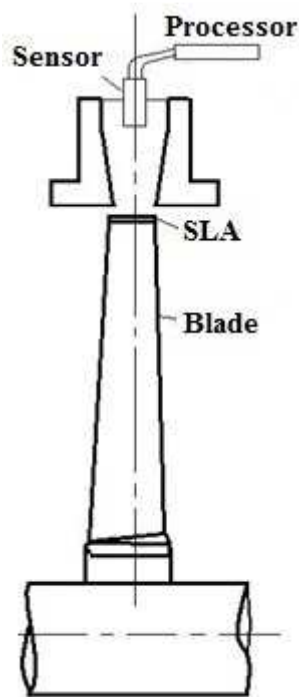


Figure 2.22 Schematic of Radionuclide's method for blade vibration

As the blade carrying the radioactive nuclides moves past the sensor, the gamma radiation by the sensor increases until a peak value is reached when the blade is directly under the sensor. Thereafter the gamma radiation reduces as the blade moves away from the sensor. The radiation sensed by sensor begins to increase again when the next blade having radioactive nuclides begins approach the sensor. The signal is responsive to the movement of the radioactive nuclides past the sensor such that sensor produces an input signal which

representative of blade is passing events. A processor extracts vibration information from the input signal. A blade is selected for monitoring purposes by designating its degree location relative to a reference position some angular distance constituting a small window. As the selected blade passes a sensor its output signal properly conditioned to form a pulse is gated during the time period corresponding to the window. The sequential pulses of the sensors form a pulse train which is modulated by any blade vibration. An FM detector is provided for demodulating the pulse train to derive vibration information.

2.3.9 Optical Method

Optical system consists of a transmitter for emitting a light beam on to the moving blade and a receiver for receiving the light beam reflected by the moving blade [12]. A light beam is directed onto the moving blade and being reflected from the latter at an angle of reflection greater than 45 degree and directed to a receiver as shown in Figure 2.23. The blade vibration is calculated from the signal thus received.

A light beam formed by a laser beam is directed by the transmitter into the flow passage and onto a moving blade. The moving blade has a shroud band for reflecting light toward the transmitter. From the reflecting surface the light beam is directed as reflected light beam to the receiver. The transmitter and the receiver are separated from one another in such a way that an angle greater than 90 degree is obtained between the incident light beam and the reflected light beam. On the reflecting surface the light beam illuminates a part area which is less than 1 mm². Due to the separate arrangement of transmitter and receiver it is possible to take a reflection measurement even in the flow passage filled with flow of steam.

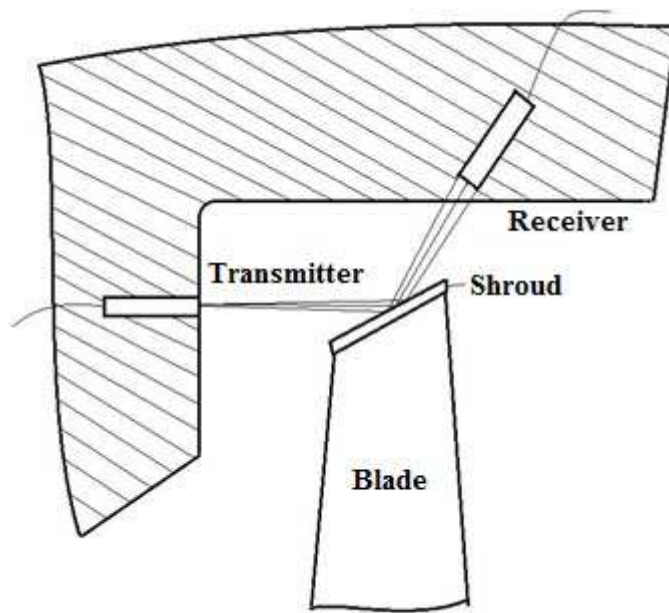


Figure 2.23 Schematic of optical method for blade vibration.

2.3.10 Casing Internal Pressure Measurement

For gas turbines, internal gas pressure acting on the casing wall is used for detecting deterioration of blade faults [22]. Every blade is surrounded by typical gas pressure profile. Detection of change in the pressure profile in the form of distortion in the periodic pressure trace is used to monitor the blade condition. The detection method mainly relies on extraction of features in the pressure signal caused by the seeded fault in the blade through experimental and numerical simulation of pressure signal.

Blade vibration is measured by the demodulation of the measured pressure signal such that an estimate of the blade vibration amplitude can be made. Demodulation of pressure signal is not straight forward as the measured signals are found not conducive for conventional demodulation. It requires novel way of demodulation. It has been shown with some initial experimental verification that the stochastic portion of the internal pressure signal contains set of harmonics of the shaft speed plus and minus the blade natural frequency which

can be a measure of blade natural frequency. Though the initial results are encouraging, lot of work need to done before it can be used for in-service measurement of blade vibration.

The patent filed by Edward suggests monitoring back pressure in a turbine to assess the feasibility of blade vibrations. The patent is about a method of limiting blade vibration by closely monitoring back pressure at each stage of the long blades in low pressure turbine [23].

2.3.11 Casing Vibration

The approach of indirect measurements has been known for a long time [1]. Accelerometers at the casing of a compressor near the blade tips was first investigated by Mathioudakis et al [24] to measure the blade vibrations. The collected vibration signals are rich in frequency contents. This method has shown a great deal of uncertainties when blade vibrations are to be monitored in presence of all working fluid in the machine and associated instabilities in the acoustical and housing/foundation problems. Working on gas turbines, Mathioudakis tried to reconstruct gas pressure through inverse filtering the casing vibration. The reconstructed pressure signal was then used for detecting blade vibration by examining the change in the pressure profile in the form of distortion in the periodic trace of pressure signal.

Casing vibration is also used for detecting blade vibration when the engine speed is swept such that the blade is forced to vibrate in resonance [10]. On a simple test rig, blade vibration was detected at single speed from the stochastic component of casing vibration. Wavelet analysis is used for analyzing casing vibration along with the internal pressure signal and the emanating acoustic signal in order to measure blade vibration. The analysis technique showed difference between healthy blade and the blade seeded with fault in the experiments. During coast down of engine, wavelet analysis of casing vibration was used to detect loose blades. Generally, some level of mistuning exists in the natural frequency of the blades due to

difference in fitments and tolerances. These variables also contribute to the noise while carrying out wavelet analysis.

There are obvious advantages of using casing vibration for detecting natural frequency of turbine blade on an as-installed machine. Though it appears simple to analyze casing signals during steady state operation, the technique of connecting the signal of blade natural frequency excited by the off design operating condition in the engine is still in its infancy.

2.3.12 Closure

Each one of the blade vibration measurement techniques cited in this chapter has its own merit and demerit with regard to complexity, intrusiveness, difficulty in implementation and calibration. Even then, none of the methods gives the basic information about which blade mode is excited and what is the margin between excitation frequency and the blade natural frequency. The widely prevailing blade tip timing method with all the complexities gives vibration amplitude of individual blade tip. However, vibration of a single blade leads to vibration of the whole stage and with the time damaged blade fails due to fatigue. By this, it appears that when high vibration of blade tip is detected, there is very little time before failure. Till now there is no published report on advance information provided before failure.

Chapter 3

Development of a Methodology for Detecting Blade Vibration and its Experimental Verification

This chapter presents foundation of the method evolved for detecting blade vibration and is organized in two parts. Firstly we present an experimental method of detecting blade vibration in a rotating fan. The metallic fan with 9 blades is rotated by a variable speed motor. The fan in the experiment represents a turbine stage as the dynamics in both the cases are comparable. It is well documented that on long turbine blades, the steam not only moves axially from lower stages to last stage but also speeds up within the blade channels in the radial direction. These are termed as leakages from the tip of the blades especially in the unshrouded free standing blades. The steam issuing out from the tip of the blades strikes the casing with a certain intensity and frequency. The frequency of striking corresponds to the product of speed of rotation and number of blades called as blade passing frequency (BPF). This phenomenon is simulated in the experiment with the metallic fan. The leaked air issues out from the tip of the blades. A metallic ring around the blades represents the casing. On the ring, a microphone is mounted in such a way that it faces the tip of the blade to measure intensity and frequency of air pressure striking the ring.

In the latter half of this chapter, an analytical solution is presented to the phenomena observed in the experiment. It was demonstrated that when the rotating blades vibrate, the intensity of air pressure striking the ring reduces significantly as measured by the microphone.

3.1 Problem Definition

The aim of this study is to arrive at a robust proposal of detecting blade vibration non-intrusively. For any operating power plant a non-intrusive method of detecting blade vibration is most desirable from implementation point of view. Unlike for the bearings and shaft, the rotating turbine blades are not directly accessible for measuring its vibration. The proposed method relies on technique which does not need placing sensors in the steam/gas flow path inside the turbine. The blades rotating inside the casing are strongly coupled with the casing structure in the presence of the working fluid/gas in the turbine. The entire environment inside the casing is filled with general random noise due to steam/gas flow, deterministic steam/gas pressure pulsations corresponding to the rotor speed and pulsations caused by blade of different stages of the turbine. All these random and deterministic steam/gas excitations coexist in the volume of the casing identified respectively as white noise, 1X component (shaft speed) and BPFs of different stages assembled on the rotor. Each turbine stage generates its own unique frequency and amplitude of pressure pulsation. The turbine casing is subjected to excitation by each of these independently existing pressure pulsation signals and the casing responds with appropriate deflection depending on the impedance at each of the deterministic frequencies.

The rigid casing responds to internal pressure pulsations with amplitude proportional to the intensity of pulsations. Figure 3.1 shows typical response of rigid component having natural frequency ω_n excited by forcing function $\omega \lll \omega_n$. The Figure also shows plot of

phase between response and force function. It can be seen that when $\omega \ll \omega_n$, the ratio of amplitude of response to amplitude of forcing function is equal to one and the phase is equal to zero. That indicates that the rigid flanges of the casing transmit low frequency vibrations without any distortion.

The proposed method deals with analysis of the casing signal through separation of the dominant periodic components related to blade vibration contained in the stochastic portion of the casing response to the dynamic pressure field inside the casing.

Figure 3.2 shows schematic cross section of inside of a turbine and accelerometer mounted on the casing. The location of the accelerometer on the casing is chosen such that impedance of the location is conducive for picking up even low intensity signals without distortion. Since the range of measurement is large, in order to cover high and low frequency signals, the accelerometer is mounted with studs screwed on to the casing. Typical frequency spectrum of casing measured by accelerometer mounted on the casing is shown in Figure 3.3. The prominent hump around 30 KHz is the mounted natural frequency of the accelerometer. The Figure 3.3 indicates that the steam flow excitation inside the turbine is essentially wide banded extending beyond 50 KHz. In the low frequency region of the band, the discrete peaks correspond to blade passing frequencies (BPF) of different turbine stages. BPF is the product of speed and the number of blades in each stage. The enlarged view of the lower frequency region is shown in lower part of Figure 3.3. The four color bands in the lower zoomed spectrum shows the position of the four BPFs in the spectrum. If the number of blades in a stage is 96 and the shaft speed is 1500 rpm (25 Hz) then the BPF of the stage will be at 2400 Hz. Figure 3.4 shows two individual spectrums. The one in red color is during when no steam is flowing in the turbine and the spectrum in blue color is when the steam flow is established in the turbine operating at 300 MW. BPF peak appears when the steam flows on the blades. Hence the presence of BPF component in the signal is due to impingement of steam issuing

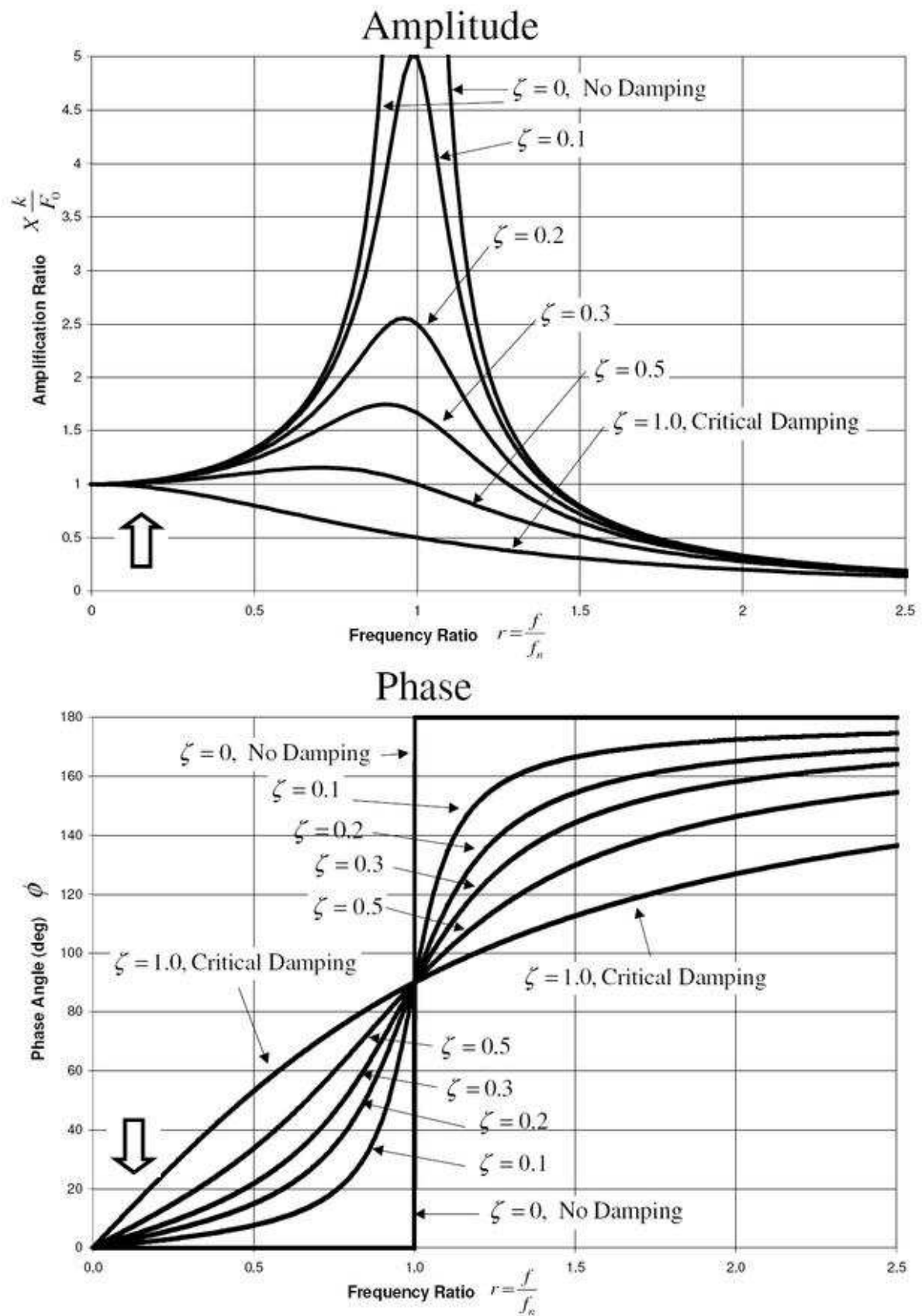


Figure 3.1 Response and phase angle during forced excitation

radially outward from the tips of the blades. The steam works on the blades and the leakage steam is thrown in the radial direction. The rigid casing responds to steam excitation at BPF.

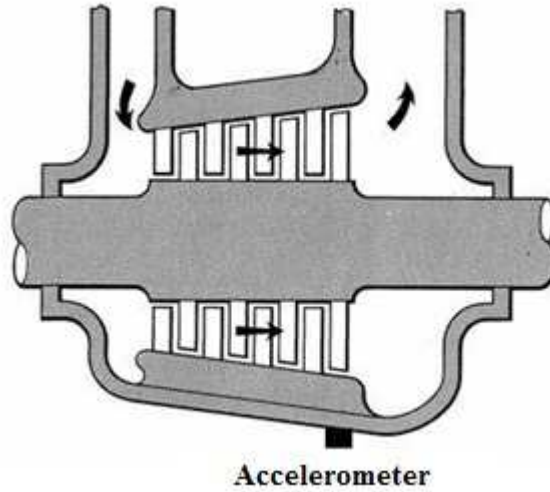


Figure 3.2 Schematic of turbine casing and position of accelerometer on the casing

The amplitude and the feature of the casing response at BPF depend on the condition of the tips of the blades of the stage.

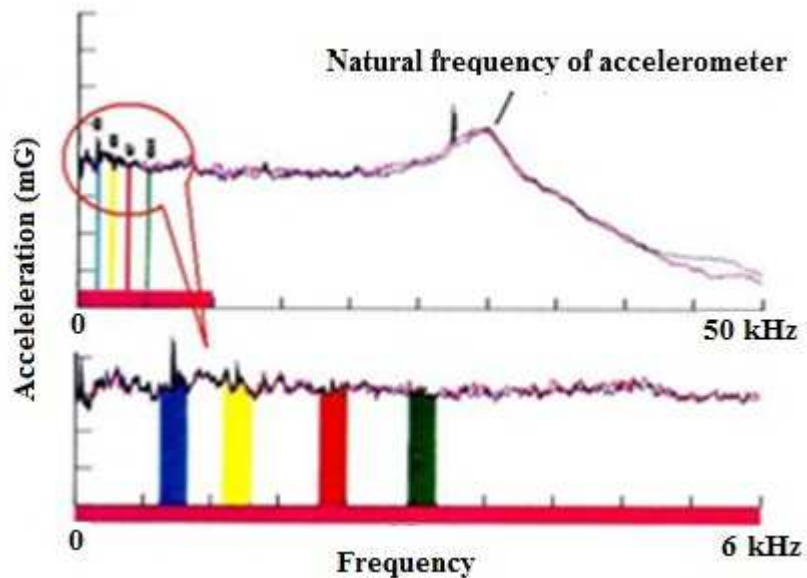


Figure 3.3 Wide band frequency response of the casing

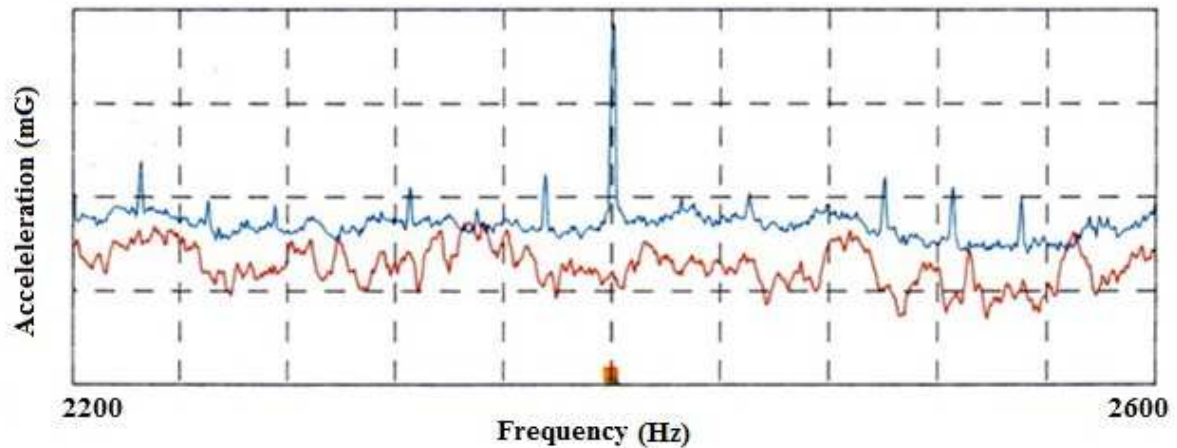


Figure 3.4 Individual spectra of BPF at 2400 Hz.

Every stage in a turbine generally has different number of blades. That makes BPF of each stage different and well separated in the frequency spectrum. As the presence of BPF in the signal is due to rotation of the blades in the turbine, all the attributes of the BPF namely the amplitude at BPF, the long term trend of the amplitude, modulation of its amplitude etc have to be directly related to the condition of the blade. Identifying the relationship between the character of BPF and the dynamics of turbine blades is the problem definition of the thesis. This is presented in the next Para.

3.2 Relationship between BPF and Blade Vibration

Laboratory experiment was carried out involving rotating fan and jet of air to excite the blades of the metallic fan. The fan in the setup simulates the rotating turbine, its blades as turbine blades and the air jet is meant to excite the blades of the fan to vibrate.

Figure 3.5 shows schematic of the experimental setup. The fan wheel is coupled to a variable speed motor for experiments at different speeds. With different fans consisting of different blades were tested at different speeds. The pressure in the air jet was varied to optimize excitation on the blades. In order to increase the amplitude of blade vibration at its

resonance, the air jet nozzle was connected to a shaker for vibrating at required frequencies. Such arrangement enables fixed frequency excitation over and above the white noise excitation imparted by the air jet. The jet of air simulates non-synchronous excitation on the blades similar to turbulent steam excitation on the rotating turbine blades inside the casing. A dynamic pressure transducer is mounted on a ring structure enveloping the fan and facing towards the tip of the blade. The transducer picks the air pressure pulsation due to rotation of the fan. As the ring structure was not rigid enough, accelerometer could not be used. However, the information in the dynamic pressure sensor in the experiment is similar to information in the accelerometer signal obtained from the turbine casing. As covered in



Figure 3.5 Schematic of experimental setup

chapter 2, the acceleration signal of the turbine casing is the result of excitation of the casing by pressure fluctuations in the steam/gas turbine.

Speed of the fan was chosen such that the BPF and natural frequency of the fan blade is not influenced by any other vibration in the setup. Before the test, natural frequency of flap

wise mode was identified by modal testing using impulse hammer. The fundamental modal frequency was at 182 Hz. Figure 3.6 (a) shows frequency spectrum of pressure signal. The Y axis is in pressure units. The peaks marked in the Figure correspond to speed of the fan and the BPF of the fan. The speed was 24.5 Hz and the BPF was at 220.625 Hz. Figure 3.6 (b) shows the same spectrum as in Figure 3.6 (a) except for increase in the amplitude at natural frequency of the blades at 181.250 Hz and decrease in the amplitude of BPF. The decrease is about 1.3 mPa. Increase in the amplitude of natural frequency was achieved by the air jet excitation. The pressure transducer is able to measure not only the BPF but also the signal corresponding to the blade vibration. The analysis shows that the amplitude of BPF decreases when the blades vibrate. This cause and effect relationship connects BPF and the natural frequency of the blade. The other frequency peaks in the spectra like 400 Hz and about 450 Hz are frequencies of the local acoustics generated due to air impingement during operation of the fan. Experiments were also carried out with cracked fan blades to analyse the

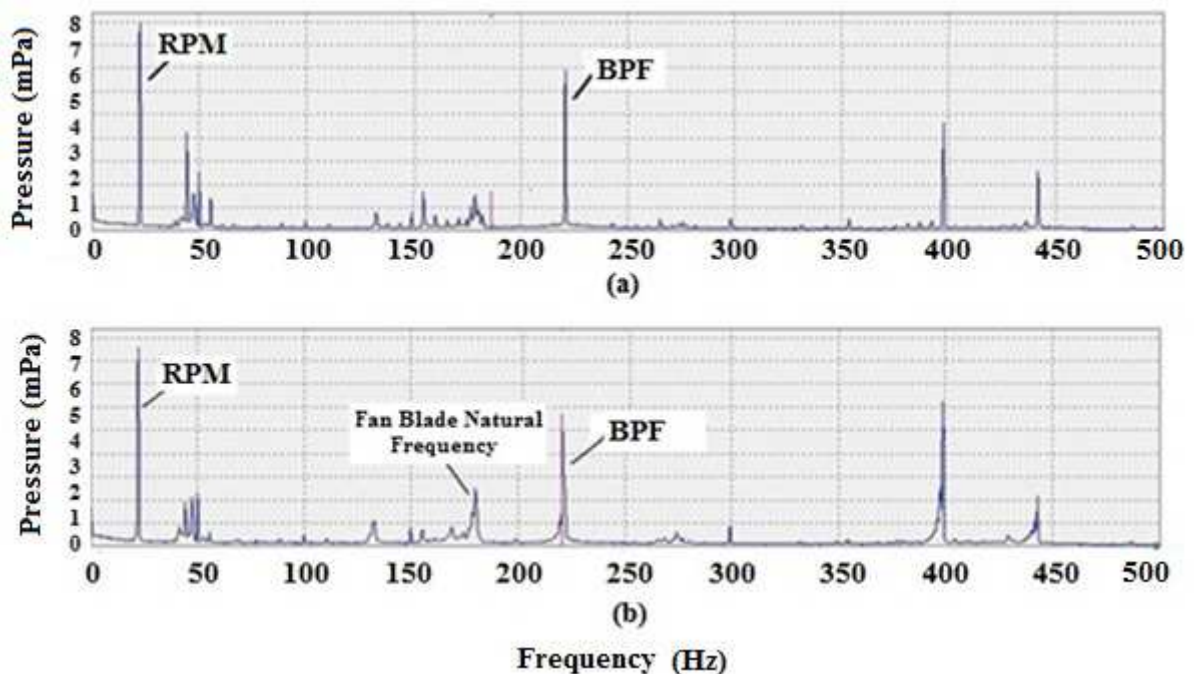


Figure 3.6 Spectrum of pressure signal (a) BPF & RPM (b) BPF, RPM & blade natural frequency

possibility of detecting cracked blades using the same technique Table 1 shows amplitude of BPF and the amplitude of the blade natural frequency.

Table 3.1 Amplitude of BPF and Blade Natural frequency in the setup

S.No	Amplitude of BPF (mPa)	Amplitude at blade natural frequency (mPa)
1	7.0	1.5
2	6.21	2.0
3	5.08	2.4
4	4.87	2.6

The proposed method of detecting blade vibration through simulated experiments was successful in connecting BPF and the natural frequency of the blade. Steady amplitude of BPF indicates no blade vibration whereas varying amplitude of BPF indicates blade vibration. The experiment also showed that for a given fan, running at constant speed the amplitude of BPF is not affected by any other variation except the blade vibration.

3.3 Close Form Equation to Predict Reduction in Magnitude at BPF Due to Blade Vibration

Mathematical solution was attempted to show that when blades vibrate the amplitude at BPF reduces. Figure 3.7 shows illustration of rotating pressure wave inside the casing along with the blades. BPF is sinusoidal pressure wave rotating inside the casing as shown in the If there are N numbers of blades in a stage, the time varying pressure in the casing can be written as

$$P(t) = A \sin(\omega t) \tag{3.1}$$

where ω is BPF in radian/sec and A is the amplitude.

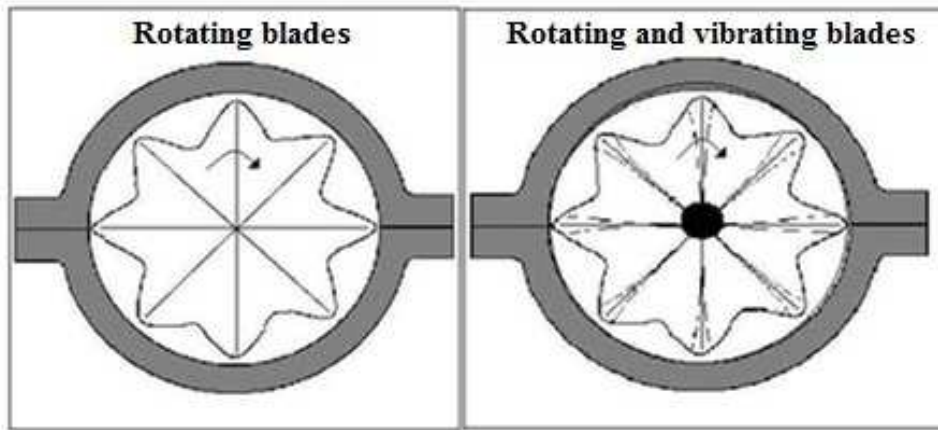


Figure 3.7 Illustration of pressure wave inside a turbine & effect of blade vibration

Out of N blades if one blade sets into vibration, it deflects from its equilibrium position and introduces lag in its arrival time at a given position in comparison to the other blades in the stage. It is assumed that the natural frequency of the blade is significantly lower than the BPF of that stage which is true for the long blades of LP turbine.

The amplitude at BPF with one blade vibrating can be written as

$$P(t) = A \left\{ \frac{(N-1)}{N} \sin(\omega t) + \frac{1}{N} \sin(\omega t + \phi) \right\} \quad (3.2)$$

If M number of blades vibrate, this relationship becomes

$$P(t) = A \left\{ \frac{(N-M)}{N} \sin(\omega t) + \frac{M}{N} \sin(\omega t + \phi) \right\} \quad (3.3)$$

When one blade out of N blades vibrates, its contribution to overall amplitude reduces by $1/N$ when taken with the delay in phase with respect to non vibrating blades. The remaining $(N-1)$ blades contribute more to overall vibration amplitude A without any delay. As more and more blades vibrate, contribution for the reduction of overall amplitude increases when delay in phase is considered with respect to non vibrating blades. When all the blades vibrate, due to phase delay with respect to condition of no blade vibration, the amplitude reduces. Amplitude of BPF is always compared with conditions when the blades are vibrating with that when the blades are not vibrating. In an operating plant when the blades are constantly vibrating, amplitude of BPF remains constant. Only on a long term amplitude trend of BPF, this can be

identified. The curves are obtained by running MatLab program written to solve equation 3.2. Vibration of more and more number of blades leads to higher phase difference and the amplitude of $P(t)$ decreases as shown in Figure 3.8. The single sinusoidal wave characterizes oscillation of BPF.

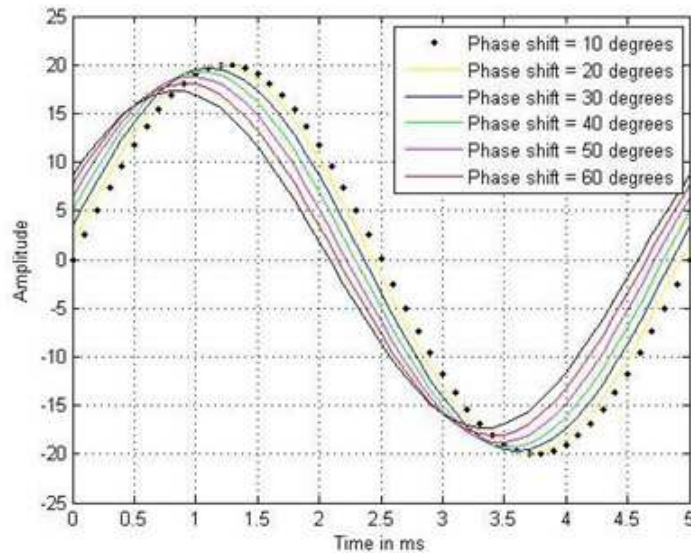


Figure 3.8 Amplitude reduction with increase in phase shift due to blade vibration.

Figure 3.9 shows reduction in the magnitude of $P(t)$ with increasing phase angle due to increasing magnitude of vibration of the blades.

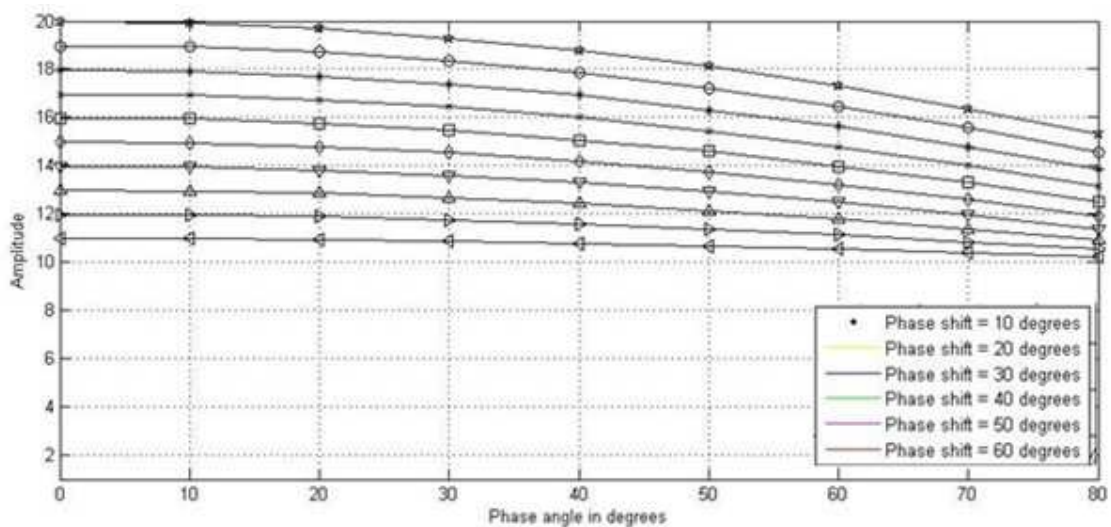


Figure 3.9 Reduction in the amplitude at BPF due to increasing vibration of the blades.

3.4 Closure

The proposed method of detecting blade vibration has been successful in relating BPF and the natural frequency of the blade in simulated experiments. Constant amplitude of BPF component indicates no blade vibration whereas changing amplitude of BPF component indicates blade vibration. The experiment also showed that for a given speed of the fan, the amplitude at BPF is not affected by any other variation except for the blade vibration. Amplitude of BPF is the intensity of impingement of air issuing from the fan blade on the casing during rotation of the fan. In the experiment, the impingement intensity is measured by a pressure transducer. When the blades vibrate, the intensity of impingement reduces and hence the amplitude of BPF reduces. The next chapter describes application of the proposed technique in turbine blades of an operating plant.

Chapter 4

Application of Blade Vibration Detection Method on Low Pressure Turbine of 900 MW Nuclear Turbine

The application of the of the proposed blade vibration detection technique to the LP casing of the turbine operating in 900 MW nuclear power plant is further discussed in this chapter. In an operating plant, it is not possible to excite a blade by a jet of air as was done in the previous chapter. However, the long blades have tendency to vibrate due to slightest excitation by the flowing steam. As listed in Chapter 2, there are several known and unknown reasons for the blades to vibrate. In the hostile steam environment, especially towards the last stages in a nuclear turbine, blades vibrate [25][26]. Among many reasons, the primary reason for the the blades to vibrate is during the transients created during power alteration. It is normal for the plant operators to alter the power generation, however small, in a day or at least in a week.

As brought out in Chapter 3, the BPF of any stage is the information carrier about the blades of the stage. The underlying phenomenon behind source of BPF is same, be it a fan, steam turbine, gas turbine or compressor. Besides, the response of the casing in all these cases due to excitation by BPF can be easily measured by general purpose accelerometers mounted on the casing. As the BPF is in kHz range even for the last stage of LP turbine, the

distortion to the BPF component by the rigid casing is less. Hence, the deterministic BPF in the casing vibration signal can be readily identified on any turbine.

In this chapter, the application and validation of the proposed blade vibration detection technique on LP turbine of a 900 MW Nuclear turbine are presented.

4.1 Problem Definition

The turbine in the nuclear plant consists of 1 HP and 2 LP. Each LP has 9 stages. The 9th stage is the last (exhaust) stage with 58 free standing blades. The rotating speed of the turbine is 1500 RPM (25 Hz). The numbers of blades on the other stages and the corresponding BPFs are given in Table 2 below.

Table 4.1 List of BPFs and number of blades in the last 6 stages of LP turbine

Stage No.	Number of blades	BPF (Hz)
9 th	58	1450
8 th	96	2400
7 th	152	3800
6 th	204	5100

General purpose accelerometers were mounted on the rigid parting plane of the LP casing and casing vibration data was recorded during pre defined interval. Figure 4.1 shows the BPF component of all the last 4 stages before the entry of the steam in the turbine and after the entry of steam. The red and the blue overlaid spectra in the Figure show the two cases. The BPF peak is distinctly present in the spectrum indicating the ease of obtaining BPF from the casing.

In an operating plant there are no provisions to deliberately induce vibration in the blades to analyze the effect of blade vibration on the amplitude at BPF. However, the literature on dynamics of the blades in steam environment say that the last stage long blades do vibrate during transients and sustain until normalcy returns to mode of operation. In the following, we describe the results of analysis of the recorded casing vibration data during certain transients in the form of change in power generation which is adjusted based on the grid demand.

4.2 Casing Vibration Analysis

The first approach was to identify the process transients that could be significant and has potential to induce vibration in the blades. Different power generation level from the generator is achieved by different steam flow in the turbine. As the proposed technique is uniquely dependent on the presence of steam in the casing for transfer of blade related information to the casing, vibration data captured during power change was analyzed.

Figure 4.2 shows the overall trend of power for 30 days. On 3rd day the plant was generating about 540 MW. This was changed to 810 MW which continued for two days and then reduced back to about 510 MW. This duration was selected for detailed analysis. Vibration data acquired for about 5 minutes in every 2 hours was analyzed and an averaged spectra was generated for every 2 hours. In all, 36 spectra were generated for detailed analysis over a period of 72 hours.

Figure 4.3 shows 3D waterfall spectra of all the 36 spectra are generated from FFT program from the acceleration time signal measured by accelerometers mounted on the casing of the LP turbine close to the parting plane. The BPF component of 9th stage at 1450 Hz can

be seen prominently in the centre with nearly steady amplitude. The other peak is the side

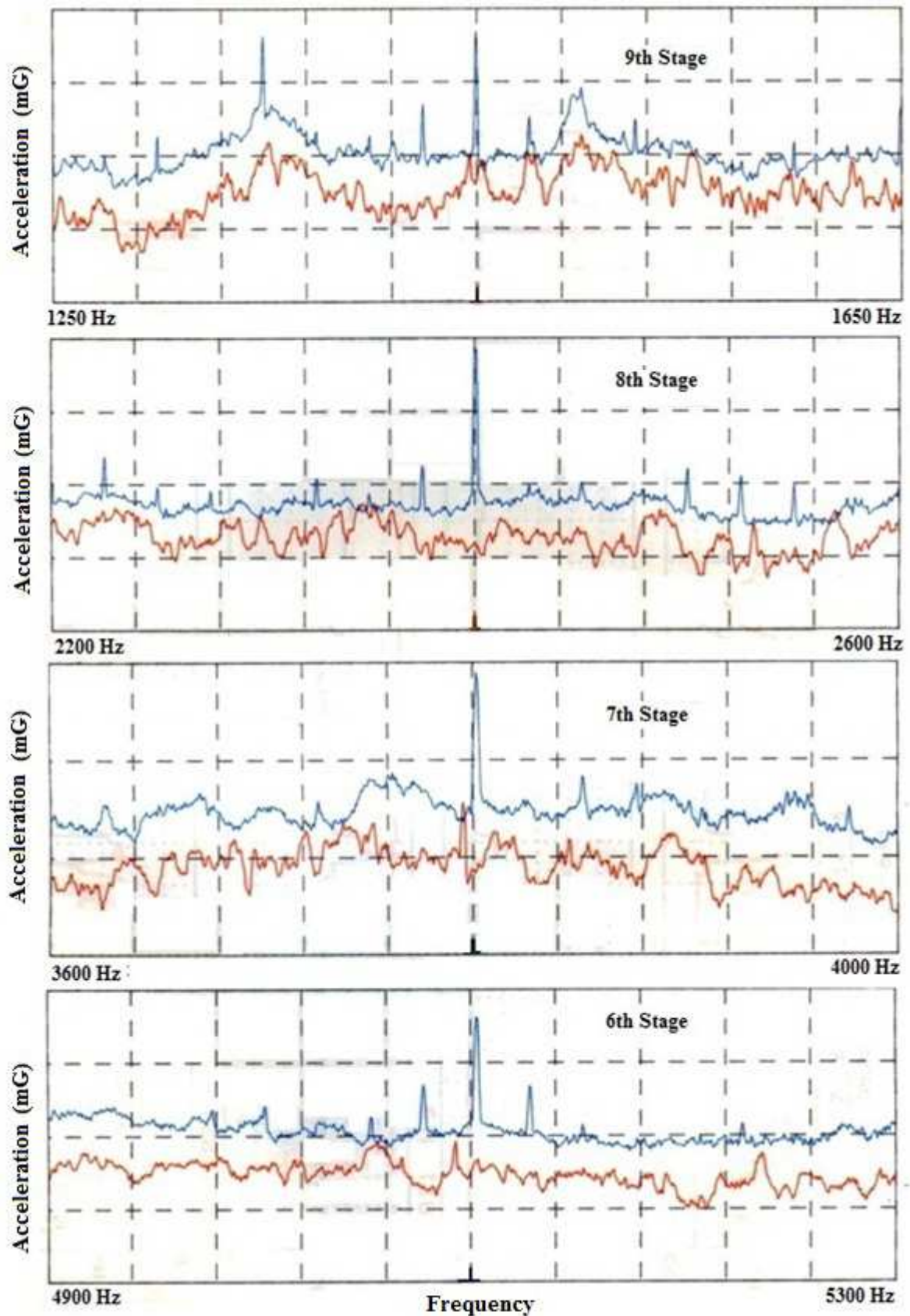


Figure 4.1 BPF peak of the last four stages measured from the casing of LP turbine

band to BPF spaced 25 Hz away from it. The other side band appears due to modulation of BPF by the speed signal at 25 Hz. There were no discernible changes in the amplitude trend of BPF. The amplitudes are in mG units of acceleration. The other peaks are side bands to BPF due to its modulation by turbine speed spaced 25Hz on either side of BPF. The peak at 1350 Hz in the 9th stage may be 54th harmonic of the speed component (25Hz). It has been found to be inconsistent in its appearance in the spectra. The accelerometers are mounted on the outer casing of one LP turbine near the parting plane.

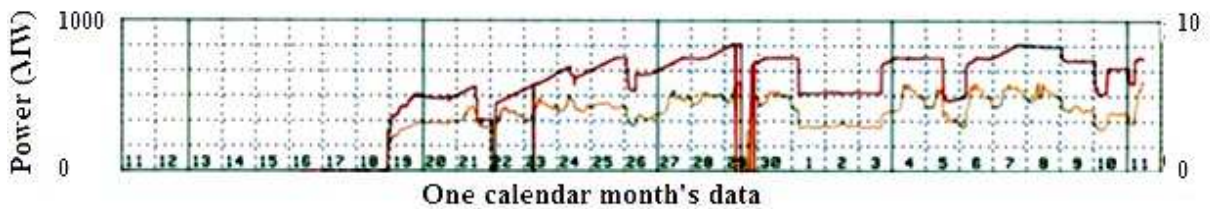


Figure 4.2 Trend of Generated Power and Current of 990 MW turbine

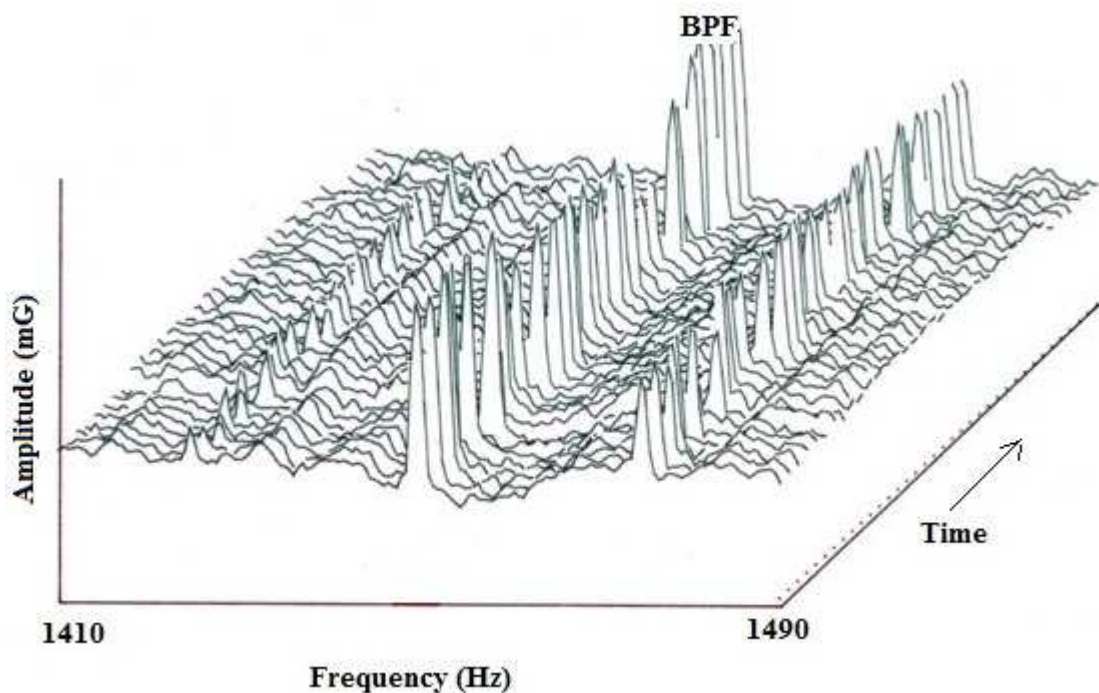


Figure 4.3 Waterfall spectrum of showing BPF of 9th stage at 1450 Hz.

Figure 4.4 shows BPF component of 8th stage at 2400 Hz seen prominently in the centre. Side bands spaced ± 25 Hz on either side of BPF can also be seen caused by modulation of BPF of 8th stage by the speed component at 25 Hz.

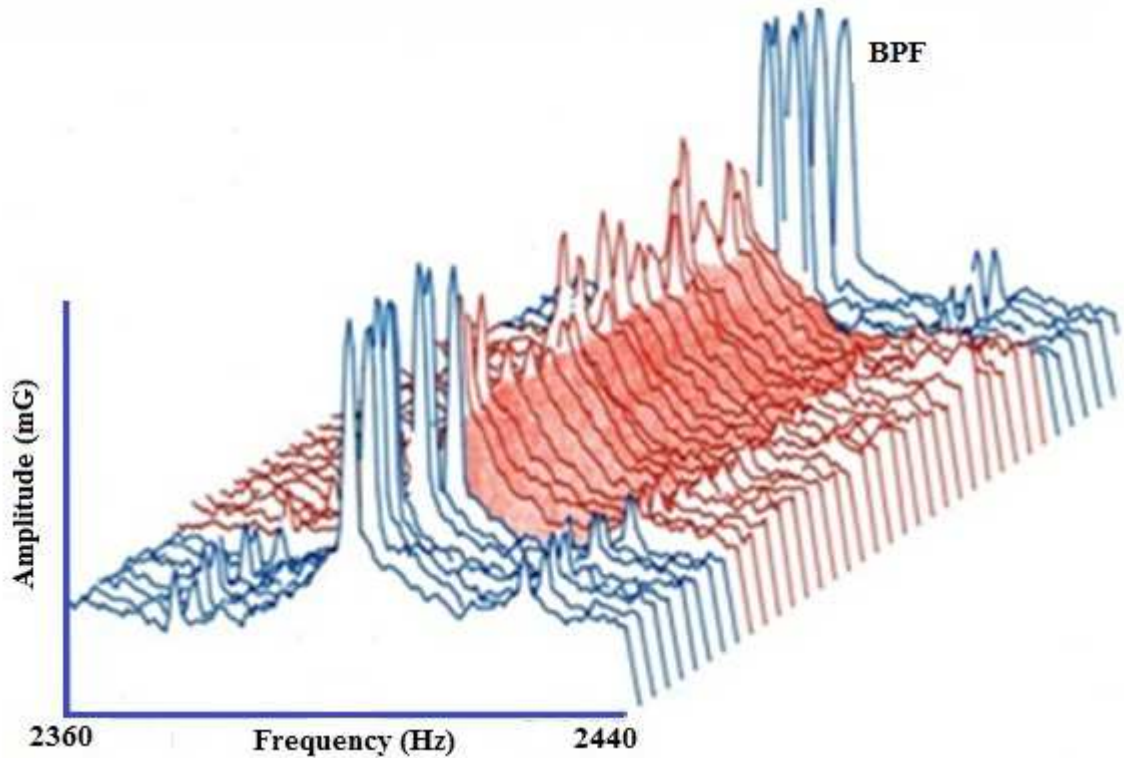


Figure 4.4 Waterfall spectrum of showing BPF of 8th stage at 2400 Hz.

Additionally, the BPF peak can be seen with significantly changing in amplitude starting from the 9th spectra. The first 12 spectra correspond to signals captured on the 3rd day and so 9th spectra correspond to signal at 18 hrs. As can be seen from Figure 4.2 at around 18 hrs the power changes from 510 MW to around 750 MW. The additional steam flow demanded for increased power generation has caused the amplitude at BPF to reduce. The long blades are susceptible to vibration due to change in quantity steam and the local steam path across the blades. In case of 8th stage blades the steam turbulence increased due to steam extraction port on the downstream. Such disturbances are known to cause blade vibration known as steam extraction noise induced blade vibration. Spectra with reduced amplitude at

BPF continue till the 30th spectrum corresponding to 12 hrs noon on 5th day. From 31st spectrum, the amplitude at BPF increases which corresponds to power generation of slightly less than 510 MW. The trend of amplitude at BPF during the entire 30 days of data was found to follow the trend of power generated.

The BPF peak at 2400 Hz is a sine wave signal of dynamic steam pressure impinging on the casing due to rotation of 8th stage blades. Abrupt reduction in the amplitude (spectra in RED) during operation at higher power (> 810 MW) actually signifies reduction in the intensity of pressure signal. As mentioned in Chapter 3, such reduction in amplitude at BPF cannot be explained without the participation of the blades. While the BPF continues to be at 2400 Hz as the speed of the turbine does not change, reduction in amplitude of BPF needed more investigation. When BPF and the blades are connected as cause and effect relationship, further analysis was carried out to assess the operating condition of the blades at different power.

Having established the relationship between amplitude at BPF and natural frequency of the blade, the possibility of blade vibration was needed to be realized in an operating turbine. From the nature of known sources of excitation on the blades, which are either harmonic or random, the blades significantly vibrate in one of its natural frequencies described in Chapter 2 Para 2.2.2. As fatigue is a common factor in all types of blade failures, the lower modes have higher potential to contribute to fatigue in the blade. Additionally, the long blades get excited with little disturbance and vibrate in the fundamental mode. The fundamental natural frequency of long blades is normally within 100 Hz for long blades. Casing vibration was analyzed to investigate the signal of blade vibration.

Figure 4.5 shows water fall spectrum in the frequency band of 70 to 100 Hz. The red and the blue spectra are identically numbered as in Figure 4.4. A continuous and prominent peak is seen at 75 Hz with same amplitude. 75 Hz corresponds to 3rd harmonic of the speed.

This comes because of the residual unbalance in the turbine rotor. In the close neighborhood, a peak at 78 Hz appears in the red colored spectra corresponding to power of around 810 MW. The blue colored spectra on either side of the red colored spectra correspond to power generation around 500 MW. The color of the spectra is shown in red and blue to emphasize the presence or absence of the peaks in discussion. In this case the presence or absence of 78 Hz component. As can be seen in the Figure 4.5, the frequency peak at 78 Hz is seen only in the red colored spectra. As each spectrum is generated once in 2 hrs, the 22 red colored spectra correspond to 44 hrs of operation. That is to say that for 44 hrs, the blade was vibrating at 78 Hz.

In the turbine, the steam issues out of the tip of the rotating blades and impinges on the casing at a regular frequency termed as BPF at 2400 Hz. Amplitude of BPF is a measure of force of impingement in a narrow circle on the inside of casing at BPF. Accelerometers mounted on the casing senses these forces as acceleration signal. If the rotating blade is also vibrating, the intensity of impingement reduces due to smeared action of impingement on wider circle on inside surface of the casing even though the frequency of impingement (BPF) remains the same on account of no change in the speed of rotation and number of blades in the stage remaining the same. Hence amplitude of BPF reduces when the blades vibrate.

From the Campbell diagram of the 8th stage, provided by the manufacturer, it was confirmed that 78 Hz is the first mode of the free standing blades of 8th stage. On reviewing Figure 4.5 and Figure 4.6 together, it can be seen that when the blades vibrate the amplitude of BPF reduces. This relationship is exactly similar to the relation established between BPF and the natural frequency of the blade in the experiment explained in Chapter 3, Section 3.2. The reason for the blades in the 8th stage to vibrate is due to increased steam turbulence caused near the steam extraction port on the downstream of 8th stage. Figure 4.6 shows cross

section of the exhaust side of the LP turbine. Due to increased steam flow during increased

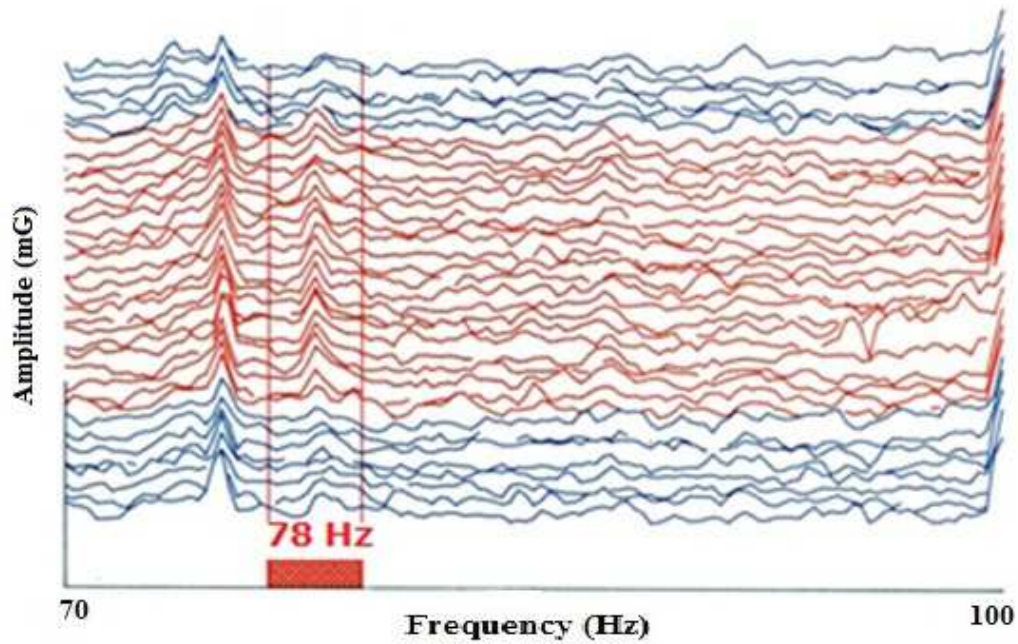


Figure 4.5 Waterfall spectrum of casing vibration showing blade natural frequency at 78 Hz

power generation (510 MWe and 810 MWe), the steam noise increases near the steam extraction port. The random steam noise excites the blades to vibrate.

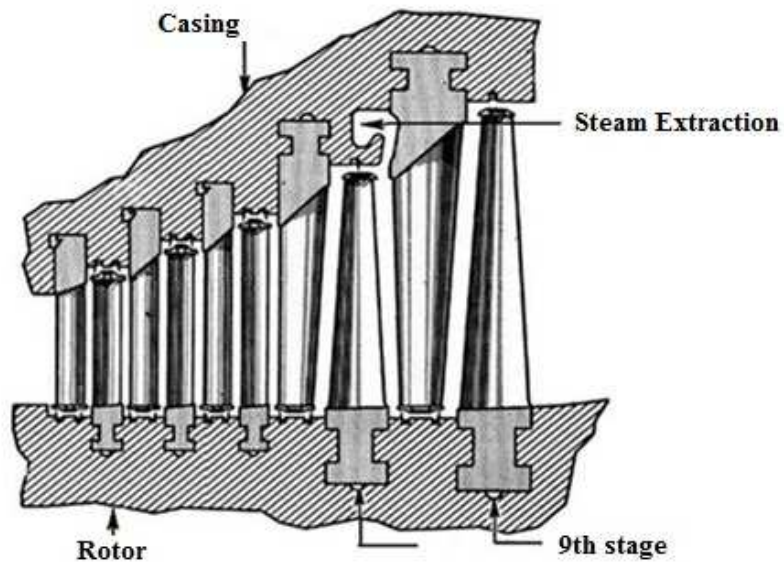


Figure 4.6 Cross section of exhaust side of the LP casing

In a separate CFD study carried out by M/s Hitachi, it is shown that the steam eddies formed due to steam extraction excites the blades to vibrate significantly. Such excitations are random in nature and so the blades vibrate in lower mode natural frequency. Figure 4.7 shows CFD results provided by M/s Hitachi [27]. The eddies formed due to steam extraction excites the blades to vibrate in their lower mode.

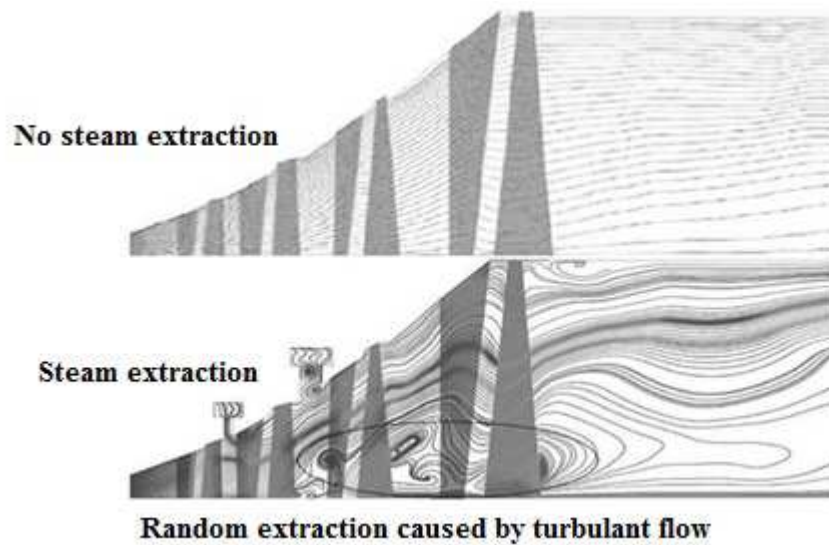


Figure 4.7 Results of CFD study carried out by M/s Hitachi [27]

4.3 Closure

The application of detecting blade vibration technique by analyzing casing vibration acquired on LP turbine of a 900 MW nuclear power plant was demonstrated. As described in Chapter 2, the long blades are excited by several known and unknown sources in a steam turbine. In this chapter, it was demonstrated that the blades vibrate in its natural frequency due to random steam excitation caused by steam extraction. The vibrating blades reduce the amplitude at BPF thus validating the conclusion of Chapter 3. It was also demonstrated that by trending the amplitude at BPF, which is easily measureable from the casing vibration data, it is possible to

detect blade vibration in an operating power plant. The consistent results obtained in chapters 3 and 4 demonstrate the robustness of the technique. From diagnostic point of view, it is important to identify the condition at which the blades have tendency to vibrate. In this case, increased steam noise due to steam extraction is shown to be the cause of blade vibration. This helps in validating the Campbell diagram of the stage provided by the turbine manufacturer. Before an individual blade fails due to the high vibration, the blade has to vibrate along with other blades in one of the identified modes. By detecting the mode of blade vibration by the proposed method, we can say that there is a possibility of stray blade to fail if the blades continue to vibrate.

The subsequent chapters deal with the vibration of turbine blades under plant load operation.

Chapter 5

Study of Vibration of Turbine Blade Subjected to Part Load Operation

In this chapter, the application of blade vibration detection technique on the turbine operating at part load is looked in to. In almost every power plant the turbine operates at part load for significant portion of time. This is also called off design condition. Such operation could be due to various reasons ranging from low grid demand to technical problems for running at full load. During off design operation, the steam conditions vary along the steam path due to reduced steam mass flow. There are zones of different pressure, radial flow, counter flows and flow recirculation (flow instabilities) etc. Such operating conditions are not healthy for the blades. They lead to blade vibration which in turn can lead to blade failures. Unit operation with reduced mass flow also causes reduction of the steam flow velocity. This results in change in incident angle on the blade along the leading edge (change of stage velocity triangle). The flow entering into the long blades of exhaust stage with negative incidence angle strikes the suction surface of the blade airfoil and excites the blades. The pressure fluctuation, flow recirculation and counter flows in conjunction with the negative incidence angle flow striking on the blades induce vibration in the blade [29].

We recreate low load and low vacuum condition for a short time in an operating plant to excite the long blades. Casing vibration acquired during the part load operation is analyzed to trend the amplitude at BPF.

5.1 Problem Definition

The turbine operating at part load is a 220 MW PHWR nuclear power plant. The turbine has one HP module and one LP module. Steam enters LP from the centre and splits into left and the right LP. Each side of the LP consists of 5 stages. The 5th stage blades are laced, 4th stage blades have lacing rods and the 3rd to 1st stage blades are shrouded at the free end. Due to inadequate heat transfer capability of the moderator system, the plant was operating at 165 MW. The long last stage blades are 975 mm long and laced. There are 78 blades in the last stage and the turbine operates at 3000 RPM (50 Hz). The intended purpose of the lacing wire is to damp unwanted blade vibration by the action of friction. To a large extent the introduced lacing wires are effective in controlling blade vibration. If the damped blades have to vibrate with significant amplitude, the process has to be perturbed.

In the following, the method adopted to perturb the blades to vibrate and the analysis results of recorded casing vibration data acquired during part load operation are described.

5.2 Casing Vibration Analysis

The first approach was to identify the process transients that could be significant and has potential to induce vibration in the blades. While the approach is to trend the amplitude at BPF, to influence changes in the amplitude it was necessary to certainly induce vibration in the blades. Low vacuum in the condenser is one parameter that has potential to induce blade vibration due to change in the steam incident angle on the blade along the leading edge

(change of stage velocity triangle). Thus the flow entering the long blades of exhaust stage with negative incidence angle due to low vacuum strikes the suction surface of the blade's airfoil and excites the blades. Such vibration in the blade is also called self excitation. Under self excitation the blades vibrate at natural frequency and it continues until such condition prevails in the turbine. Casing vibration data acquired during low vacuum in the condenser is analyzed.

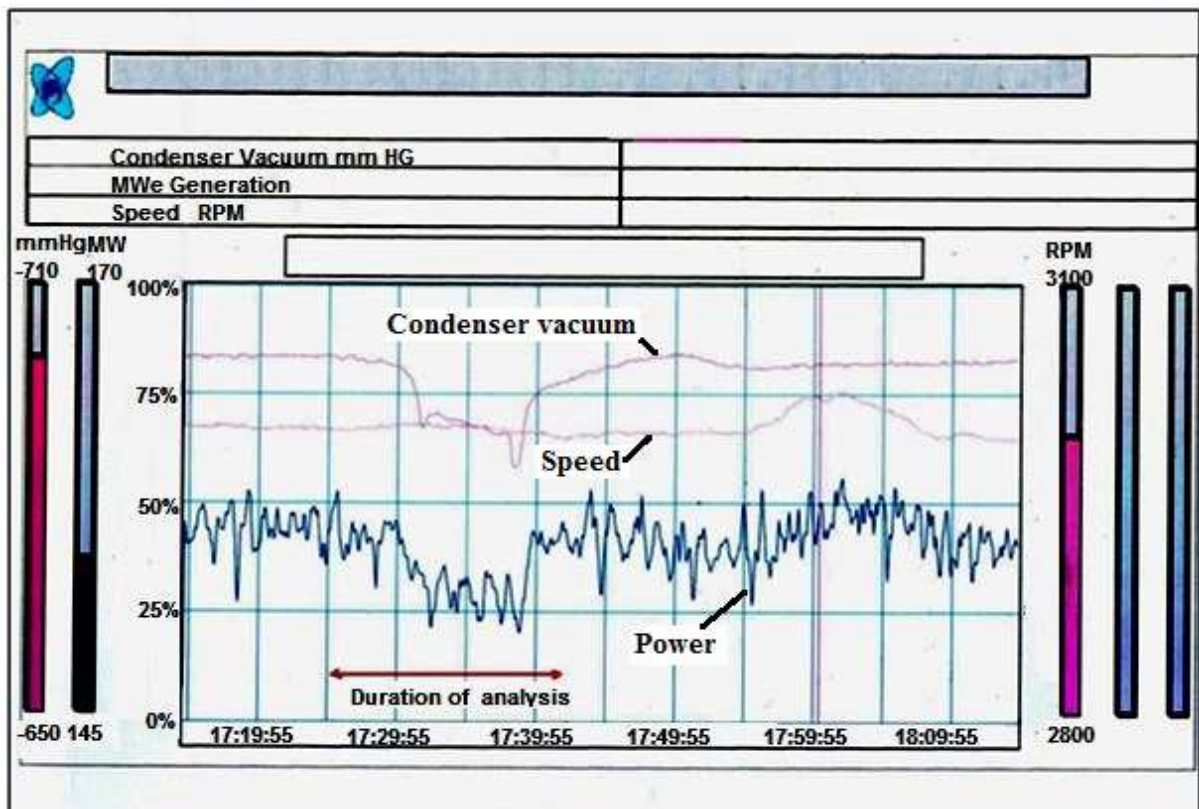


Figure 5.1 Variation of turbine load, condenser vacuum and speed with time

Figure 5.1 shows variation of power, speed, and vacuum in the condenser. For about 15 minutes between 17:29 and 17:44 hrs, the condenser vacuum reduced from -700 to -680 mm HG and power reduced from 155 MW to 152 MW. The red line with arrow at ends indicates the duration of low vacuum. During the created transient, casing vibration was analyzed. Figure 5.2 shows the waterfall spectrum of BPF of the last stage for the identified 15 minute duration. The waterfall spectrum is obtained by analyzing the acceleration time

domain signal measured by the accelerometer mounted on the casing of the LP turbine. The time domain signal is converted to frequency spectrum and all the spectra are cascaded in waterfall spectrum. The prominent peak at 3882 Hz is the BPF. The amplitude of BPF shows a pattern of variation. Comparison between Figure 5.1 and 5.2 shows similarity between trend of turbine process (power and vacuum) and amplitude trend of BPF. When vacuum decreases, the amplitude of BPF decreases and then recovers back when the vacuum is normalized. As shown in Chapter 3 and 4, in the present case too, the amplitude at BPF reduces for a transient existing or created externally inside the casing. It was earlier consistently shown that primary reason for amplitude at BPF to reduce is blade vibration. The relation between reduction of amplitude of BPF and blade vibration at natural frequency was established in Chapter 3. If that has been validated, it was important to analyze and detect signal of blade vibration during part load operation and re-establish the relation between BPF with natural frequency of the blade. Casing signal was analyzed in the low frequency band.

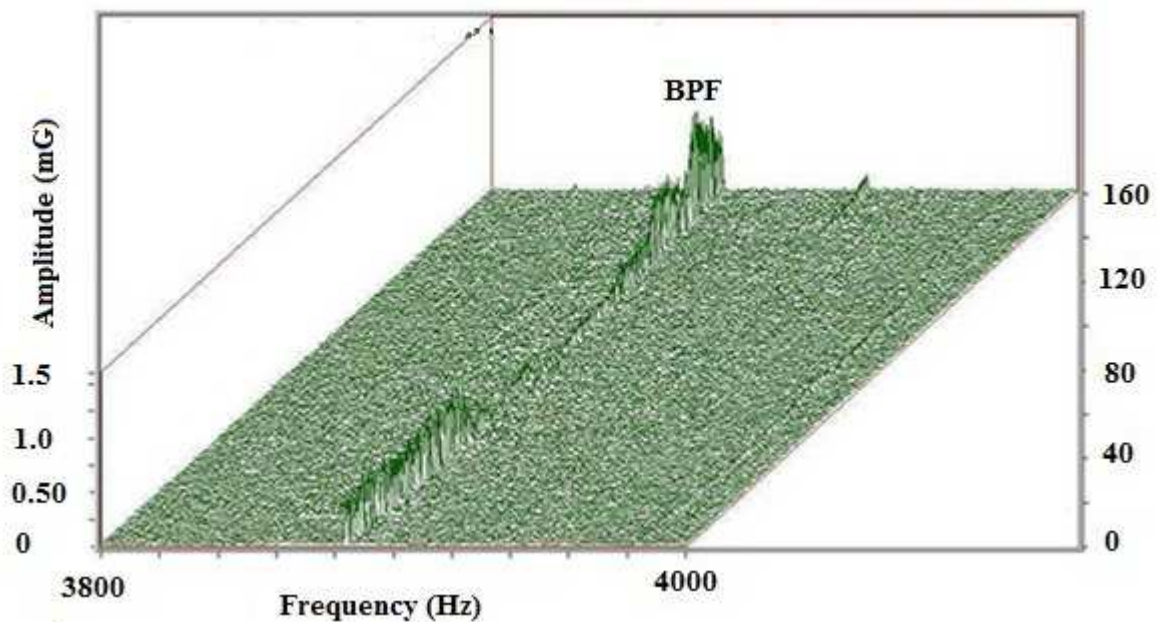


Figure 5.2 Waterfall frequency spectrum showing BPF of last stage LP blades

Figure 5.3 shows the waterfall spectrum in the band of 101–140 Hz. A frequency peak at 107 Hz emerges above the background during low vacuum in the condenser accompanied by low load. As brought out earlier, the last stage is laced at the free end which inhabits blade vibration. In spite of the effect of damping, the low vacuum condition in the condenser is able to excite the blades and the low level of blade vibration is transmitted to the casing. As the last stage blades are laced, all the blades will vibrate with similar amplitude in the first mode. The method does not detect vibration of individual blade but detects combined stage amplitude with respect to background. This method is a demonstration of the sensitivity of the technique to capture even low level of blade vibration [30-33].

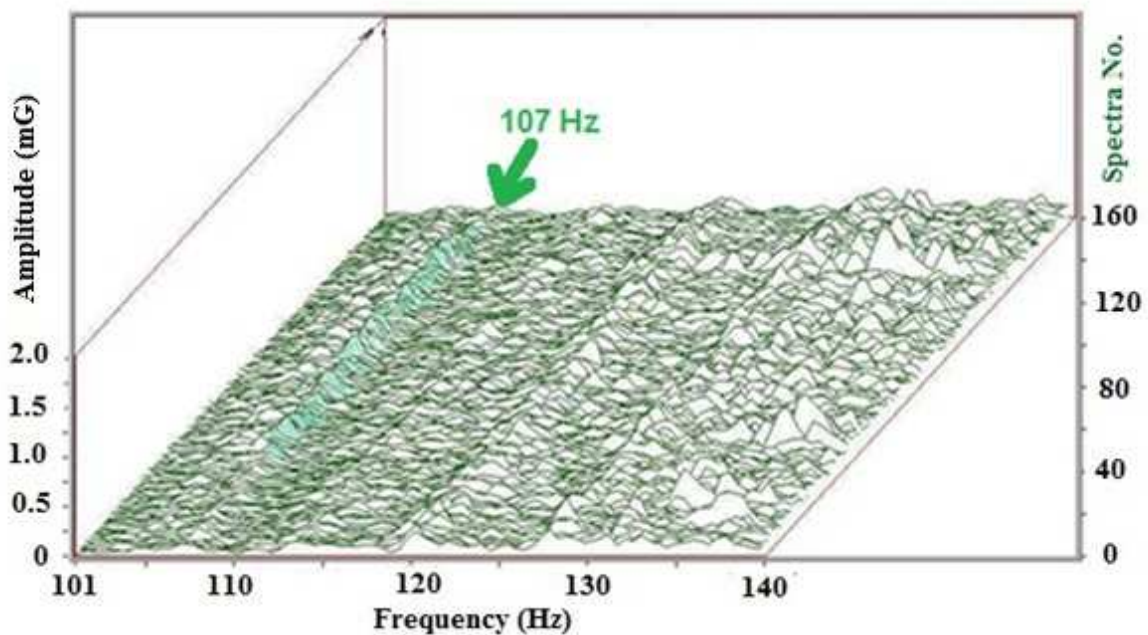


Figure 5.3 Waterfall spectrum showing blade natural frequency at 107 Hz

The time duration during which, the amplitude of BPF reduces and increase of amplitude of 107 Hz in the low frequency spectrum shows a close match. This comparison establishes direct relationship between BPF and blade natural frequency. This relationship closely matches with the results given in section 3.2. From the Campbell diagram provided by the manufacturer it was confirmed that 107 Hz is the first mode of the long blades. An

independent result published based of finite element modeling of the last stage blades confirm the first mode and its frequency close to 107 Hz. Figure 5.4 illustrates the mode shape of the combined model of disk and the blades. In this mode, all the blades vibrate axially in phase with respect to the turbine shaft. Such a mode is also called an umbrella mode. This mode happens to be the lowest mode and the one which gets easily excited during transients as explained in section 5.2. This mode is 0-0 mode as illustrated in Figure 2.9.

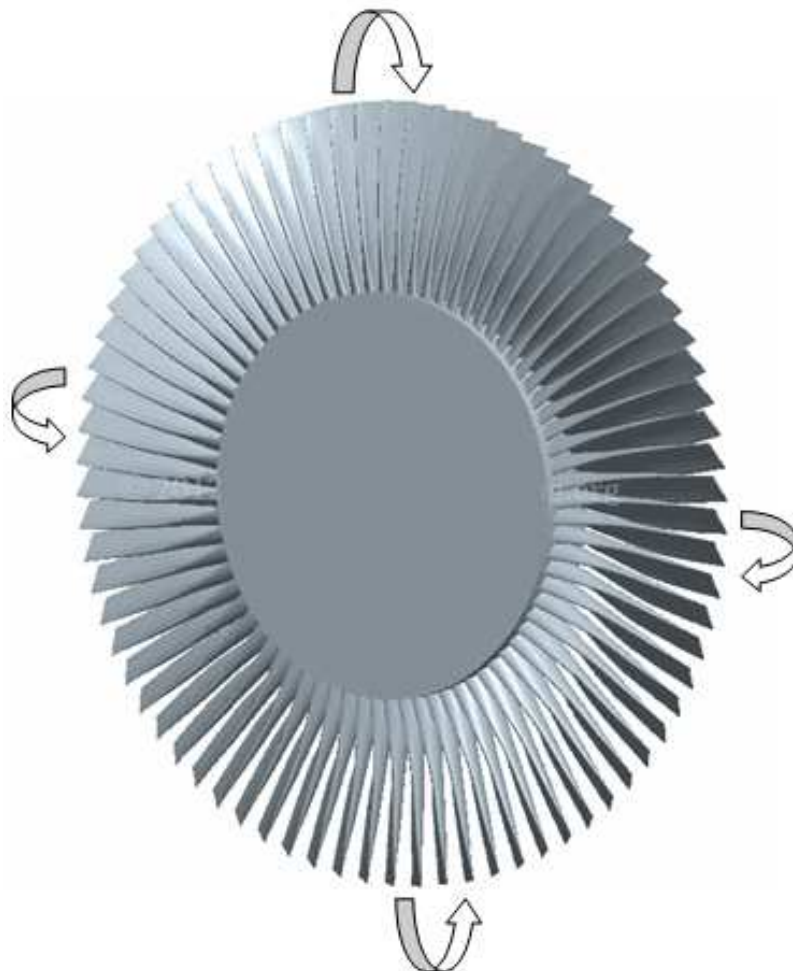


Figure 5.4 1st Mode shape (Umbrella) and frequency (107.7098 Hz) of the last stage [34]

Table 3 shows results obtained by two different published works. The results in S.No. 1 are published by J. S. Rao and results of S. No. 2 are produced by BHEL from the test done in Hyderabad. Both are for the same stage of the turbine. This work was done by the author with reference to turbine fire accident in Narora atomic power station in 1993. The turbine in Narora plant and the turbine dealt in Chapter 5 are of identical design. Thus, the results are relevant and comparable. The present work is consistent with the results published independently.

Table 5.1 First mode frequency of the last stage bladed disk

S. No.		Single blade	Disk	Bladed flexible Disk	Bladed rigid disk
1	FE method Published[34]	102.02 Hz	760 Hz (1 Nodal Diameter)	107.7098 Hz Umbrella Mode	113 Hz
2	Test	103 Hz (Tunnel test at BHEL)	-----	107 Hz (Result of present work)	

5.3 Closure

The application of detecting blade vibration technique on a turbine operating at part load is demonstrated in this chapter. In the present case, the blades were inhibited to vibrate even under part load operating condition because of the effect lacing wire. Blade vibration was induced by slightly lowering the vacuum in the condenser under part load. Under low vacuum, a correlation was established between decreasing value at BPF and blade vibration in first mode. The results are consistent with the published work done by other researcher and the blade manufacturer (BHEL). Whatever be the reason for blade vibration, if they are vibrating it transmits the signal to the casing whose response can be used to detect blade

vibration. The consistent results obtained in Chapters 3, 4 and 5 demonstrate the versatility of the technique.

Chapter 6

Application of Present Technique on Detecting Compressor Blade Vibration in a Power Plant

The versatility of the detecting technique is demonstrated in this chapter by applying it on a compressor of a 250 MW gas power plant. The moving pressure fields in the casing due to the pressure profiles around the rotor blades cause harmonically varying pressure field inside the casing. In addition, vibration of individual rotor blades causes modulation of the rotating pressure profiles around the rotor blades. It was shown in Chapters 4 & 5 how the steam turbine casing vibration can be analyzed for deducing blade vibration parameters. Compressors in a gas based power plant compresses the incoming air and sends the pressurized air to a burner chamber from where the hot and pressurized gas is directed to a turbine to rotate and generate power. Unlike the long blades in LP turbine in a steam based power plants, blades in compressors are short, wide, and very rigid. However, under conditions conducive for vibration, rigid blades also vibrate. There are many reported incidences of blade failure primarily due to fatigue.

We demonstrate the effectiveness of the detection technique on compressors which had incidences of repeated blade failure due to un-understood reason.

6.1 Problem Definition

Like in steam turbines, in axial flow compressors the flow proceeds throughout the casing essentially parallel to the axis of the machine. The compressor consists of adjacent rows of rotor blades and stator blades. The rotor blades are mounted on the rotor drum and the stator blades are fixed to the casing. The blades are of aerofoil section based on aerodynamic theory. The air stream follows the blade contour. The annulus area is reduced from inlet to outlet to keep the flow velocity constant whereas the air pressure increases by flow of air in the diverging passage of the moving blades. The stationary blades aid in increasing the pressure energy by diffusion process and in guiding air flow from lower stages to higher stages without shock.

The first 4 rows named as R1 to R4 consists of 26, 28, 34 and 36 blades respectively. Figure 6.1 shows typical cross section of axial flow compressor. The rotor rotates at 3000 RPM and the air that also flows radially impinges on the casing. The temperature on the outer surface of the casing at the inlet end does not reach high (100 degree C) and so general purpose accelerometers can be mounted on the casing. In the following, we describe the application of detecting blade vibration by analysis of casing response.

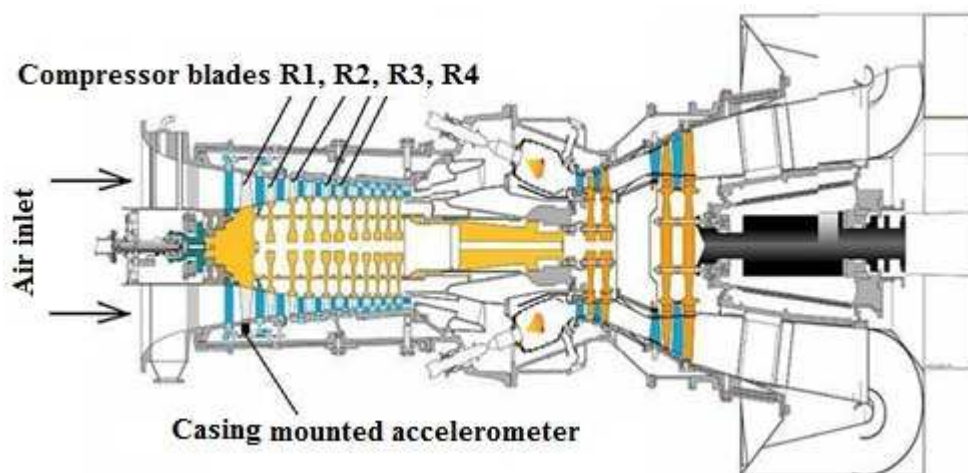


Figure 6.1 Typical cross section of axial flow compressor

6.2 Casing Vibration Analysis

Casing vibration analysis was carried out on a working plant. Figure 6.2 shows water fall spectrum of casing vibration response in the band of 200 to 550 Hz. The vertical lines correspond to harmonics of the rotor speed. These are also called engine orders which excite the blades if the blade natural frequency happens to coincide with the engine orders. The Campbell diagram provided by the turbine manufacturer essentially gives the same information as given by the spectrum in Figure 6.2. They indicate steam excitation frequencies in a turbine. Due to speed variation, the higher harmonics do not coincide with multiples of 50. The higher harmonics are nothing but the engine orders shown in the Campbell diagram. Whereas the 10th harmonic must have coincided with 500 Hz but due to synchronous speed being less than 3000 RPM the 10th harmonic is coinciding with around 478 Hz. Just beside the 10th harmonic, a frequency appears consistently for the time of recording.

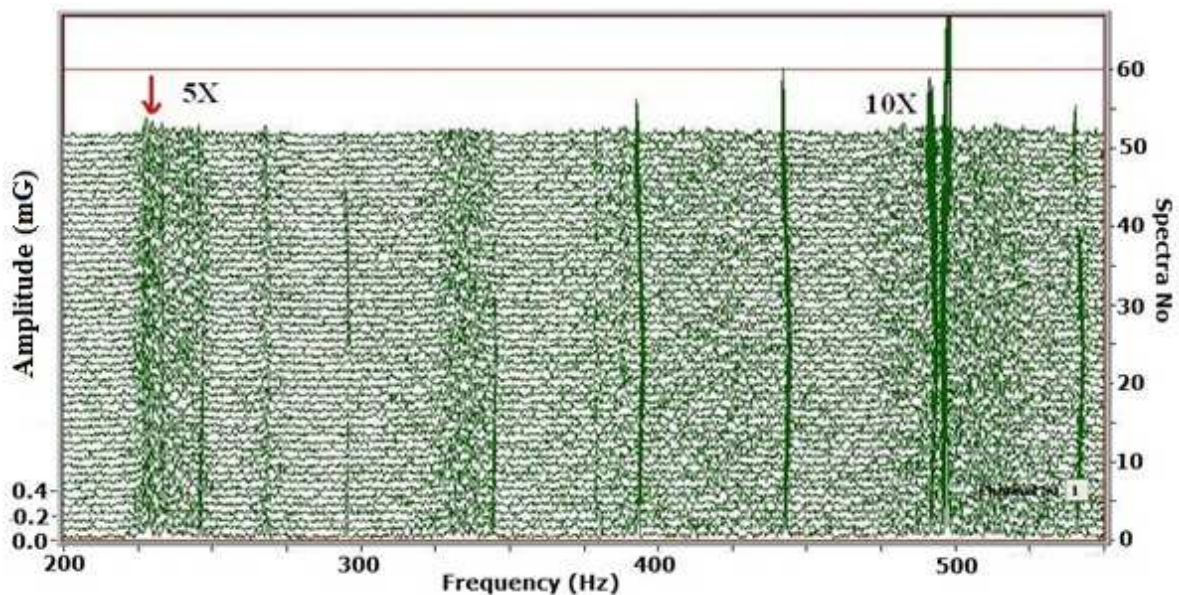


Figure 6.2 Waterfall spectrum of casing vibration response

Designers normally tune the components of the compressors to ensure sufficient margin between any natural frequency and the engine order. In this case however one frequency appeared very close to 10th harmonic. To make sure about the origin of the frequency, it was required to create a short transient in the operating compressor. In the available option, dropping of load was acceptable to the operators. By dropping the load, the air intake into the compressor gets disturbed from normal condition [35].

During the measurement, the load was dropped by 10 MW for 10 minutes and normalized. Water fall spectrum of casing response in the band of 200 to 550 Hz during load drop is shown in Figure 6.3. As a consequence of load drop, the unknown frequency close to 10th harmonic responds and moves closer to the 10th harmonic as can be seen in Figure 6.3.

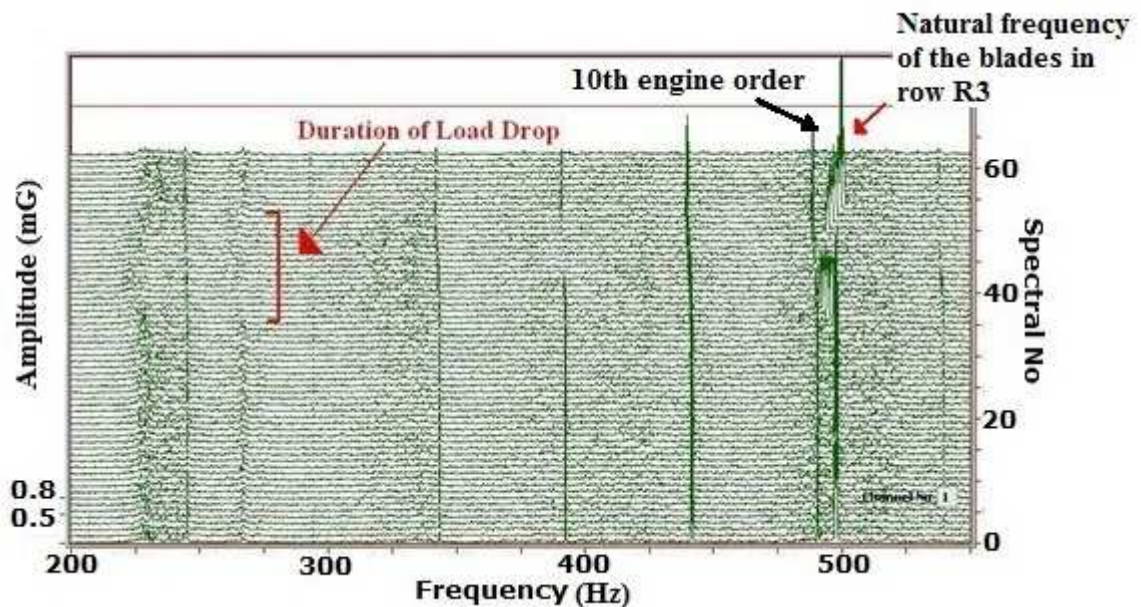


Figure 6.3 Water fall spectrum of casing vibration response during load drop

Figure 6.4 shows amplitude trend of BPF of row R3. The dip in the amplitude can be seen when the load was dropped after confirming the sensitivity of the frequency peak to the transient, modal test was performed on the compressor blades on a spare rotor stored in the

plant to identify the natural frequencies of the blades. As the blades are short in size, the effect of centrifugal force on the blade's natural frequency is expected to be less and so the natural frequency measured in static condition will be close to the natural frequencies during rotation. Table 4 shows the measured natural frequencies of the blades in rows R1 to R4.

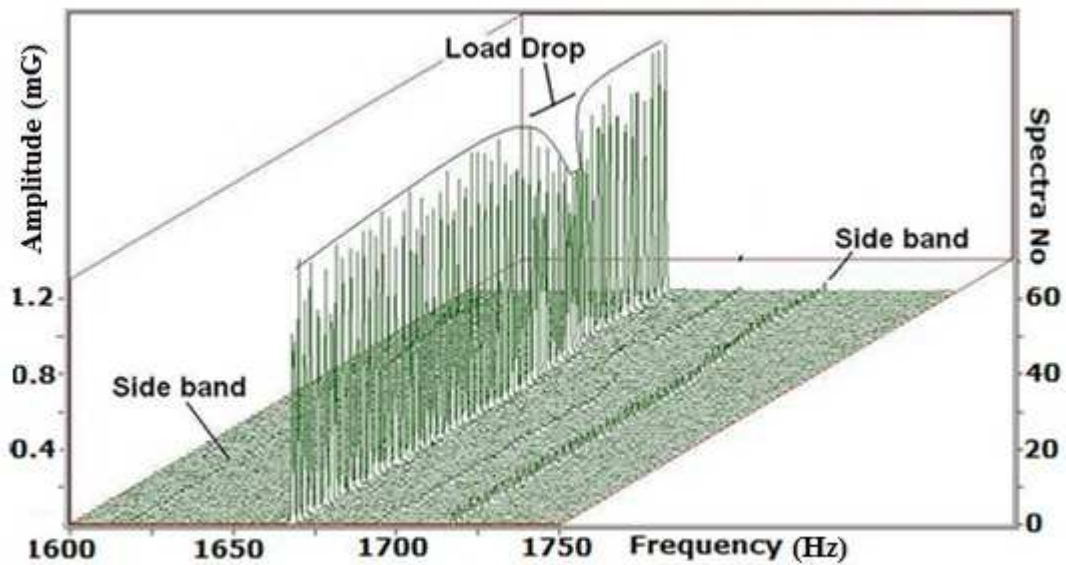


Figure 6.4 Amplitude trend of BPF of row R3

In order to verify the natural frequency of the blade in row R3, experimental modal analysis test was carried out with instrumented impulse hammer and accelerometer. One accelerometer was placed on one blade and the blade was rapped with impulse hammer. Rowing hammer method was adopted. The impulse signal and the response signals were analyzed using an analyzer to obtain frequency response function. The averaged frequency response function in real and imaginary mode was obtained as shown in figure 6.5. The peaks in real and imaginary plots marked with arrows and are the natural frequencies of the blade. The first bending mode is detected at 508 Hz. The frequencies listed under row R3 in Table 4

can be seen in the graph of Real and Imaginary plots. In one of the previous accidents in the plant, blades in row R3 had repeatedly failed.

Table 6.1 List of natural frequencies of the blades in 4 rows of the spare rotor

Row R1 (Hz)	Row R2 (Hz)	Row R3 (Hz)	Row R4 (Hz)
1A-575	1F-456	1A-508	1A-346
1T-796	1T-606	1T-740	1T 590
865	912	2F-975	865
1F-968	2T-1228	3F-1462	1040
2T-1165	2F-1331	2T-1659	1212
1306	1659	3T-2353	1337
2F-1493	3T-1881		1731
1606	3F-2250		2T-1928
3F-1903	A: Axial	F: Flap	T:Torsional

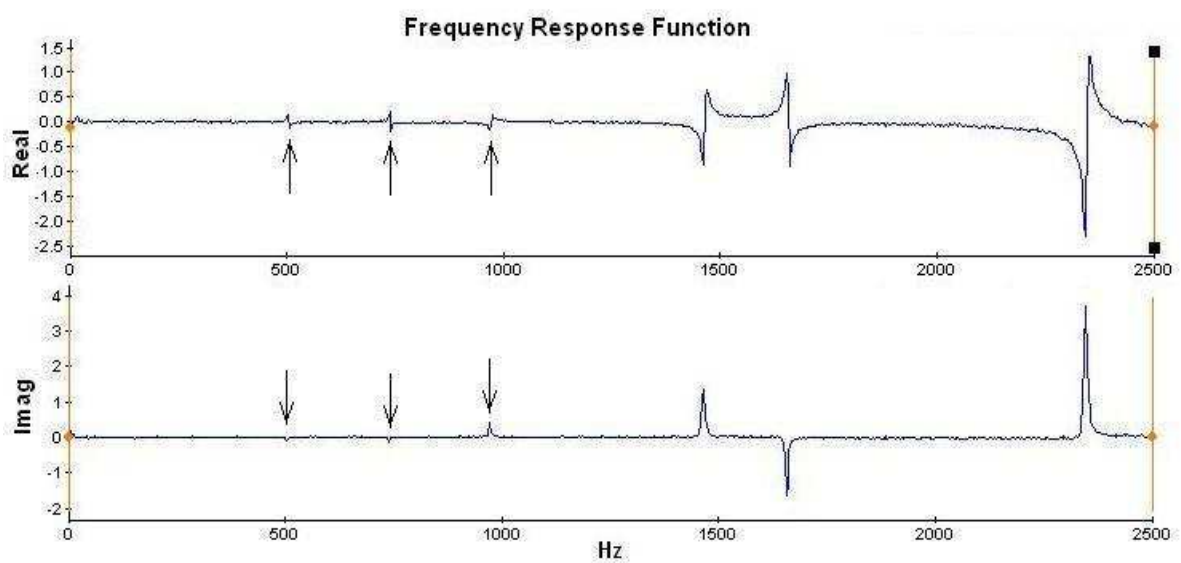


Figure 6.5 Frequency Response Function of row R3 blade

The tell-tale mark on the failed cross section of the blade shown in Figure 6.6 indicate fatigue due to axial mode. excitation. Because of closeness of the axial mode around 508 Hz, to the 10th engine order as shown in figure 6.3, the blade failed in fatigue.

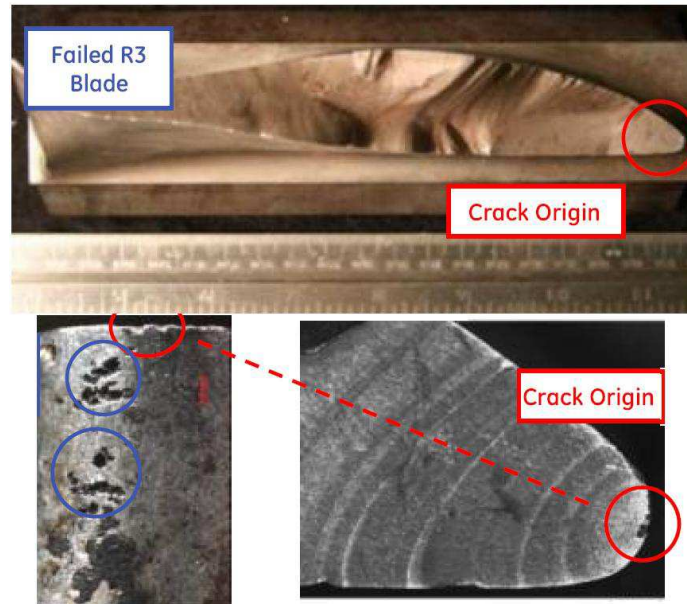


Figure 6.6 Cross section of the failed blade with beach marks

The beach marks indicate active axial mode. The analysis confirmed that the axial mode blades are continuously excited by 10th harmonic. Harmonic excitation of the blades leads to high stress in the roots leading to eventual failure.

6.3 Closure

Casing response effectively carried the information about blade vibration of the compressor during operation. The amplitude at BPF of row R3 reduces when the load was dropped establishing the relationship between BPF and the natural frequency of the blade. The modal analysis carried out on the static blades was found acceptable for rotating blades. Even though the blades are short, wide and rigid, it still vibrates continuously due to harmonic excitation by the 10th engine order. The tell-tale beach marks on the failed surface of the blade

confirmed that axial mode of the blade is excited by the 10th harmonic. The Campbell diagram of the stage confirmed axial mode at the frequency measured by modal analysis.

Chapter 7

Numerical Investigation of Fluid Structure Interaction between Blade and the Surrounding Steam

In this chapter the model of actual LP blade is subjected to condition conducive for self excitation. Self excitation in long steam turbine blades sets in at low load and low condenser vacuum when the tip of the blades vibrates. The frequency of vibration during self excitation is the natural frequency of the blade. Quite often the turbines operate at low load accompanied by low vacuum in the condenser due to variation in the condenser cooling water temperature. The blade vibration modulates the steam and the steam in turn excites the blades. This phenomenon of exchanging energy between steam and the blade continues as long as conducive conditions prevail in the turbine. In many power plants in India, due to wide fluctuations in energy demand and temperature of cooling water, the off design condition regularly prevails. Vibration induced in the blades due to such self excitation causes fatigue that could lead to failure on a long run. To assess the behavior of the blade under simulated low load and low vacuum condition, fluid structure interaction using standard finite element package was carried out. In the following, we present the results of fluid structure interaction between the blade and the surrounding steam medium that simulates flow along the top leading edge of the blade at an angle that induces self excitation.

7.1 Problem Definition

In fluid structure interaction, the fluid domain is most conveniently described in Eulerian reference frame while the structure is described in Lagrangian formulation. A fluid flow field can be thought of as being comprised of a large number of finite sized fluid particles which have mass, momentum, internal energy, and other properties. Mathematical laws can then be written for each fluid particle. This is the Lagrangian description of fluid motion. Another view of fluid motion is the Eulerian description. In the Eulerian description of fluid motion, change in flow properties at a fluid element that is fixed in space and time (x,y,z,t) , rather than following individual fluid particles.

However, these formulations are incompatible as they need continuous adaptation of the mesh without modifying the topography of the mesh. In problems involving large deformation within the computational domain it is generally difficult to adapt the mesh quality. This is normally overcome by continuously performing re-meshing using Lagrangian formulation. Re-meshing however introduces artificial diffusivity and would be difficult to perform the computation with sufficient robustness in 3D problems. This problem is solved by use of Lagrangian multiplier. The method allows coupling of fluid and structural domain with dissimilar element distribution using Lagrangian multiplier in a fictitious boundary representing the actual structure.

The governing equations for viscous incompressible fluid in a closed domain are

1. Conservation of mass
2. Newtonian second law (conservation of momentum) the change in momentum equal the sum of forces on a fluid particle
3. First law of thermodynamics (conservation of Energy) the rate of change of energy equals the sum of rate of heat addition to and work done on the fluid particle.

These have to be satisfied for the entire fluid mechanics problem.

In many situations of general interest, the flow of gases is compressible: i.e., there are significant changes in the mass density as the gas flows from place to place. For the case of compressible flow, the continuity of mass and the momentum equation is augmented by the energy conservation equation, as well as thermodynamic relations that specify the internal energy per unit mass, and the temperature in terms of the density and pressure.

Conservation of mass in Eulerian description is given by,

$$\frac{\partial \rho}{\partial t} + \nabla \cdot (\rho u) = 0 \quad (7.1)$$

In two dimensional flows, it is given as,

$$\frac{\partial \rho}{\partial t} + \frac{\partial}{\partial x}(\rho u) + \frac{\partial}{\partial y}(\rho v) = 0 \quad (7.2)$$

Conservation of momentum in Eulerian description is given by,

$$\nabla \cdot \sigma + f = \rho \left(\frac{\partial u}{\partial t} + u \cdot \nabla u \right) \quad (7.3)$$

In two dimensional cases, this becomes,

$$\frac{\partial \sigma_x}{\partial x} + \frac{\partial \sigma_{xy}}{\partial y} + f_x = \rho \left(\frac{\partial u}{\partial t} + u \frac{\partial u}{\partial x} + v \frac{\partial u}{\partial y} \right) \quad (7.4)$$

$$\frac{\partial \sigma_{xy}}{\partial x} + \frac{\partial \sigma_y}{\partial y} + f_y = \rho \left(\frac{\partial u}{\partial t} + u \frac{\partial v}{\partial x} + v \frac{\partial v}{\partial y} \right) \quad (7.5)$$

σ_x , σ_y , are total stress components

f_x , f_y are body force vector

Total stress components in terms of viscous stress components and hydrostatic pressure is given by

$$\sigma_x = \tau_x - p, \sigma_y = \tau_y - p \text{ and } \sigma_{xy} = \tau_{xy} \quad (7.6)$$

The Newton's law of viscosity relates viscous stress τ with velocity gradient. Hence for isotropic Newtonian fluid

$$\tau_x = 2\mu \frac{\partial u}{\partial x} \text{ and } \tau_y = 2\mu \frac{\partial v}{\partial y} \text{ and } \tau_{xy} = 2\mu \left(\frac{\partial u}{\partial y} + \frac{\partial v}{\partial x} \right) \quad (7.7)$$

μ = viscosity of fluid

Conservation of energy for incompressible fluid is expressed as

$$\rho c \left(\frac{\partial T}{\partial t} + u \frac{\partial T}{\partial x} + v \frac{\partial T}{\partial y} \right) = K \left(\frac{\partial^2 T}{\partial x^2} + \frac{\partial^2 T}{\partial y^2} \right) + q + \phi \quad (7.8)$$

C = mean heat capacity at constant volume

q = internal heat generation

k = thermal conductivity of the isotropic fluid

ϕ = viscous dissipation

For the structure, Lagrangian description of motion is used to express the global conservation laws. Because of the fixed material in solids, the conservation of mass is satisfied. The Newton's second law of motion satisfies conservation of momentum and in isothermal condition, the energy conservation is satisfied by considering the equation of motion.

The primary concern in fluid structure interaction (FSI) is computation of fluid forces that act on deformable structures [36]. Hydrodynamic forces act on the structure which is modeled to carry out dynamic analysis to predict failure, stresses, damage etc. Application of FSI methods help to predict the fluid forces by solving the governing equations and using appropriate coupling between fluid and the structure. The coupling between fluid and the structures computes coupling forces on the FSI. The coupling algorithm computes the contact force to be applied from the fluid to the structure and the other way around. The nodal forces at the contact interface are updated at each time step to account for the contact forces.

7.2 Modeling Long Turbine Blade

A single blade has been modeled to examine the effect of tangential flow and off-tangential flow on the vibration characteristics of the blade. The stainless steel blade is 945 mm long and weighs about 19 Kg. As per the Campbell diagram, the first mode of the blade is 107 Hz. In Section 4, detection of vibration of this blade for casing vibration was discussed.

In order to closely match the blade geometry, the surface coordinates of the blade was read by Coordinate Measuring Machine (CMM) into CAD tool Solid-works software. These curves were imported in pre-processor tool; Hyper-mesh of RADIOSS finite element solver. As the root of the blade is not important to the present study, it has not been shown. Cross sections of the blade at the two end i.e. bottom and tip were meshed with 2-D shell elements in such a way that each of them have similar number of elements along the curve and at the same time fine enough to capture the bending moments. The blade is modeled as 8-noded brick (Hex) elements. Dynamic analysis of the blade confirmed the first bending mode at 105 Hz. This simulates free standing blade in the turbine. RADIOSS finite element solver was used to solve simulation of dynamics between the blade and the surrounding fluid [37]. Since the blade is submerged in the fluid domain, the fluid is modeled as rectangular domain enclosing the blade. Figure 7.1 shows the meshed blade housed in the meshed fluid domain.

Primary objective of modeling the fluid and the structure is to assess the response of the blade to the fluid jet that strikes the leading edge of the blade at design angle of incidence and large angle of incidence. This simulates steam incidence angle on the blade during full load and high vacuum in condenser and part load and low vacuum in condenser respectively. In the fluid model, fluid velocities are defined along the leading edge equivalent to speed of the blade. A typical set of finite elements including shell, solid, bar, and spring elements, rigid bodies as well as loads, number of materials, and contact interfaces available in RADIOSS is used in the study.

7.3 Fluid Structure Interaction

To accommodate interaction between blade and the fluid, master-slave approach is adopted. Lagrangian elements of the blade acts as master node and Eulerian elements of the fluid act as slave node. When the slave node is in close proximity and is within the predefined

gap from the master elements, a spring element gets added between master and the slave node which remains active until slave node goes beyond the gap value. The energy and momentum between master and slave is exchanged via these spring elements. Choosing the gap value and



Figure 7.1 Model of the blade and the surrounding fluid

the interface stiffness value are crucial for accuracy of modeling. In this case 1.5 times the average size of Lagrangian element is chosen as the gap between blade boundary and fluid. The spring stiffness is computed by using maximum fluid velocity, its density and gap value [36].

Blade vibration due to interaction with the jet of steam flowing across the blade at different angle of incidence is analyzed. The angle of incidence changes due to reduced steam flow and high back pressure. Blade vibration sustains until the negative incidence angle is maintained. Due to large angle of incidence, as shown in Figure 7.2, blades vibrate.

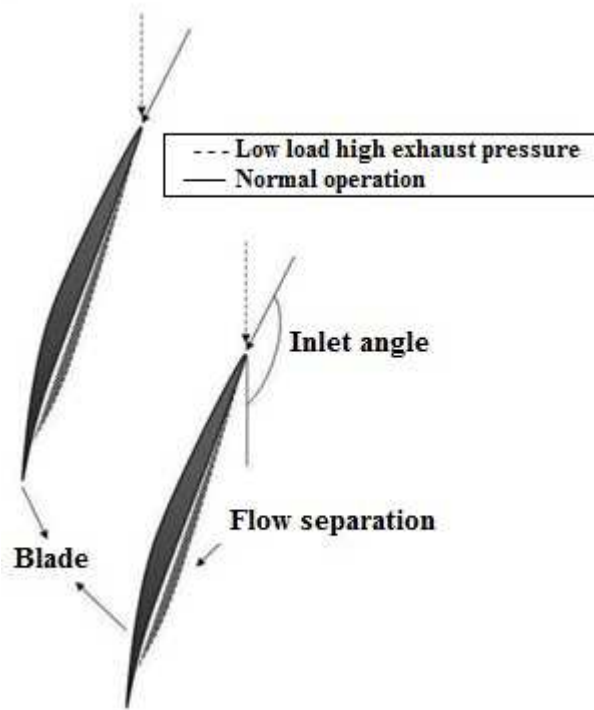


Figure 7.2 Steam inlet angle on the blade.

Blade vibration modulates the flow around the blades and vice-versa. This phenomenon is called self excitation of the blade. Figure 7.3 shows the flow of steam across the cross section of the blade. Figure 7.4 shows gross oscillatory nature of vibration corresponds to the first bending mode of the blade at different angle of incidence.

It can be seen that as the angle becomes more, the amplitude of oscillation of the blade increases indicating severity of stall/ self excitation. The model of the blade behaves in similar manner as seen in the operating plant [38][39].

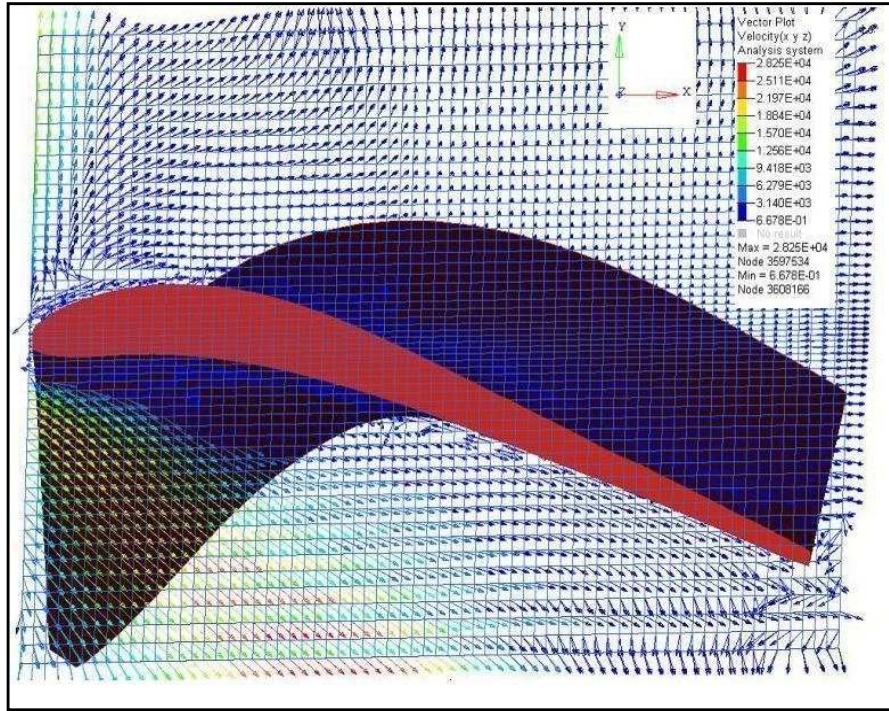


Figure 7.3 Flow of steam across the blade

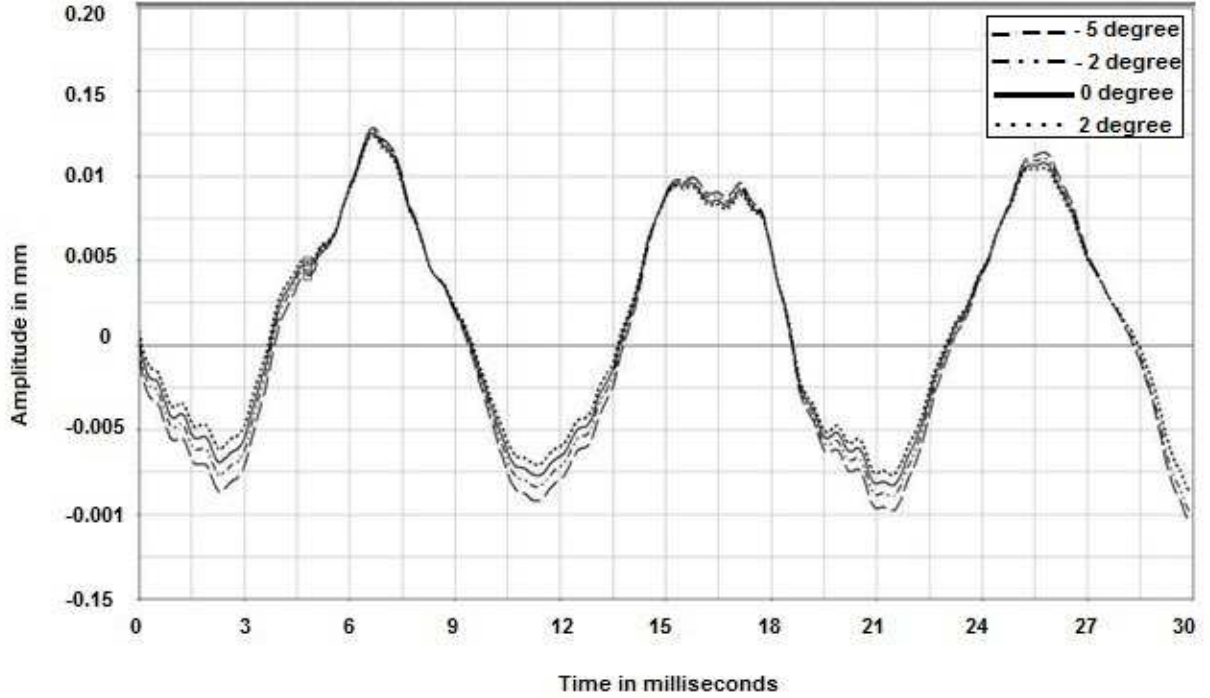


Figure 7.4 Increase in blade vibration due to large steam inlet angle

7.4 Closure

Self excitation in long steam turbine blades sets in at low load and low condenser vacuum when the tips of the blades vibrate. The frequency of vibration during self excitation is the natural frequency of the blade. Quite often turbines operate at low load accompanied by low vacuum in the condenser due to variation in the condenser cooling water temperature. The blade vibration modulates the steam and the steam in turn excites the blades. Until this condition prevails in the turbine the blades vibrate in its natural frequency.

There is limited work reported on simulation of self excitation in turbine blades especially in steam turbines. Chapter 5 demonstrated how the technique was successfully used for detecting self excitation in last stage blades of due to part load operation. This chapter demonstrated self excitation in the blades by simulating condition conducive for self excitation under fluid structure interaction in a commercial finite element package. The blade and the steam were modeled separately and the coupling between the two was achieved through interface spring element between master and slave element. The results of the simulation study closely matched with the results of measurement carried out in the operating power plant. The turbine mentioned in section 5.1 operates at part load that is 220 MWe turbine operates at 165 MWe. The reduced power needs less steam flow. At such part load, the steam incidence angle becomes negative. Due to negative incident angle of steam, the natural frequency of the blade is excited and is measured on the casing at 107 Hz. In the simulation also, it is shown that the amplitude of natural frequency of the model blade increases. The increase is shown in time domain for better illustration.

Chapter 8

Conclusions, Contributions and Future Work

This chapter presents the main conclusions of the work done under comprehensive study on the detection of turbine blade vibration. In principle there are many techniques proposed by researchers and academicians based on the laboratory models with intrusive sensors for either blade tip timing measurement or strain measurement by mounting strain gages directly on the blade. In most of the cases, the techniques are either complicated to implement or offer limited direct information about the health of the blade. The following conclusions are derived on the proposed method of detecting blade vibration based on the analysis of casing vibration.

8.1 Conclusions

The new method of detecting blade vibration has been successful in relating BPF and the natural frequency of the blade in the simulated experiment involving variable speed fan and air jet impingement. Constant vibration amplitude at BPF indicates no blade vibration whereas varying amplitude at BPF indicates blade vibration.

The new method was implemented on low pressure turbine of a 900 MW nuclear power plant and demonstrated that long blades vibrate in its natural frequency due to random steam

excitation caused by steam extraction. The results closely match with the results of simulated laboratory experiment.

The new method was successfully implemented for detecting long blade vibration induced by part load operation in 220 MW nuclear power plant. The blades vibrate due to self excitation caused by low load and low condenser vacuum created in the turbine temporarily. Blade vibrates until the condition conducive to blade vibration prevails in the turbine. The measured blade natural frequency during plant operation closely agrees with published results.

The new method was applied on compressor of 250MW gas turbine to detect compressor blade vibration. Even though the blades are short and rigid, they are excited by transient created by suddenly lowering the load on the turbine. The measured blade natural frequency closely agrees with the natural frequency indicated in the Campbell diagram of the compressor stage.

The phenomenon of self excitation in turbine blades due to part load operation was simulated in a commercial finite element package dealing with fluid structure interaction. The increase in amplitude of blade vibration at its natural frequency due to variation in the incidence angle of steam impingement on the leading edge was demonstrated.

The new method is easy to implement even on a working turbine. The signal analysis technique can be easily implemented without processing with complicated signal processing tools. The strength of the blade related vibration signals can be measured by general purpose accelerometer mounted on the turbine casing.

8.2 Contribution

Primary contribution of the work done is towards evolving a robust but simple technique of monitoring turbine blade vibrations non-intrusively through analysis and

successful application of the technique on operating turbines of different class, make and design. This has been demonstrated successfully for the benefit of power industry.

8.3 Future Work

There are still many reported incidences of blade failure in power plants. In most of the root cause analysis reports, the tell-tale marks on the failed surface point to strong presence of fatigue before failure. This indicates possibility of blade vibration leading to micro cracks and its growth with time. The presence of crack on any part of the blade has a potential to fail during operation. As a part of future work, the blade vibration monitoring technique will be carried forward to detect cracked blades in the turbine. The technique of detecting blade vibration in an operating turbine combined with detecting crack in the blade during operation will be able to address monitoring the overall health of the turbine comprehensively.

References

1. Alexander Leyzerovich. Large Power Steam Turbines. Penn Well Books. ISBN 0-87814-717-9/ ISBN 0-87814-716-0. 1997
2. Bates, R.C.: Steam turbine blades: considerations in design and a survey of blade failures, EPRI Project Report No 912-1 CS-1967, August (1981)
3. J Krzyzanowski. On efficiency measurements on large steam turbine low pressure stages. Proceedings of Institute of Mechanical Engineers Vol. 211 Part A, page 347-355, 1997
4. Dewey, R., Rieger, N., McCloskey, T.: Survey of steam turbine blade failures. EPRI CS3891 Project 1856-1, March (1985)
5. Knappett D & J.Garcia. Blade tip timing and strain gage correlation on compressor blades. Proceedings of the Institution of Mechanical Engineers Part G, 222 (GA) pg 497-506 2008
6. Helmut G Maumann. Steam turbine blade options: How to specify or upgrade. Proceedings of the 11th Turbo machinery symposium, Texas, 1982
7. Kearton W.J. Steam turbine theory and practice. Pitman, London 1999.
8. Yeon-Suri Choi et al Investigation of blade failure in a gas turbine. Journal of Mechanical Science and technology , 24 (10) 2010 page 1969-1974
9. Sandeep kumar et al. Monitoring Low cycle fatigue damage in turbine blade using vibration characteristics. Mechanical System and signal processing 21(1): 480-501, 2007
10. H Kanki et al Vibration diagnostic expert system for steam turbine. CISM courses and lectures No 352, International centre for mechanical sciences 1993 page 144-147
11. G Janicki et al Turbine Blade Vibration Measurement Methods for Turbo-charges, American Journal of Sensor Technology, 2014 2 (2), pp 13-19.
12. Overview of blade vibration monitoring capabilities, Hood technology ,Page 1-21 June 2011
13. Kazuhiro Tamura et al Non-contact vibration measurement of the rotor blades that play a pivotal role in the reliability of gas turbines Technical review Vol 51, No 1, March 2014 Page 10-15

14. Jaromir Strnd et al, Diagnostic methods of bladed disc mode shape evaluation used for shrouded blades in steam turbines, 12 European workshop on advanced control and diagnosis, Journal of Physics: Conference series 659, 2015 page 1-8
15. Dvrst.F.A Melling & Whitelaw Principles and practices of Laser Doppler Anemometry. Academic press <http://www.dantecmt.com/Ida/princip/Indes.html>
16. J. R. Kadambi et al, Turbomachinery Blade Vibration and Dynamic Stress Measurements Utilizing Nonintrusive Techniques, Journal of Turbomach 111(4), 468-474 (Oct 01, 1989)
17. Maynard K.P. Trethewey M.W. Application of torsional vibration measurement to blade and shaft crack detection in operating machinery. Maintenance and reliability Conference, Gatlinburg, Tennessee, May 2001.
18. M. Sunar and S.S. Rao, Recent Advances in Sensing and Control of Flexible Structures via Piezoelectric Materials Technology, ASME Applied Mechanics Reviews 52 (1999), 1–16.
19. Ronald L. Bannister, Turbine blade vibration detection apparatus US patent 4413519 A 1983
20. Michael Twerdochlib, Microwave system for monitoring turbine blade vibration US patent 5479826, 1996
21. P. W. Viscovich, Turbine blade vibration monitor for non-magnetic blades ,US patent 914953 A 1990
22. Forbes G L & Robert B Randall. Non contact gas turbine blade vibration measurement from casing pressure and vibration signals- a review. Proceedings of the 8th IFToMM International Conf. in rotor dynamics Sept 2010 KIST Seoul, Korea
23. Edward David Thompson et al Steam turbine blade vibration monitor back pressure limiting system and method. US patent 20150128596, 2015
24. Mathioudakis, K., E. Loukis, and K.D. Papailiou, Casing vibration and gas turbine operating conditions. 1989. Toronto, Ontario, Canada: Publication by American Society of Mechanical Engineers (ASME), New York, NY, USA.
25. W.Gershutz et al Experimental Investigations of Rotating flow instabilities in the last stage of a low pressure model steam turbine during windage, Proceeding of IMechE, Vol. 219, Part A Journal of Power and Energy, Page 499-510, 2005

26. Benjamin Megerle. Unsteady aerodynamics of low pressure steam turbine operating under low volume flow condition. Ph. D. Thesis, Ecole Polytechnique Federale de Lausanne, 2014
27. Tateki Nakamura, Hamaoka Unit-5 Nuclear Turbine Incident and its countermeasures Japan Society of Maintenology , 2009-2011
28. Thomas H Mccloskey, Troubleshooting turbine path damage mechanisms, Proceeding of the 31st Turbo machinery symposium 2002, page 105-145
29. Nicolo Bachschmid et al Blade vibration measurements and excitation force evaluation. Proceedings of the 9th IFToMM International conference on rotor dynamics Vol. 21, Series on Mechanisms and Machine Science Springer International publishing Switzerland pp 65-78 May 2015
30. Blade vibration triggered by low load and high back pressure, A.Rama Rao, B.K.Dutta, Engineering Failure Analysis 46 (2014) 40–48
31. M. Petrovic et al, Off Design Flow Analysis of Low Pressure Steam Turbines, Proceeding of Institute of Mechanical Engineers, Vol. 211, Part A, Page 215-224,1997
32. M. A. Barron- Meza. Vibration analysis of a self excited elastic beam. Journal of applied research and technology ,Vol. 8 No 2 August 2010, page 227-239
33. Z Mazur et al Steam turbine blade failure analysis. Engineering Failure Analysis Vol. 15 ,2008, page 129-141
34. J. S. Rao, Turbo machinery blade vibration, Narosa Publications, 2000
35. Vibration analysis for detecting failure of compressor blade. A. Rama Rao & B.K. Dutta Engineering Failure Analysis, 25 (2012) 211–218
36. J. De Hart et al, A two-dimensional fluid structure interaction model of the aortic valve , Journal of biomechanics, Vol. 33, 2000, Page 1079-1088
37. RADIOSS Theory and Manual, “Large displacement finite element analysis” January 2009
38. A.Rama Rao, B.K.Dutta, “In situ Detection of Turbine Blade Vibration and prevention. Journal of Failure Analysis and Prevention”. DOI 10.1007/s11668-012-9597-6 Published online 01 August 2012
39. M Petrovic et al “ Off-design flow analysis of low pressure steam turbines” Proceeding of IMechE Part A Vol 211, 1997, Page 215-224